

Review

High-Performance Piezoelectric Energy Harvesters and Their Applications

Zhengbao Yang,^{1,3,*} Shengxi Zhou,^{2,*} Jean Zu,^{3,*} and Daniel Inman^{4,*}

Energy harvesting holds great potential to achieve long-lifespan self-powered operations of wireless sensor networks, wearable devices, and medical implants, and thus has attracted substantial interest from both academia and industry. This paper presents a comprehensive review of piezoelectric energy-harvesting techniques developed in the last decade. The piezoelectric effect has been widely adopted to convert mechanical energy to electricity, due to its high energy conversion efficiency, ease of implementation, and miniaturization. From the viewpoint of applications, we are most concerned about whether an energy harvester can generate sufficient power under a variable excitation. Therefore, here we concentrate on methodologies leading to high power output and broad operational bandwidth. Different designs, nonlinear methods, optimization techniques, and harvesting materials are reviewed and discussed in depth. Furthermore, we identify four promising applications: shoes, pacemakers, tire pressure monitoring systems, and bridge and building monitoring. We review new high-performance energy harvesters proposed for each application.

Introduction

Mechanical energy harvesting is a process by which vibration, kinetic energy, or deformation energy is converted to electrical energy. There are a variety of energy sources available for energy harvesters, ranging from the human body to wild animals, from industrial machinery to vehicles, from large-scale buildings to bridges, and from water flow to wind. Energy harvesters are regarded as promising independent power sources for low-power electronic devices such as wireless sensors, portable devices, and medical implants. Different from the most commonly used chemical batteries, energy harvesters function like power generators, endlessly harvesting energy from the surroundings. Thus issues associated with batteries such as limited lifespan, large size, environmental pollution, and high maintenance cost are mitigated by harvesting solutions. Along with the rapid development of low-power integrated circuits (ICs) and high-efficiency energy storage solutions, the energy-harvesting technology is expected to ultimately give rise to an era of self-powered autonomous operation in healthcare, automotive applications, and environmental monitoring.

Energy harvesters have been intensively studied for the last two decades. A wide range of investigations have been conducted to improve performance in a variety of aspects. There are a number of excellent reviews published, which focus on materials,^{1–3} micro-electromechanical systems (MEMS)-scale devices,^{4–11} nonlinear broadband methods,^{12–14} circuits,^{15–17} and different conversion methods.^{18–24} The goal of this study is to provide an in-depth review on the state-of-the-art techniques that lead to high-performance energy harvesting via the piezoelectric effect. Instead of discussing methods proposed to improve performance in different aspects

Context & Scale

With the rapid advances in wireless sensors, implantable electronics, and wearable devices, the demand for high-power-density and long-lifespan power sources is becoming increasingly stronger. Energy harvesting, emerging as an alternative energy solution to batteries, holds great potential to achieve self-powered autonomous operations of such low-power electronic devices, and thus has recently attracted much attention from both academia and industry. The piezoelectric effect is widely adopted to convert mechanical energy to electrical energy, due to its high energy conversion efficiency, ease of implementation, and miniaturization. This paper presents a comprehensive and critical review of state-of-the-art research on piezoelectric energy harvesting. From the viewpoint of applications, we are most concerned about whether an energy harvester can generate sufficient power under variable excitation. Therefore, here we concentrate on methodologies leading to high power output and broad operational bandwidth. A variety of designs, nonlinear methods, optimization techniques, and harvesting materials are reviewed and discussed in depth. The study also evaluates different figures of merit



broadly, we concentrate on the most essential properties to end users. From the perspective of applications, power output and operational bandwidth are the two metrics most useful to product development engineers. The insufficient power output and the sensitivity to environmental variations are the main barriers preventing current energy harvesters from being widely adopted in engineering practice. To improve power output and extend working bandwidth, researchers have explored different designs, nonlinear methods, optimization techniques, and materials, which are included in this review. To further improve the performance of piezoelectric energy harvesters (PEHs), it is important to discuss them in specific application environments. Here we identified four most promising and widely studied applications: shoes, artificial pacemakers, tire pressure monitoring systems, and building and bridge monitoring systems. For each application, we characterize the excitation sources, detail design methodologies, and comprehensively review application-oriented designs proposed in the past 10 years. The hope of this review is to help guide future research and promote future applications of PEHs.

The article begins with a brief introduction of fundamental knowledge for piezoelectric energy harvesting. We then review nonlinear methods for extending the operational bandwidth and approaches to obtain high power output, followed by a comprehensive performance evaluation of recently proposed PEHs. Finally, we present a detailed review of high-performance energy harvesters for the four identified applications.

Fundamentals of Piezoelectric Energy Harvesting

The direct piezoelectric effect is the basis for PEHs. It is governed by the following constitutive equations, which connects the mechanical domain (stress T and strain S) with the electric domain (electric field E and charge density D):

$$\begin{bmatrix} \text{Converse} \\ \text{Direct} \end{bmatrix} = \begin{bmatrix} S \\ D \end{bmatrix} = \begin{bmatrix} s^E & d^t \\ d & \epsilon^T \end{bmatrix} \begin{bmatrix} T \\ E \end{bmatrix}, \quad (\text{Equation 2.1})$$

where s^E is the compliance under a constant electrical field, ϵ^T is the dielectric permittivity under a constant stress, and d and d^t are the matrices for direct and converse piezoelectric effect, where the superscript t stands for the transpose.

Most energy harvesters operate in a frequency range much lower than the resonant frequency of the employed piezoelectric elements. Thus the piezoelectric elements can be approximately regarded as parallel plate capacitors. For a piezoelectric element (surface area S and thickness t) loaded with a stress σ , we can roughly calculate the accumulated charge Q on the electrode, the voltage V over the element, and the total converted electric energy U as

$$\begin{aligned} U &= \frac{1}{2} QV = \frac{1}{2} (d \times \sigma \times S) \bullet (g \times \sigma \times t), \\ &= \frac{1}{2} d \times g \times \sigma^2 \times \text{Volume} \end{aligned} \quad (\text{Equation 2.2})$$

where the current constant d and voltage constant g correspond to the specific coefficients of the operational mode. The simplified Equation 2.2 indicates that a material or operational mode with a high $d \times g$ value will show a high power density when the piezoelectric material is directly stressed.

Equation 2.2 can be used to evaluate different piezoelectric materials. Those commonly used in energy harvesters include aluminum nitride (AlN), ZnO, BaTiO₃, polyvinylidene fluoride (PVDF), PZT, PMN-PT (Pb[Mg_{1/3}Nb_{2/3}]O₃-PbTiO₃), PZN-PT

and presents a systematic performance comparison on recently proposed energy harvesters. Furthermore, we identify four promising applications: shoes, artificial pacemakers, tire pressure monitoring systems, and bridge and building monitoring. The excitation characteristics of each application are analyzed and corresponding harvesting methods discussed.

The piezoelectric energy-harvesting technology has experienced significant progress in the past 10 years. However, research on energy harvesters is mostly conducted without specific applications, and reliability and system integration have not been well examined. More research is expected to deal with these issues to facilitate in turning decades of research efforts on energy harvesting into tangible benefits in our daily life.

¹Department of Mechanical and Biomedical Engineering, City University of Hong Kong, Kowloon, Hong Kong, China

²School of Aeronautics, Northwestern Polytechnical University, Xi'an, China

³Department of Mechanical and Industrial Engineering, University of Toronto, Toronto, ON, Canada

⁴Department of Aerospace Engineering, University of Michigan, Ann Arbor, MI USA

*Correspondence: zb.yang@cityu.edu.hk (Z.Y.), zhoushengxi@nwpu.edu.cn (S.Z.), zu@mie.utoronto.ca (J.Z.), daninman@umich.edu (D.I.)

<https://doi.org/10.1016/j.joule.2018.03.011>

Table 1. Piezoelectric Materials and Their Properties

| | BaTiO ₃ | PZT-4 | PZT-5A | PZT-5H | PZT-8 | PVDF | PMN-33%PT | PZN-6%PT |
|----------------------------|--------------------|-------|--------|--------|-------|------|-----------|----------|
| d_{31} (10^{-12} C/N) | -78 | -123 | -171 | -275 | -97 | -23 | -920 | -1,400 |
| d_{33} | 149 | 289 | 374 | 593 | 225 | 33 | 2200 | 2,400 |
| d_{15} | | 496 | 584 | 741 | 330 | | | |
| g_{31} (10^{-3} Vm/N) | 5 | -11.1 | -11.4 | -9.1 | -11 | 216 | -17.1 | 24.3 |
| g_{33} | 14.1 | 26.1 | 24.8 | 19.7 | 25.4 | 330 | 44 | 41.7 |
| g_{15} | | 39.4 | 38.2 | 26.8 | 28.9 | | | |
| k_{33} | 0.48 | 0.7 | 0.71 | 0.75 | 0.64 | 0.15 | 0.93 | 0.9 |
| Mechanical Q _M | 300 | 500 | 75 | 65 | 1,000 | 3–10 | 69 | |
| Dielectric loss | | 0.4% | | 2% | 0.4% | | 0.42% | |
| Curie temperature (°C) | 115 | 328 | 365 | 193 | 300 | 100 | 145 | 100 |

See Khan et al.,² Caliò et al.,²⁵ Uchino,²⁶ Zhang et al.,²⁷ and Yang and Zu.²⁸

(Pb[Zn_{1/3}Nb_{2/3}]O₃-PbTiO₃), and various piezoelectric composites. Table 1 summarizes the properties of these piezoelectric materials. AlN and ZnO have a much weaker piezoelectric effect than the other listed materials. They are usually adopted in thin film configurations in micro scale where figures of merit are different from those of bulk materials. Properties of AlN and ZnO are thus not compared here. As shown in Table 1, usually we have $d_{15} \gg d_{33} > d_{31}$. For PZT, $d_{31} \approx 0.5d_{33}$. The single crystals PMN-PT and PZN-PT demonstrate the highest piezoelectric properties, but are more sensitive to temperate change, more susceptible to fatigue, and more difficult to manufacture than lead zirconate titanate (PZT). Therefore, PZT is still the most popular piezoelectric material in energy harvesters.

PZT is a perovskite ceramic, manufactured via a complicated process. First, fine PZT powders of the component metal oxides PbZr_{1-x}Ti_xO₃ are mixed at a specific proportion (x). It has been demonstrated that the piezoelectric effect is maximized when $x \approx 0.5$ (Yuhuan²⁹). Around $x = 0.5$, the crystalline PZT is in the vicinity of the morphotropic phase boundary between the ferroelectric monoclinic and rhombohedral phases, and an increased number of domain structures coexist. The compound powder is then heated and formed (dry or isostatic press, etc.) into the desired shape. Following this, the elements experience a sinter firing process and attain a dense crystalline structure. The crystalline elements are ground to specifications and covered with surface electrodes for the last process, polarization. PZT is a polycrystalline material with polar domains of random orientations (Figure 1A); thus it does not show a macroscopic piezoelectric effect until being polarized. In the polarization process, a strong DC electric field is provided through the electrodes at a temperature a little below the Curie temperature. With the assistance of heat, the randomly oriented polar domains can move more freely to be aligned with the external electric field (Figure 1B). After cooling and the removal of the electric field, the polar domains are locked into a pattern of near alignment (Figure 1C). As a consequence, the material possesses permanent polarization and exhibit the desired piezoelectric effect.

According to the directions of polarization and stress, energy harvesters can be categorized into two main operation modes: d_{31} and d_{33} . As illustrated in Figure 2, in the d_{31} mode, the polarization direction "3," i.e., the electric field, is perpendicular to the direction of the applied stress "1." This is the most commonly used operation mode, and widely exists in bending-beam structures. In contrast, the

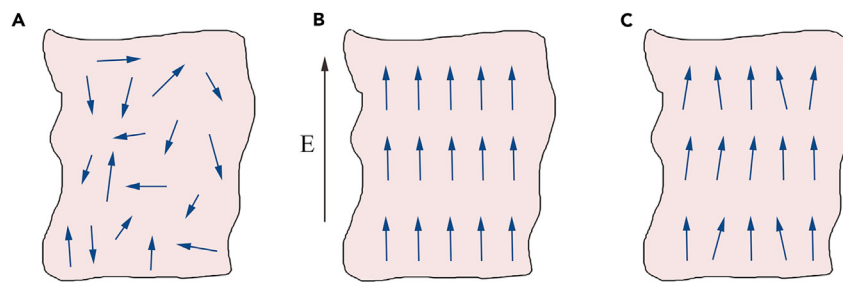


Figure 1. Polarization of Polycrystalline Piezoelectric Ceramic

- (A) Random orientation of polar domains prior to poling.
(B) Poling under a constant electric field.
(C) Remnant polarization after the removal of the electric field.

polarization and the applied stress are in the same direction in the d_{33} mode. The d_{33} mode appears in direct compressive/tensile harvesters or harvesters with the interdigitated electrode. In both the d_{31} and d_{33} modes, electrodes are made perpendicular to the poling direction, i.e., the electric field is aligned with the polarization. Some energy harvesters also employ the shear mode, where the charge constant d_{15} plays the role. Piezoelectric elements working in the shear mode need a special treatment as the electrodes are formed on surfaces parallel to the poling direction.

The stiff piezoceramics are not able to capture much mechanical energy if they are directly attached to a vibration host. The classic solution is to attach a piezoelectric element on a flexible beam structure. The cantilever, as shown in Figure 3, is the most commonly used structure. The substructure is covered with one piezoelectric element (unimorph) or two (bimorph) near the high-stress fixed end, and often attached with a tip mass to lower resonant frequency and increase the vibration-induced stress. The cantilever energy harvester is an inertial linear resonant energy harvester and has been used widely in the literature as a benchmark for performance comparison. It operates by first harnessing vibration energy from ambient excitation sources such as building oscillations, human motions, and vehicle vibrations, thereafter converting the harnessed mechanical energy to electrical energy for powering portable or wireless sensor modules.

Broadband Nonlinear Energy Harvesting

Governing Equations

Considering that linear resonant harvesters are incapable of harvesting energy from broadband or frequency-varying excitations, researchers have developed some frequency tuning approaches, such as multi-cantilever structures, bistable composite plate designs, and passive and active stiffness-tuning technologies.^{12–14,30,31}

From the viewpoint of stochastic resonance,³² Gammaletti et al. brought the bi-stable mechanism to the vibration energy-harvesting field, and numerically and experimentally demonstrated the unique advantage of bistable energy harvesters (BEHs) under random excitation.³³ The nonlinear magnetic interaction was used to induce nonlinear responses of an inverted pendulum beam. Under harmonic excitations, Erturk et al.³⁴ presented a typical Duffing system, consisting of a magnetic beam attached with piezoelectric patches and two fixed external magnets as shown in Figure 4A. A set of dimensionless electromechanical equations were

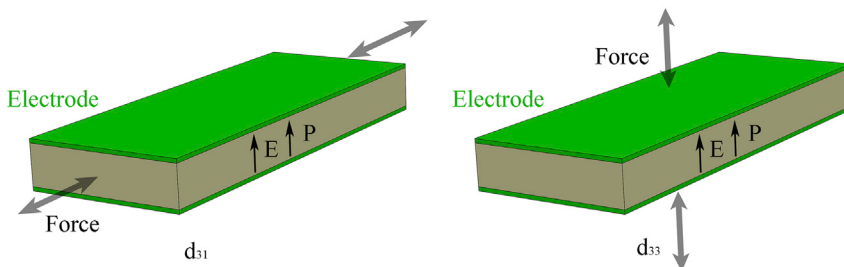


Figure 2. Illustration of the d_{31} and d_{33} Operation Modes

employed to describe the dynamic characteristics. The corresponding governing equations are:

$$\ddot{x} + 2\zeta\dot{x} - \frac{1}{2}x(1-x^2) - \chi v = f \cos \Omega t, \quad (\text{Equation 3.1})$$

$$\dot{v} + \lambda v + \kappa \dot{x} = 0$$

where v is the dimensionless voltage across the load resistance, χ is the dimensionless piezoelectric coupling term in the mechanical equation, κ is the dimensionless piezoelectric coupling term in the electrical circuit equation, and λ is the reciprocal of the dimensionless time constant ($\lambda \propto 1/R/C_p$, where R is the load resistance and C_p is the equivalent capacitance of the piezoelectric layers). All the parameters used in this model are dimensionless and not completely related to the real experiments. Nevertheless, this model can be used to qualitatively depict and analyze the nonlinear dynamic responses of bistable harvesters.

Zhou et al.³⁵ designed an alternative nonlinear broadband energy harvester with rotatable magnets to further extend frequency bandwidth by altering the magnet inclination angle (Figure 4B). This system consists of an elastic substrate, tip magnet attachments, external magnets, and two piezoelectric layers at the root. The exhibited nonlinear dynamic behaviors vary depending on the inclination angle α of the external magnets relative to the horizontal (Figure 4B) over a certain frequency range. Additionally, the configuration potentially saves space since nonlinear frequency response can be altered by simply rotating the magnets rather than changing the magnet spacing. A quantitative electromechanical model was derived based on the Rayleigh-Ritz method and Euler-Bernoulli beam theory. The corresponding governing equations are:

$$M\ddot{x} + C\dot{x} + Kx - \theta v = F + F_m \quad (\text{Equation 3.2})$$

$$C_p\dot{v} + \frac{v}{R} + \theta \dot{x} = 0,$$

where M is the equivalent mass, K is the equivalent stiffness, C is the equivalent damping, θ is the equivalent electromechanical coupling term, $x(t)$ is the tip displacement of the harvester in the transverse direction, $v(t)$ is the voltage across the electrical load, and $F(t)$ is the external mechanical force as the excitation term.

F_m is the magnetic force fit to a polynomial of the form

$$F_m = \mu x + \lambda x^3, \quad (\text{Equation 3.3})$$

which is identified by using a sensitive dynamometer in experiments. The coefficients of the magnetic force polynomial denoted by μ and λ depend on the angle α .

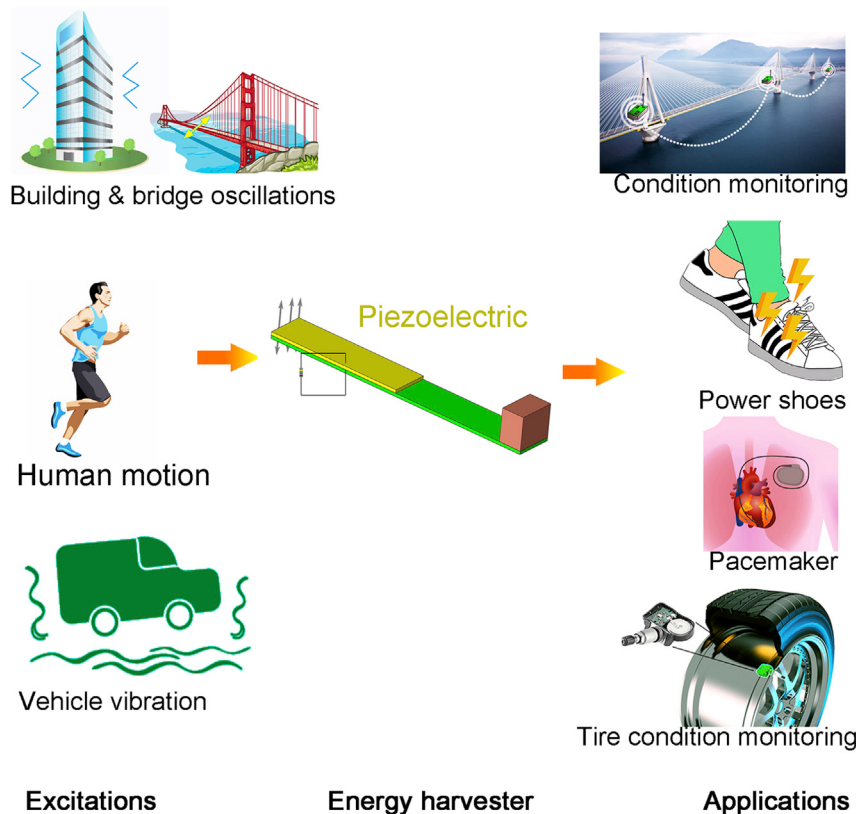


Figure 3. The Typical Energy Harvesting Operation Process

The most commonly used cantilever configuration is shown here as an example.

For modeling the magnetic force, Stanton et al.³⁶ proposed an analytical method for the bistable energy harvester shown in Figure 5. The magnetic field generated by a magnet **A** upon another magnetic **B** was given by

$$\mathbf{B}_{AB} = -\frac{\mu_0}{4\pi} \nabla \frac{\mu_A \cdot \mathbf{r}_{AB}}{\|\mathbf{r}_{AB}\|_2^3}, \quad (\text{Equation 3.4})$$

where $\|\cdot\|_2$ and ∇ denote the Euclidean norm and vector gradient operators, respectively. μ_0 and μ_A are the permeability of the free space and the magnetic dipole moment vector, respectively. \mathbf{r}_{AB} is the effective distance from the magnet **A** upon the magnetic **B**. The potential energy in the field is expressed as $U_m = -\mathbf{B}_{AB} \cdot \mu_B$. The magnetic force can be obtained by making a differential on U_m .

Energy-Harvesting Performance and Analysis

Under variable harmonic excitations, nonlinear energy harvesters have been proven to be able to exhibit a broadband performance. Researchers have successively explored monostable, bistable, and tristable systems. Sebald et al.³⁷ experimentally verified that their nonlinear monostable harvester can work in the frequency range of 26–36 Hz under the excitation level of 3.2 m s^{-2} , whose bandwidth is much wider than its linear counterpart. Tang et al.³⁸ designed a monostable harvester with a magnetic oscillator that works well under weak excitations. Compared with the equivalent linear harvester, the monostable harvester obtained a 41% increase in the magnitude of the power at an excitation level of 2 m s^{-2} , and a 100% increase in the operating bandwidth. Yang et al.^{39,40} designed a high-efficiency compressive-mode monostable harvester that produced a maximum power output of

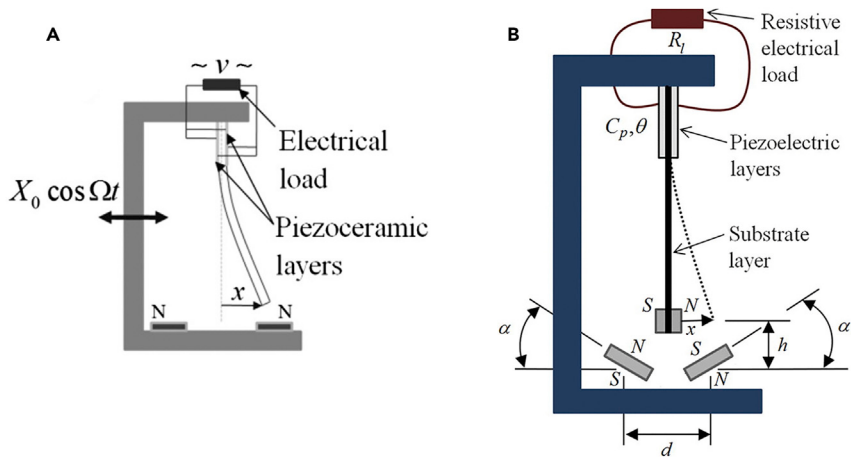


Figure 4. Typical Magnetic-Based Nonlinear Energy Harvesting Structures

(A) Duffing bistable energy harvester. Reproduced from Erturk et al.³⁴ with permission from AIP Publishing LLC.

(B) Rotatable nonlinear energy harvester. Reproduced from Zhou et al.³⁵ with permission from AIP Publishing LLC.

54.7 mW and an operational bandwidth of 12 Hz, under an excitation level of 4.9 m s^{-2} . Stanton et al.⁴¹ achieved a novel bidirectional hysteretic response of a monostable cantilever harvester by tuning a set of coupled magnets. Both hardening and softening responses were exhibited in the simulation and invoked in experiments. Yang et al.⁴² proposed a new method to tune the nonlinear responses of monostable harvesters by tilting the structures. The capability of shifting the dynamic responses between hardening nonlinearity and softening nonlinearity gives energy harvesters a great environmental adaptability. Erturk et al.^{34,43} explored the high-energy orbits in a Duffing BEH over a range of excitation frequencies, and numerically and experimentally verified the energy-harvesting enhancement of the BEH. Zhou et al.³⁵ obtained high-energy output voltage in a wide frequency range of 4–22 Hz by changing the magnet inclination angle shown in Figure 4B. Later, based on the same nonlinear energy-harvesting device, Zhou et al.^{44,45} and Kim et al.^{46,47} proposed a tristable energy-harvesting concept. The theoretical and experimental results demonstrated that the tristable energy harvester with shallow potential wells can more easily undergo high-energy inter-well oscillations under low-level excitations than its bistable counterparts because of their higher potential.

To analyze nonlinear systems, researchers have proposed a variety of theoretical models and solutions. Both the harmonic balance method⁴⁸ and the multiple scale technique⁴² have been used to solve the governing equations of monostable systems. Stanton et al.⁴⁹ deduced the fundamental harmonic balance solutions of the intra-well and inter-well oscillations for BEHs. Based on this research, Harne and Wang⁵⁰ obtained the harmonic balance solutions with both fundamental and third harmonic terms of BEHs. Meanwhile, they observed the third harmonic response in experiments, which is in accordance with the earlier work provided by Massna and Daqaq.⁵¹ For the tristable systems that have more nonlinear terms and complex nonlinear dynamics, Zhou et al.⁵² and Panyam et al.⁵³ successively employed the harmonic balance method and the perturbation method to obtain the theoretical solutions. They found that tristable energy harvesters have multi-solution frequency ranges under harmonic excitations. The chaotic response characteristics of nonlinear energy harvesters were explored by Cao et al.⁵⁴ via the phase trajectory, power

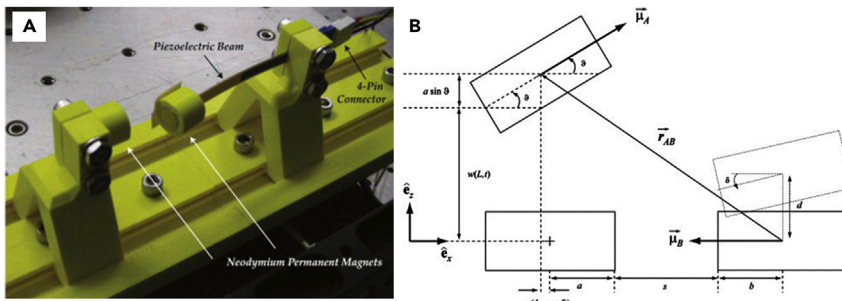


Figure 5. Repulsive Magnetic Force-Based Bistable Energy Harvester

(A) Experimental setup.

(B) Detailed view of the geometry used to outline vector parameters of the analytical magnet model. Reproduced from Stanton et al.³⁶ with permission from Elsevier.

spectrum, Poincare map, and bifurcation diagram. The predictive criteria to determine the harmonic excitation conditions for the presence of chaotic response were investigated via Melnikov theoretical methods.^{55,56}

In addition to investigating ideal harmonic excitations, random excitations have also been systematically investigated. Litak et al.^{57,58} numerically simulated the responses of the bistable harvester proposed by Erturk et al.³⁴ under random base excitations, and observed the stochastic resonance phenomenon. It is claimed that if the variance of the excitation were known, the harvester could be optimized to maximize the power harvested under random base excitations. Cottone et al.⁵⁹ numerically and experimentally verified that a buckled-beam-based bistable harvester produces more power under random base excitation compared with its linear counterpart. Daqaq^{60,61} explored the Fokker-Plank-Kolmogorov equation to describe the responses of bistable harvesters and approximately solved this equation by using the finite element method. The work of Zhao and Erturk⁶² indicates that a bistable harvester can have a better energy-harvesting performance than linear harvesters only if it was optimally designed to work in the neighborhood of a specific random excitation intensity. For the much lower or higher excitation intensity levels, linear harvesters actually generate larger power output near their resonant frequencies. Under random base excitations, Li et al.⁶³ found that tristable harvesters with shallower potential wells generate more power than bistable harvesters, which is in agreement with the conclusion for harmonic base excitation cases.^{44–47}

There are some new structures proposed for the design of nonlinear energy harvesters. Different from the aforementioned nonlinear energy harvesters that can only harness vibration energy from one direction, Su et al.^{64,65} developed a two degrees of freedom (2DOF) broadband magnet-induced dual-cantilever PEH. As shown in Figure 6A, it consists of outer and inner beams and magnets attached to the tips. The magnets induce a nonlinear repulsive force between the two beams, and make the structure bistable. In experiments, it exhibits broadband characteristics and has two voltage peaks in the excitation frequency range under some excitation levels. Arrieta et al.^{66,68} proposed a bistable composite plate for energy harvesting, as shown in Figure 6B. This bistable plate was obtained based on a special heat treatment technology and is capable of bearing high-level excitations. Note that a high level excitation is necessary to make high-energy inter-well oscillations in this design. Betts et al.^{69,70} presented an optimization strategy of bistable composites, which enables improved power output by discovering the optimal configurations based on the statics of the device. The optimal device aspect ratio,

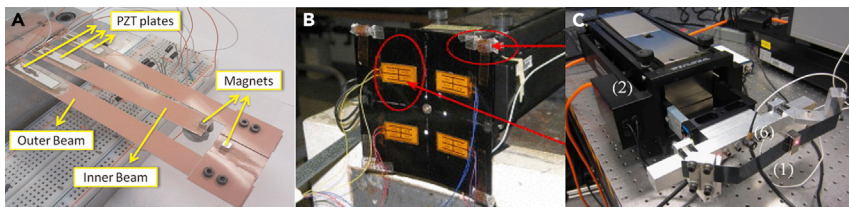


Figure 6. New Nonlinear Energy Harvesters

(A) 2DOF bistable harvester. Reproduced from Su et al.⁶⁴ with permission from SAGE Publications.

(B) Bistable composite plate. Reproduced from Arrieta et al.⁶⁶ with permission from AIP Publishing LLC.

(C) M-shaped nonlinear energy harvester. Reproduced from Leadenham et al.⁶⁷ with permission from Elsevier.

stacking sequence, thickness, and piezoelectric area were considered in their research. Leadenham and Erturk⁶⁷ designed an M-shaped asymmetric nonlinear energy harvester for broadband vibration energy harvesting. As shown in Figure 6C, a pre-bent monostable beam structure, the M-shaped configuration may exhibit both limited maximum deflections to protect piezoelectric elements and favorable nonlinear dynamic response at low excitation levels, thanks to the large stretching capabilities. Compared with the corresponding linear system, the M-shaped nonlinear energy harvester offers a maximal 8,900% bandwidth enhancement at the root-mean-square base excitation levels of 0.07 g.

Energy-Harvesting Enhancement Strategies

Nonlinearity has been widely recognized as an effective method to extend the working bandwidth for energy harvesters. However, one should note that such nonlinear energy harvesters have multiple vibration orbits and a region of hysteresis under most excitation conditions. Furthermore, their expected performance enhancement can be realized only when system vibrates at the highest orbit. It is difficult to maintain nonlinear harvesters in the high-energy oscillation states, especially under weak excitations. With zero initial conditions, nonlinear harvesters usually follow the low-energy orbits, resulting in small-amplitude voltage responses. To overcome this issue, Zhou et al.⁷¹ presented an initial impact method for facilitating nonlinear energy harvesters to overcome the potential barriers and achieve high-energy inter-well oscillations under low-level excitations. Figure 7A shows the schematic of a mechanism for imparting additional energy based on the transfer of momentum. In principle, an emitter and receiver could be used to send and receive a projectile to impact the free end of the harvester. The harvester will then obtain a new velocity (or kinetic energy) that is appropriate to respond in high-energy inter-well oscillations. Via this method, the effective bandwidths of bistable and tristable harvesters were increased to 15 Hz and 12 Hz from 3 Hz to 5 Hz in experiments, respectively.

Later on, Mallicket et al.⁷² introduced an electronic control method to switch from the low- to the high-energy orbit of a nonlinear electromagnetic energy harvester by employing the strong interaction between its electrical and mechanical degrees of freedom. In principle, this method can be applied to nonlinear energy harvesters of different sizes and transduction methods after some modifications. As shown in Figure 7B, a voltage $\gamma\dot{x}$ is induced in the coil (internal resistance R_C) of the nonlinear energy harvester, where \dot{x} and γ are respectively the velocity of the mechanical oscillator and the electromagnetic coupling coefficient. The electric power is extracted through the load resistance R_L that is connected in series with the coil. In addition, a voltage source V_A (with internal resistance R_A) is connected across the coil, which,

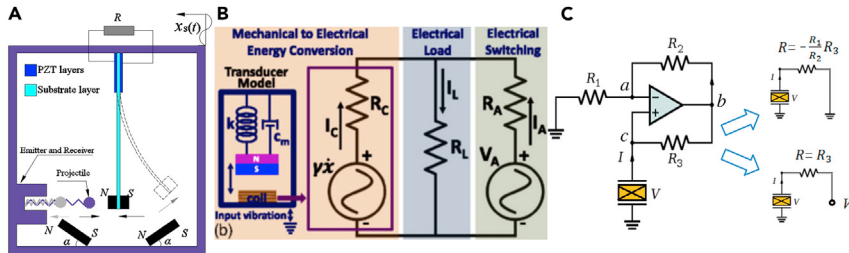


Figure 7. High-Energy Orbit Implement Strategies

(A) Impact-induced method. Reproduced from Zhou et al.⁷¹ with permission from AIP Publishing LLC.

(B) Electrical actuation method. Reproduced from Mallick et al.⁷² with permission from The American Physical Society.

(C) Voltage impulse perturbation method. Reproduced from Lan et al.⁷³ with permission from EDP Sciences.

over a short period, forms electric voltage to perturb the system to switch the state. This method was claimed to be able to improve the energy conversion efficiency over a broad bandwidth under frequency-amplitude-varying excitations using a small energy budget.

Recently, to trigger high-energy-orbit responses of nonlinear PEHs, Lan et al.⁷³ presented a voltage impulse perturbation approach using negative resistance. The detailed circuit design is shown in Figure 7C. A negative resistance can be designed by tuning resistors R_1 , R_2 , and R_3 in the circuit. When the circuit works as a negative resistance, current flows into the piezoelectric element, providing an external excitation to the system. Meanwhile, a response voltage across on the resistances is produced, which influences the mechanical oscillation of energy harvesters. Via this method, high-energy orbit oscillations of both monostable and BEHs were experimentally induced.

Hosseiniloo et al.⁷⁴ proposed a robust and adaptive sliding mode controller to shift the nonlinear energy harvester to the desired attractor by a short entrainment on the desired attractor. Their numerical results show that this method can successfully move the harvester to the desired attractor in a reasonable period of time, but no experiments were conducted.

Summary

The research discussed above indicates that nonlinearity is an effective way to improve the energy-harvesting performance. Nonlinear energy harvesters have theoretically and experimentally demonstrated broader operating bandwidths than their linear counterparts. However, one should note that nonlinear energy harvesters have multiple vibration orbits under most excitation conditions, and the expected performance enhancement can be realized only when nonlinear energy harvesters vibrate at the highest orbit. It is difficult to maintain nonlinear harvesters in the high-energy oscillation states, especially under weak excitations. With zero initial conditions, nonlinear harvesters usually follow the low-energy orbits, resulting in small-amplitude voltage responses.

How to maintain nonlinear energy harvesters in the high-energy states is a critical problem. Using active control is a feasible way to tune nonlinear systems, but consumes a certain amount of energy. More research is expected on the active control technique to improve its robustness under varying conditions, and make the energy

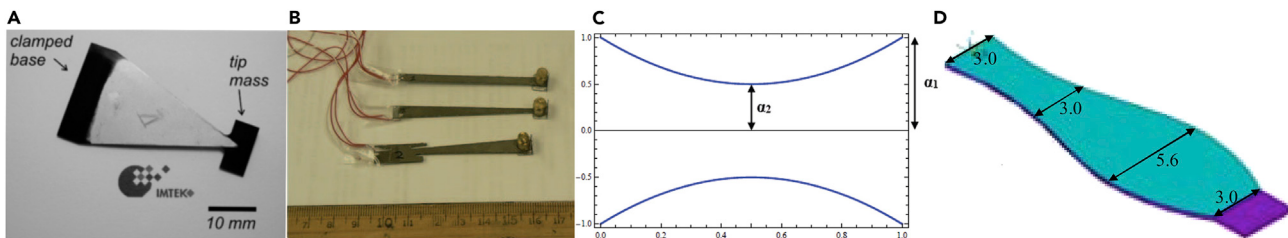


Figure 8. Cantilever Energy Harvesters of Different Beam Shape

- (A) Triangular cantilever beam. Reprinted with permission from Dietl et al.⁷⁷ Copyright 2010, SAGE Publications.
- (B) Tapered and reverse tapered cantilevers. Reproduced from Goldschmidtboeing et al.⁷⁸ with permission from IOP Publishing Ltd.
- (C) Beam with a width of a quadratic profile. Reproduced from Ben Ayed et al.⁷⁹ with permission from SAGE Publications.
- (D) Optimized beam shape with a fixed length. Reproduced from Park et al.⁸⁰ with permission from KSME & Springer.

consumed trivial compared with the energy harvested. Passive control methods are worthy of investigation, although their adaptability may not be as good as that of the active methods. Another critical problem that nonlinear energy harvesters are facing is how to efficiently transfer and store the generated broadband or random electric energy. Currently, most research mainly focuses on the broadband dynamic characteristics of nonlinear systems under the open-circuit condition or simply with resistive loads. More work is expected on the development and optimization of conditioning interface circuits for nonlinear energy harvesters.

High Power Output

Researchers have explored a variety of methods to improve the performance of energy harvesters from the perspective of structures, materials, and circuits. It is impossible to include all of the methods and designs in one review. Here we mainly analyze new structures and materials for increasing power output. Readers who are interested in energy-harvesting circuits can refer to the review papers.^{15,16} The following analyzes these new methods and designs in seven categories: geometry-modified cantilever; topology optimization; curved structures; electrode optimization; d_{15} mode under shear/torsion excitations; new structures operating under tension/compression excitations; and new piezoelectric materials and composites.

Geometry-Modified Cantilever

Classic PEHs employ rectangular cantilever beams where piezoelectric elements experience a bending stress that varies linearly along the length direction. The bending stress is maximized at the fixed end and tends to be zero at the free tip. As a consequence, issues such as overstrain and fatigue may occur around the fixed end. In contrast, the piezoelectric material around the free tip does not play its full role. To obtain a uniform and large strain distribution on the employed piezoelectric materials in cantilever PEHs, researchers have modified usual rectangular shape to consider different geometries.

Tapered cantilevers are well-known optimized shapes. As early as 2005, Roundy et al.^{75,76} proposed the idea of replacing rectangular cantilevers with the trapezoidal file to improve power output. Experiments indicated that beams with a nonuniform width have a 30% gain in power output over rectangular counterparts. Diel and Carcia⁷⁷ examined a family of beams ranging from rectangular beams to triangular beams theoretically and experimentally (Figure 8A). The study indicates that the beam shape has little effect on efficiency, but significantly affects the maximum tolerable excitation strength and the maximum achievable output power. Goldschmidtboeing and Woias⁷⁸ presented a theoretical model based on the

Rayleigh-Ritz method for width-varying cantilever energy harvesters, and optimized three beam shapes: rectangle, linear taper, and reverse taper (Figure 8B). Furthermore, Ayed et al.⁷⁹ studied two types of width profiles for cantilever PEHs as a linear and quadratic function of the position (Figure 8C). They modeled a unimorph cantilever with a tip mass using the one-mode Galerkin method, and estimated that the quadratic geometry is capable of yielding nearly 100% more energy than a rectangular shape.

Besides focusing on different geometries of energy harvesters themselves, researchers have also implemented performance optimization from the system level. Park et al.⁸⁰ considered the limited application space of an energy harvester, and set a fixed length cantilevers with a variable width to maximize the output power. A finite element model was built using ANSYS to find the highest-power-output shape for cantilever beams subject to tip impact excitations. It identified an optimal design with a unique wide tip as shown in Figure 8D. Experiments demonstrated a 37% improvement on the power output compared with the rectangular counterpart using the same amount of material.

Thickness optimization was undertaken theoretically by Paquin and Amant,⁸¹ who proposed a semi-analytical model based on the Rayleigh-Ritz approximations. The study estimated that a thickness-tapered beam with a slope angle of 0.94° can increase power output of energy harvesters by a factor of 3.6. This performance enhancement can be explained by the more uniform strain distribution formed by the tapered thickness. They did not provide experimental validation. This method is plausible theoretically but may not be feasible due to the difficulty in manufacturing thin beams with such a small slope angle.

Topology Optimization

The aforementioned approaches consider only a small number of geometric variables of well-defined shapes such as rectangles and trapezoids. General geometries have also been studied via a variety of topology optimization strategies. Here, we review some representative topology optimization investigations in energy harvesters. Note that all of the topology optimization results are presented without experimental data.

Rupp et al.⁸² applied the topology optimization method to optimize the circuit parameters and the layout of multilayer structures consisting of piezoelectric, electrode, and structural layers. The electromechanical coupling was modeled using the finite element method and the circuit was simulated as a lumped-parameter system. Figure 9A shows the studied object and the optimized design under a harmonic excitation. The optimal layout is dependent upon the substrate thickness ratio. It is obvious that the optimal shape identified by the topology optimization is different from regular geometries such as rectangles and trapezoids, which might pose some problems in the manufacturing process.

Akihiro et al.⁸⁶ did a simultaneous topology optimization on the polarization direction and the layout of the piezoelectric material in a piezoelectric patch. The solid isotropic material with the penalization (SIMP) method was used to model the piezoelectric material and the derived equations were solved by the finite element method. The situation considered here is a piece of piezoelectric patch attached on a vibration surface in high-order vibration modes. The complicated vibration modes lead to strains of opposite signs in the piezoelectric elements and correspondingly charge cancellations if a uniform electrode is used. The authors

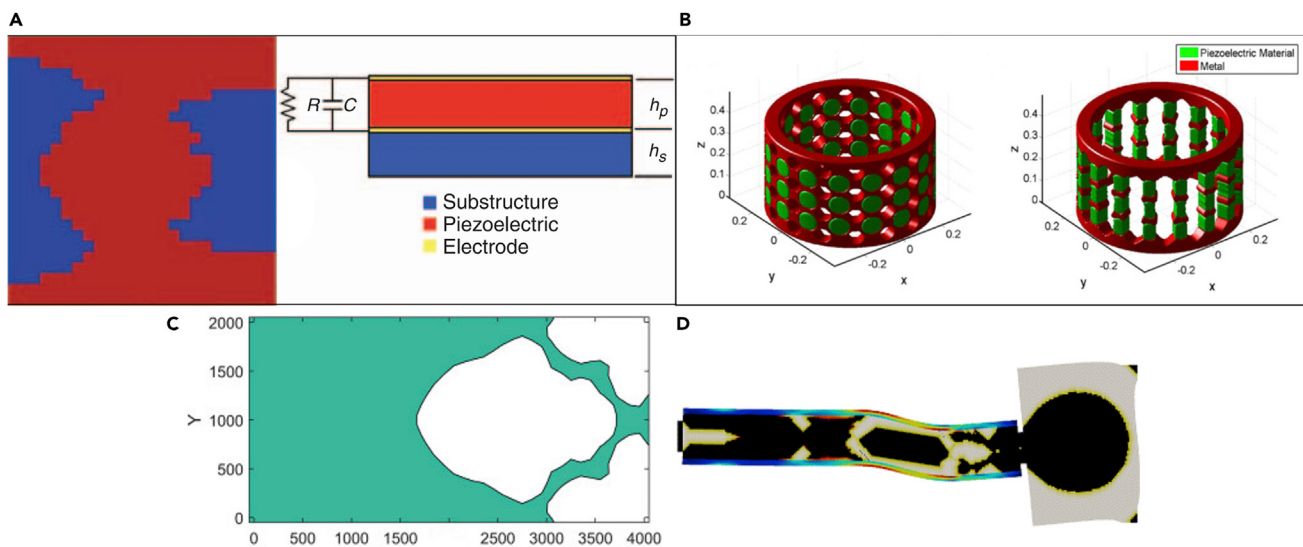


Figure 9. Topology Optimization of Energy Harvester Structures

(A) Multilayer structure with a circuit. Optimized distribution of piezoelectric material (red) on an aluminum substrate (blue). Reproduced from Rupp et al.⁸² with permission from SAGE Publications.

(B) Cylindrical energy harvester. The red (darker) to metal and the green (lighter) colors refer to the piezoelectric material. Reproduced from Rupp et al.⁸³ with permission from Elsevier.

(C) The optimized layout of the piezoelectric layer. The substrate layer remains unchanged (white). Reproduced from Nanthakumar et al.⁸⁴ with permission from Elsevier.

(D) The optimal stress constrained design of a bimorph cantilever with a tip mass. Black represents material and light-gray represents void. The color scale shows the Von Mises stress in the piezoelectric layers. Reproduced from Wein et al.⁸⁵ with permission from Springer-Verlag.

proposed to alter the poling direction to avoid charge cancellation. The method is almost impossible to be implemented due to the problem of polarization and the unpredictable excitation sources.

Chen et al.⁸³ used a level set topology optimization method to find the optimal geometry for maximizing the energy conversion efficiency. The employed level set-based method is argued to be better than other optimization methods used in energy harvesters such as the SIMP method and its variants.^{82,87,88} The SIMP method cannot converge to a solution with distinct phase states for such a complex multi-physics problem. In contrast, the level set method allows initially defined voids to merge and change shapes, resulting in a modified topology of the target structure. Figure 9B shows the optimized cylindrical PEH. The optimal design is with a volume ratio for the piezoelectric material of 51.9% and an energy conversion efficiency of 8.9%.

Most topology optimizations are conducted on bulk materials. In 2016, Nanthakumar et al.⁸⁴ did a topology optimization on nanoscale energy harvesters, considering the unique surface elasticity and surface piezoelectricity existing in ZnO nanostructures. They developed an extended finite element model based on the Kirchoff plate model, coupled with the level set topology optimization method to maximize the electromechanical coupling coefficient. Figure 9C shows the optimized layout of the piezoelectric material. The study also analyzed the competition between the surface elasticity and the surface piezoelectricity.

Wein et al.⁸⁵ performed a topology optimization on the elastic substructure and tip mass of a cantilever bimorph PEH by means of the SIMP method. In the study, the

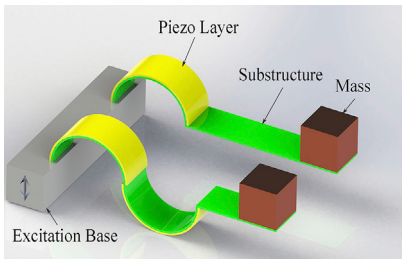


Figure 10. Schematic of Cantilever Energy Harvesters with Arc-Shaped Piezoelectric Elements

Reproduced from Yang et al.⁹⁰ with permission from Elsevier.

piezoelectric layers were kept constant and the geometries of the elastic beam and the tip mass were optimized (Figure 9D). Jia and Seshia⁸⁹ optimized the end mass size compared with the cantilever in micro cantilever energy harvesters, and found that the ideal proportion of the end mass is about 60%–70% of the total cantilever length.

Curved Structures

Although a variety of structures have been exploited in energy harvesters, the core energy transducing parts are most of time plain piezoelectric plates, discs, or stacks. In 2015, Jung developed a curved energy harvester using flexible PVDF films and succeeded in lighting up 476 LEDs under periodic palm pressing. In 2017, Yang et al.⁹⁰ introduced curved piezoceramic elements into energy harvesters. Half-tube PZT elements were employed in the cantilever architecture as shown in Figure 10. Compared with plain plates, higher and more evenly distributed stress can be formed in the curved elements. The proposed curved PZT harvester in experiments exhibited a >200% higher power density and a 60% enhancement in the energy conversion efficiency. It was asserted that more arc-shaped piezoceramic structures can be explored to improve harvester performance.

Electrode Optimization

Electrodes have been optimized to improve power output. Stewart et al.⁹¹ realized that in a traditional cantilever energy harvester, charge flows from the highly stressed root area of the cantilever to the unstrained tip area, and energy is lost in this charge redistribution process. To validate the idea, a prototype was made with 30 piezoelectric elements on an FR4 PCB board as shown in Figure 11A. When only 20 of the 30 piezoelectric elements were connected, the prototype showed the highest power output, which is 15.5% higher than when all elements were connected. Erturk et al.⁹³ did a dimensionless analysis on the strain nodes of the vibration modes of the cantilever energy harvester other than the fundamental mode, and pointed out the optimal segmented electrode configurations to avoid charge cancellation. Cho et al.⁹⁴ studied the effect of electrodes on a membrane energy harvester, and claimed that an electrode coverage of 60% demonstrated the best electromechanical coupling. Yang and Zu⁹⁵ proposed to mitigate the charge redistribution effect in flexextensional transducers by partially covering the piezoelectric element with electrodes in the middle effective region.

In 2015, Kim et al.⁹⁶ theoretically analyzed and optimized the interdigitated electrodes (IDEs) in cantilever energy harvesters. The size of the electrodes, the number of IDE fingers, and the piezoelectric thickness have significant effects on the harvester performance. It was concluded that compared with the general parallel plate electrodes, the IDEs cannot generate more power but show higher voltage responses.

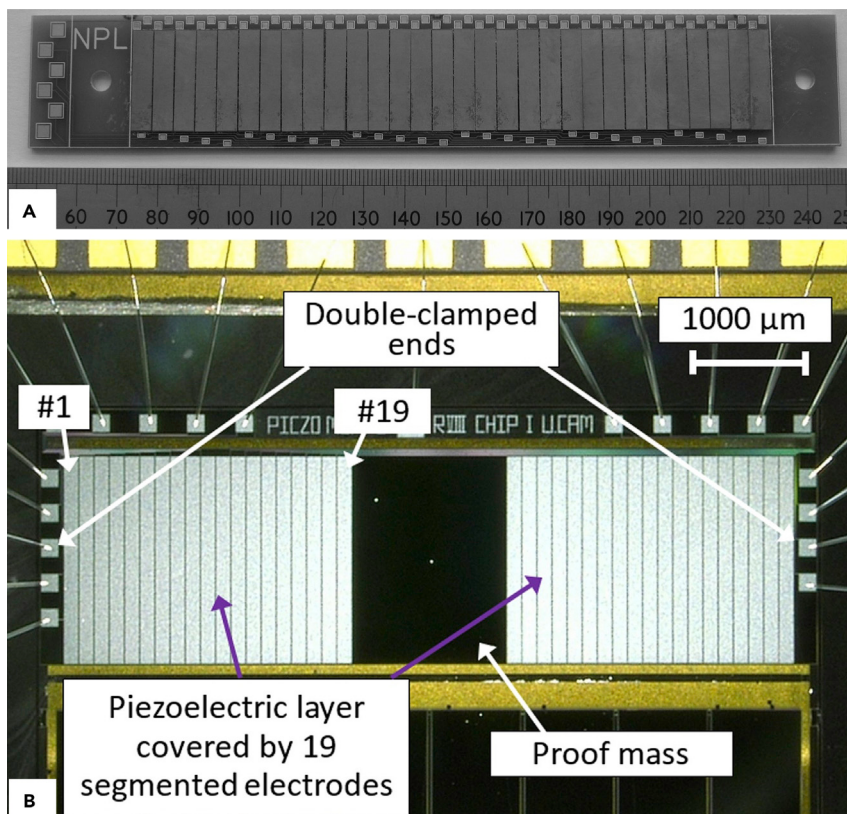


Figure 11. Cantilever Energy Harvester with Individual Piezoelectric Elements

(A) Harvester made by Stewart et al. Reproduced from Stewart et al.⁹¹ with permission from AIP Publishing LLC.

(B) Harvester made by Du et al. Reproduced from Du et al.⁹² with permission from Elsevier.

Later in 2017, Du et al.⁹² analyzed the relationship between the electrode coverage and the power output of beam-based energy harvesters. They reached a conclusion that the maximum output power of an energy harvester occurs when the electrode covers the piezoelectric layer from the maximum strain area to a position where the strain is a half of the average strain in all the previously covered area. PEH prototypes were fabricated with segmented electrodes as shown in Figure 11B. It was claimed that with the optimal electrode coverage the output power can be respectively improved by 126% and 145% for a clamped-clamped beam and a cantilever PEHs.

*d*₁₅ Mode under Shear/Torsion Excitations

From the perspective of active materials, cantilever or other bending-type energy harvesters do not work in the optimal configuration. This is because the piezoelectric coefficient *d*₃₁ is relatively smaller than *d*₃₃ and *d*₁₅. For most piezoelectric materials, the order is *d*₁₅ > *d*₃₃ > *d*₃₁. Therefore, PEHs using the large *d*₁₅ coefficient have the potential to attain a greater efficiency. Zhao et al.⁹⁷ fabricated a cantilever PEH with two *d*₁₅-mode PZT plates ($13 \times 2.5 \times 1 \text{ mm}^3$) connected in series (Figure 12A). The cantilever prototype generated a maximum power of $8.7 \mu\text{W}$ under an excitation of 14.5 m s^{-2} . Bo et al.¹⁰⁰ induced shear deformation in a PMN-PT wafer on a cantilever beam. They considered the ratio of the lateral displacement to the length of the wafer, and neglected the effect of the shear force in the shear strain calculation process. The cantilever PEH with a $13 \times 6 \times 1 \text{ mm}^3$ PMN-PT element showed a maximum power of 4.16 mW under a cyclic force of 0.05 N .

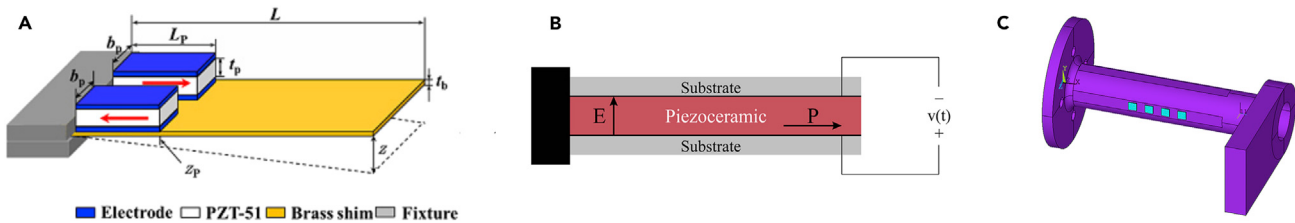


Figure 12. d_{15} Mode PEHs

(A) Cantilever PEH with two shear-mode piezoelectric elements. Reproduced from Zhao et al.⁹⁷ with permission from IOP Publishing Ltd.

(B) Vibrating sandwich beam with a piezoelectric core. Reproduced from Malakooti et al.⁹⁸ with permission from IOP Publishing Ltd.

(C) Shear-mode torsion energy harvester. Reproduced from Kulkarni et al.⁹⁹ with permission from IEEE.

In terms of modeling, Aladwani et al.¹⁰¹ developed a single degree of freedom (SDOF) model to analyze the shear-mode operation of piezoelectric materials. Malakooti and Sodano⁹⁸ developed a distributed-parameter model for a shear-mode cantilever energy harvester via the Timoshenko beam theory. As shown in Figure 12B, the desired shear deformation is formed in a vibrating sandwich beam with a piezoelectric core. The piezoelectric element is polarized in the axial direction and the induced electric field is perpendicular to the polarization in the thickness direction. The developed model estimated that the shear mode harvester subject to a harmonic base excitation is capable of generating ~50% more power compared with the equivalent cantilever bimorph harvester.

In addition to the bending excitations, torsional excitations have also been explored in d_{15} energy harvesters. Kulkarni et al.⁹⁹ presented a harvester (Figure 12C) consisting of a thin-walled tube with piezoelectric patches and an eccentric mass. The device was excited by vertical vibrations, and the eccentricity of the tip mass caused torsional stress in the tube. A prototype made of four PZT-5A shear-mode plates ($5 \times 5 \times 0.5 \text{ mm}^3$) generated a maximum root-mean-square (RMS) power of 0.57 mW under a harmonic excitation of 1 g at 620 Hz.

One should note that shear-mode PEHs face severe fabrication problems in spite of the high piezoelectric coefficient d_{15} . Complex polarization and electrode process are needed to fabricate d_{15} -mode piezoelectric elements.

New Structures Operating under Tension/Compression Excitations

Apart from cantilever and other bending-beam configurations, a variety of new structures have been developed to improve harvester performance based on the higher piezoelectric coefficient d_{33} and/or amplification effects.

Xu et al.¹⁰² presented a cantilever beam and cymbal transducer combined structure as shown in Figure 13A. Cymbal transducers have exhibited excellent performance in ultrasonic, actuation, and energy-harvesting applications,¹⁰⁵ but possess high resonant frequencies. This study combined the flexibility of cantilever beams and the force amplification of the cymbal structures in order to obtain high power output at a low frequency. A prototype, constructed with $25 \times 5 \times 1$ PMN-PT elements, a 35-mm copper cantilever, and a 4.2-g tip mass, generated a maximum power of 3.7 mW under a harmonic excitation of 3.2 g at 102 Hz. A similar structure was explored by Tufekcioglu and Dogan¹⁰⁶ under the same harmonic base excitations, and by Lee et al.¹⁰⁷ to harvest energy from flow-induced vibration.

In 2017, Zou et al.¹⁰³ explored a combined structure of cantilever and flexextensional transducers, and introduced a nonlinear magnetic force into the system. As shown in

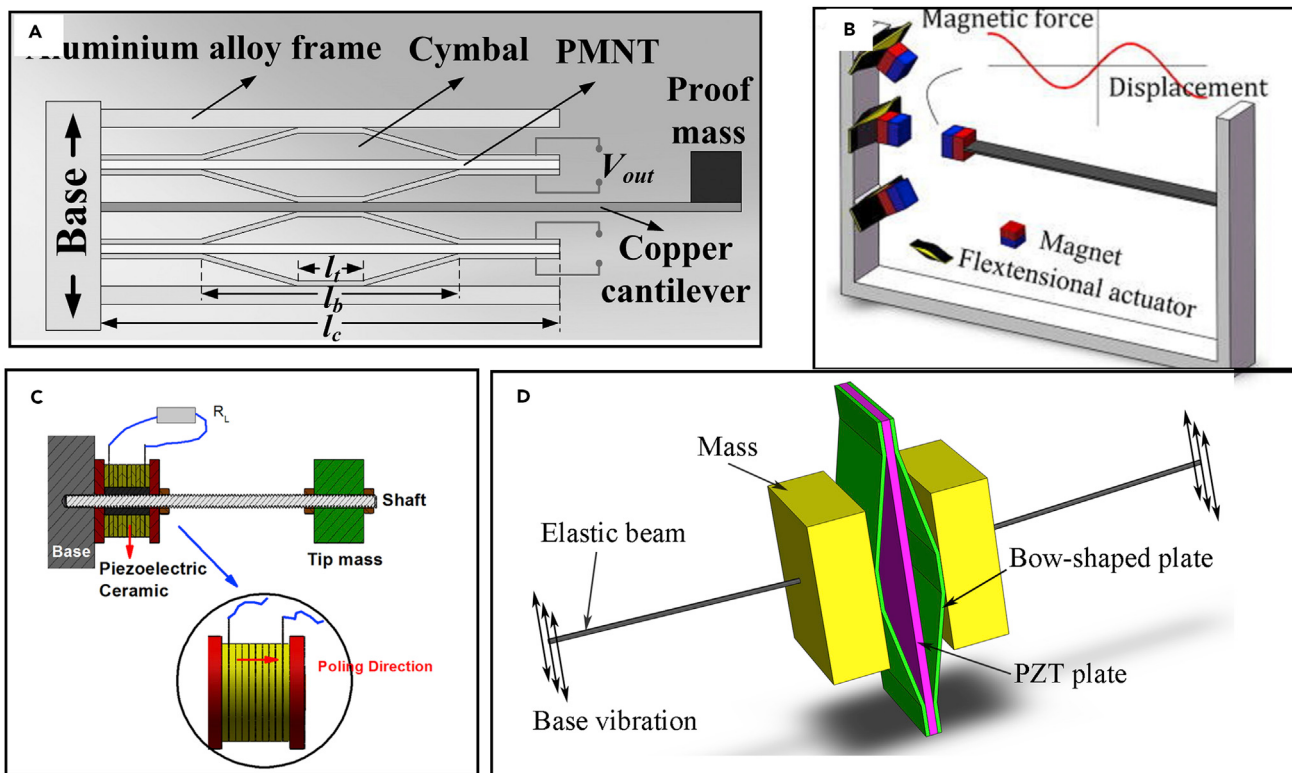


Figure 13. New PEHs Working in the Tension or Compression Mode

(A) A cantilever driving low-frequency PEH. Reproduced from Xu et al.¹⁰² with permission from AIP Publishing LLC.

(B) A nonlinear compressive-mode PEH with magnets. Reproduced from Zou et al.¹⁰³ with permission from AIP Publishing LLC.

(C) Barbell-shaped high-temperature PEH. Reproduced from Wu et al.¹⁰⁴ with permission from AIP Publishing LLC.

(D) High-performance compressive-mode piezoelectric energy harvester (HC-PEH). Reproduced from Yang et al.³⁹ with permission from Elsevier.

Figure 13B, the proposed harvester consists of a cantilever beam coupled with flexextensional transducers using magnets. The working bandwidth is significantly extended by the introduced nonlinear magnetic interaction. A prototype ($40 \times 10 \times 1 \text{ mm}^3$ PZT-5H) generated a maximum power of $387 \mu\text{W}$ under a harmonic excitation of 0.4 g at 9.9 Hz .

Wu et al.¹⁰⁴ developed a barbell-shaped PEH with the high-temperature piezoceramic $\text{BiScO}_3\text{-PbTiO}_3$. **Figure 13C** shows the barbell-shaped structure that also employs the cantilever configuration. The difference is that the piezoelectric element herein does not experience a bending stress (d_{31} mode) as in the traditional cantilever energy harvesters. In contrast, the piezoelectric stack works in the d_{33} mode, subject to the alternating normal force from the vibrating shaft. The structure was proposed to overcome the failure of the epoxy bounding layer and the piezoelectricity decay of conventional cantilever PEHs in high-temperature and large amplitude-vibration circumstances. A prototype was made of a ring piezo stack (inner diameter 8 mm; outer diameter 21 mm; thickness $\sim 20 \text{ mm}$), a 125-mm long steel shaft, and a tip mass of 100 g. The experimental data demonstrated that under a harmonic excitation with a peak-peak amplitude of 1 g, the prototype generated a maximum power of $4.76 \mu\text{W}$ at room temperature, and the power output was doubled in a high temperature range (150°C – 250°C). It was claimed that the structure could sustain large impacts and operate steadily in 100,000 vibration cycles.

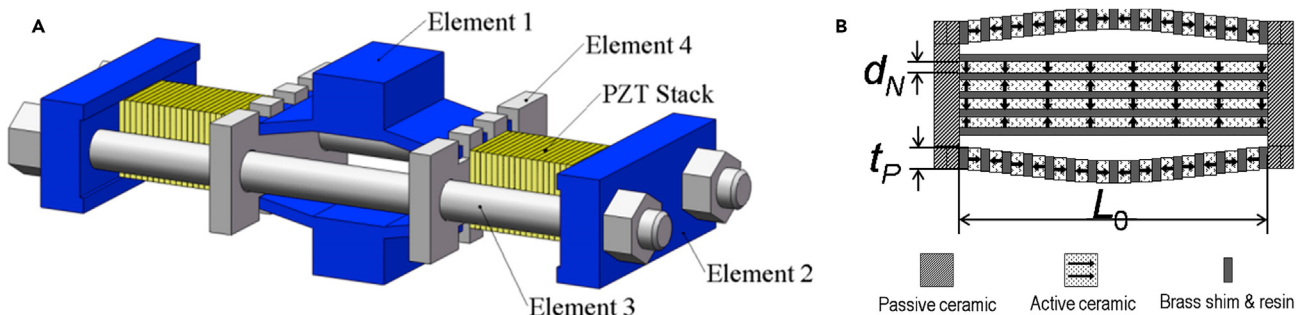


Figure 14. PEHs under Direct Force Excitations

(A) Stack-based flex-compressive PEH. Reproduced from Wang et al.¹¹³ with permission from IOP Publishing Ltd.
 (B) Bending and compressive hybrid PEH. Reproduced from Xu et al.¹¹⁴ with permission from AIP Publishing LLC.

Yang et al.^{39,40} developed a high-performance compressive-mode energy harvester by virtue of the low resonant frequency of doubly clamped beams and the amplification effect of the flexural motion. As Figure 13D shows, the proposed harvester consists of a pair of elastic beams, two mass blocks, two bow-shaped plates and a center piezoelectric plate. While working, the base vibration is first transferred through the elastic beams and absorbed by the mass blocks at the center. The vertical vibration of the center then induces tensile stress along the elastic beams. Following this, the beam motion causes the flexural deformation of the bow-shaped plates and results in a compressive stress in the center PZT plate. In the process, the excitation is amplified twice: first by the elastic beams and second by the bow-shaped plates. Due to the unique two-stage force amplification mechanism, the structure is able to generate substantial power even under weak excitations. Unlike most aforementioned harvesters, the proposed design works in the compressive mode where the piezoelectric elements only experience compressive stress. The compressive strength of PZT is claimed to be 10 times stronger than bending and tensile strengths. The compressive mode was therefore suggested for designing high-performance energy harvesters. A prototype was fabricated with a PZT-5H plate of $40 \times 15 \times 0.5 \text{ mm}^3$ and a mass of 100 g. Under a harmonic excitation with an amplitude of 0.3 g at 22.7 Hz, the prototype¹⁰⁸ produced a maximum power of 30 mW, corresponding to an average power of 15 mW.

In addition to base excitations, direct force excitations have also been investigated. Flexextensional transducers and stacks are the two most commonly used energy-harvesting structures under direct force excitations.^{109–112} To improve power output, Wang et al.¹¹³ proposed a flex-compressive PEH that can be sustained under heavy loads of thousands of newtons (Figure 14A). The bow-shaped center shell amplifies and transfers the applied load force to the symmetrically arranged piezoelectric stacks. Under a 4-Hz harmonic excitation with a 600-N amplitude, a maximum power output 17.8 mW was generated by a prototype (piezo stack: $20 \times 20 \times 36 \text{ mm}^3$). Xu et al.¹¹⁴ developed a hybrid PEH using the flexure force amplification mechanism (Figure 14B). The proposed structure resembles the conventional flexextensional transducer, but was modified with two outside curved piezo stacks. While a force is applied, the outside curved piezo stacks are compressed (d_{33}); by contrast, the center piezo stack is stretched (d_{31}). It is thus called a hybrid transducer system. A $35.5 \times 25 \times 10 \text{ mm}^3$ prototype generated 76.6 mW power under a direct normal force excitation of 15 N at 345 Hz, and a 26% energy conversion efficiency was claimed. The ultra-high power output and efficiency are mainly

contributed by the flexure force amplification mechanism and the fact that almost all inactive materials have been eliminated in the new designed structure.

New Piezoelectric Materials and Composites

Researchers have tried to improve energy harvester performance by fabricating new piezoelectric materials and composites. Morimoto et al.¹¹⁵ fabricated c-axis-oriented epitaxial PZT films on Pt/MgO substrates using the RF-magnetron sputtering technique, and transferred the films onto stainless-steel cantilevers for improved efficiency and toughness. Yeo et al.¹¹⁶ formed (001) textured PZT films on the both sides of a Ni foil by the RF-sputtering method with post annealing. Hwang et al.¹¹⁷ fabricated PZT films of 7 μm on flexible plastic substrates using the aerosol deposition method. Motivated by the extraordinarily high coupling factor and piezoelectric coefficients, single-crystal piezoelectric materials are being extensively used in energy harvesters. Xu et al.¹¹⁸ fabricated vertically aligned single-crystal PZT nanowire arrays at 230°C using the chemical epitaxial growth method. Tang et al.¹¹⁹ developed a bonding and thinning process and fabricated single-crystal PMN-PT thick films (10 μm) on silicon wafers to obtain a sufficiently powerful MEMS energy harvester. Yang and Zu²⁸ presented a systemic performance comparison between PMN-PT, PZN-PT, and PZT. Erturk et al.¹²⁰ firstly made performance analysis of single-crystal PMN-PZT unimorphs for piezoelectric energy harvesting, then Hwang et al.¹²¹ developed thin PMN-PT films for powering artificial pacemakers. Later, the same group adopted the solid-state single-crystal growth method for fabricating high-performance PMN-PZT films.¹²² Zeng et al.¹²³ developed a high-performance and stable PIMNT flake array on an ABS substrate. Xu et al.¹²⁴ synthesized high-performance and flexible nanocomposites by forming a unique hierarchical structure of PMN-PT nanowires in a PDMS base. The same group also presented a review of PMN-PT nanostructures for energy harvesting.¹²⁵ Chen et al.¹²⁶ presented micropatterned single-crystal PMN-PT ribbons for capturing both mechanical and thermal energy from the human body.

Performance Comparison

It is not straightforward to conduct a fair performance comparison on energy harvesters of different architecture, size, material, and operation mode. The difficulty in the performance comparison, on the one hand, is attributed to the lack of universal figures of merit, and on the other hand is caused by the fact that the amount of data disclosed in the literature varies considerably. Here, we review some figures of merit used to assess energy harvesters and compare high-performance harvesters proposed in the past decade.

The most commonly used metric for energy harvesters is power density, which is defined as power output over volume. However, it is not suitable to be used to compare different designs because the overall power output is not always strictly proportional to volume. The power output of inertial PEHs is related to mass (product of density and the cube of linear dimension) and the maximum displacement. Thus the averaged output power is proportional to volume^{4/3} (Marin et al.¹²⁷). Moreover, the definition of power density does not take into consideration the effect of the input excitation, which is extremely influential.

To include the excitation effect, Beeby et al.¹²⁸ proposed the figure of merit normalized power density (NPD). The NPD is the stated power output of the harvester normalized to the volume and the acceleration amplitude squared. Although the defined NPD is also not an ideal metric due to the lack of the frequency information, it presents an indication of relative performance levels. Note that here, volume can

refer to the volume of active materials or the overall volume of the system. Both calculation methods have drawbacks. The calculation only with the volume of active materials is biased and in favor of PEHs with small-size piezoelectric elements. The entire volume is not advised for use in the calculations because: (1) harvesters usually have irregular geometries; (2) the vibration amplitude varies considerably in the literature; (3) the accurate dimensions of most harvesters are not clearly documented; (4) at the system level, proper deployments, for example, those using rectification and storage circuits as the seismic mass block, significantly decrease the total volume. Considering these points, we calculated the NPD here based on the volume of active materials.

$$\text{NPD} = \frac{\text{Power}}{\text{Volume} \times \text{Acceleration}^2} \quad (\text{Equation 5.1})$$

Another widely adopted metric is efficiency, commonly defined as output electric energy over input mechanical energy. Despite of the agreement on the efficiency definition, the reported efficiency value in the literature varies considerably, as summarized by Yang et al.¹²⁹ Some¹³⁰ have claimed an efficiency value of over 80%; others¹³¹ reported an efficiency of less than 1%; yet others¹³² argued that efficiency can never exceed 50%. Yang et al.¹²⁹ presented a systematic analysis on efficiency and pointed out that the discrepancy is mainly caused by the different ways of calculating the input and output energy of inertial energy harvesters. It was found that in a vibrating energy-harvesting system, energy does not always flow in one direction from the excitation to the harvester, but also flows in reverse from the harvester to the excitation source, which is characterized by the phase difference (ϕ_x) between the external excitation and the system response. The experimentally validated efficiency expression was derived as

$$\eta = \frac{V_{\text{RMS}}^2 / R}{1/2 \times m \times (\ddot{X}_{\text{amp}}) \times (\dot{Z}_{\text{amp}}) \sin(\phi_x)}, \quad (\text{Equation 5.2})$$

where V_{RMS} , R , and m are the RMS voltage response, load resistance, and equivalent mass, respectively. X_{amp} denotes the amplitude of the response acceleration, and Z_{amp} denotes the amplitude of the excitation velocity. The authors found that the phase difference is always 90° for both linear systems and nonlinear systems around the resonant frequencies, i.e., no energy flows back to the excitation. Therefore, the efficiency calculation becomes much simpler at resonant states.

One should note that efficiency is not a comprehensive figure of merit for assessing harvester performance. It only measures the energy conversion ratio and does not reflect the size effect and the capability of trapping mechanical energy. High efficiency does not always mean high power output. An energy-harvesting system with a weak damping effect and a low-frequency excitation always exhibits a high efficiency value.

In addition to power density and efficiency, some complicated performance metrics have also been proposed, which take more parameters into consideration. Roundy¹³³ enhanced the concept of efficiency and proposed a new metric, named "effectiveness." The effectiveness considers the quality factor (Q), density (ρ), coupling coefficient (k), and transmission coefficient of energy harvesters (λ) and is defined by

$$e = k^2 Q^2 \frac{\rho}{\rho_0} \frac{\lambda}{\lambda_{\max}}. \quad (\text{Equation 5.3})$$

These parameters depend upon multiple operating conditions, and thus the operability of the defined “effectiveness” is poor. Mitcheson et al.¹⁹ developed the volume figure of merit (FoM_V) to reflect a harvester’s nearness to the performance limitation. The performance limit, i.e., the maximal available power was defined with respect to a benchmark equivalent cubic geometry (Vol), the density of gold (ρ_{Au}), and vibration frequency (w) and amplitude (Y_0), as:

$$\text{FoM}_V = \frac{\text{Useful Power Output}}{1/16 Y_0 \rho_{Au} Vol^{4/3} \omega^3}. \quad (\text{Equation 5.4})$$

A high power output is not the only goal pursued in energy harvesters. A wide working bandwidth has also been examined to ensure the environmental adaptability and reliability. Conditions to attain these two goals most of time are not aligned with each other. To increase power output, one usually tries to minimize the mechanical damping effect of inertial energy harvesters, but this entails the penalty of reduced working bandwidth. To indicate both bandwidth and power output comprehensively, Mitcheson et al.¹⁹ took one step further and proposed a bandwidth figure of merit, which is defined as the product of FoM_V and the fractional bandwidth ($\Delta w/w_n$).

Liu et al.¹³⁴ also proposed a universal metric considering both bandwidth and output power. The proposed systematic figure of merit with bandwidth information (SFoM_{BW}) for wideband PEHs is related to an averaged FoM_V, mechanical damping, density, and the fractional bandwidth. In essence, the SFoM_{BW} reflects the product of the average NPD and bandwidth.

Problems exist in the application of these complicated new figures of merit. First, all of them are derived based on the assumption or approximation of linear SDOF systems. Thus, they do not possess universality for nonlinear energy harvesters. In addition, there is no consensus on the bandwidth definition for nonlinear PEHs. For a linear vibration system, we usually use the classic definition of the 3-dB bandwidth, i.e., frequency points at which a half the maximum power is produced. Nonlinear systems have more than one stable solution over a portion of the bandwidth. The system may jump among these solutions. Also, different from linear systems, the maximum point may not occur at the center of the defined bandwidth, but at one of its extremes. Liu et al.¹³⁴ defined the bandwidth as the frequency range from the upper limit of the forward/backward frequency-sweep case to the lower limit of the opposite-direction frequency-sweep case for typical hardening/softening Duffing system. Cammarano et al.¹³⁵ analyzed the response characteristics of nonlinear PEHs and proposed to limit bandwidth to the region where only one stable solution exists. More practically, some articles reported the bandwidth as the frequency range above a certain power output level.^{40,136}

Overall, we have witnessed many attempts to redefine or develop new figures of merit that can be used to evaluate harvesters’ performance comprehensively. There is no consensus among researchers on a universal metric. The performance of energy harvesters is highly dependent on the operation conditions, dimensions, materials, and circuits employed. Different energy harvesters are developed for operation under different vibration conditions. It is inappropriate and impractical to compare various designs and approaches with one benchmark. Besides, it is very common that a publication does not present enough data to calculate a complex performance metric. We believe the most suitable standard for assessing energy harvesters is whether a proposed design meets the requirements of the targeted application under the specific constraints. Hence, parameters important to end users, such as

Table 2. Performance Comparison of State-of-the-Art Inertial Energy Harvesters: MEMS Scale

| Ref. | Material | Excitation Amplitude; g = 9.8 m s ⁻² | Frequency (Hz) | Piezo Size (mm ³ × number) | Mass (g) | RMS Power (μW) | Power Density (mW cm ⁻³) | NPD (kg m ⁻³ × 10 ³) | Note |
|-------------------------------------|----------|---|----------------|---------------------------------------|--------------------------|----------------|--------------------------------------|---|----------------------------------|
| Lee et al. ¹³⁷ 2009 | PZT | 2.5 g | 255.9 | 3 × 1.5 × 0.005 | 0.873 × 10 ⁻³ | 1.38 | 61.3 | 0.102 | aerosol PZT |
| Shen et al. ¹³⁸ 2009 | PZT | 0.75 g | 183.8 | 3.2 × 0.4 × 0.001 | – | 0.32 | 250 | 4.627 | sol-gel PZT |
| Park et al. ¹³⁹ 2010 | PZT | 0.39 g | 528 | 1 × 0.8 × 0.001 | 1.22 × 10 ⁻³ | 1.1 | 1.375 × 10 ³ | 94.1 | d ₃₃ mode |
| Morimoto et al. ¹¹⁵ 2010 | PZT | 0.51 g | 126 | 18.5 × 5 × 0.0028 | – | 5.3 | 20.46 | 0.818 | c axis-oriented epitaxial PZT |
| Tang et al. ¹⁴⁰ 2012 | PZT | 1.0 g | 514.1 | 3 × 0.8 × 0.031 | 2.89 × 10 ⁻³ | 11.56 | 155 | 1.61 | thinned buck PZT |
| Tang et al. ¹¹⁹ 2014 | PMN-PT | 1.5 g | 406 | 7.4 × 2 × 0.01 | 0.84 × 10 ⁻³ | 7.18 | 97 | 0.449 | d ₃₃ mode |
| Minh le et al. ¹⁴¹ 2015 | AlN | 0.816 g | 792 | 1 × 0.21 × 0.002 | 0.26 × 10 ⁻³ | 1.3 | 5.42 × 10 ³ | 84.7 | MgZr co-doped AlN |
| Tang et al. ¹⁴² 2016 | PZT | 3.0 g | 100.8 | 11 × 5 × 0.057 | ~0.12 | 321 | 102.4 | 0.118 | bronze substrate |
| Yeo et al. ¹¹⁶ 2016 | PZT | 0.16 g | 6 | 20 × 10 × 0.003*2 | – | 284 | 236.7 | 96.27 | 001 textured compliant structure |
| Song et al. ¹⁴³ 2017 | PZT | 0.25 g | 68 | 0.11 | 4.9 × 10 ⁻⁴ | 0.023 | 0.209 | 0.035 | MEMS; spiral shape |

power output, frequency, volume, and input excitation, should be demonstrated clearly. Meanwhile, the NPD and efficiency are recommended for the purpose of performance comparison. They are not universal metrics but can be easily calculated and present, on the basis of fundamental considerations, some knowledge of performance level.

Table 2 and **Table 3** summarize the main features of some high-performance vibration energy harvesters reported in the last 10 years. For each harvester, the table lists bibliography references, material characteristics, excitation properties, harvester sizes, output power, power density, NPD, and eventual additional notes. We intend to but are unable to assess efficiency here because of the lack of information of mechanical responses in most publications. Only papers including experimental data are listed in the tables.

As can be seen from the tables, the proposed energy-harvesting systems are heterogeneous. The output power is from hundreds of nanowatts to tens of milliwatts. The optimal working frequency ranges from 2.7 Hz to 853 Hz. Most MEMS energy harvesters show higher working frequency and power density, but much lower output power than mesoscale energy harvesters.

Applications

PEHs have been explored in a variety of fields in the past decade, including wearable devices, medical implants, vehicles, and wireless sensor networks. Here we mainly review four specific most widely studied applications: shoes, pacemakers, tire pressure monitoring system (TPMS), and building and bridge monitoring systems. In each application, we discuss the excitation sources, analyze state-of-the-art harvesters, and identify existing problems and future directions. In addition to the

Table 3. Performance Comparison of State-of-the-Art Inertial Energy Harvesters: Mesoscale

| Ref. | Material | Excitation Amplitude; g = 9.8 ms ⁻² | Frequency (Hz) | Piezo Size (mm ³ × number) | Mass (g) | RMS Power | Power Density (mW cm ⁻³) | NPD (kg m ⁻³ × 10 ³) | Note |
|--|-------------|--|----------------|---------------------------------------|--------------------------|-----------|--------------------------------------|---|--|
| Dai et al. ¹⁴⁴ 2009 | PZT-5H | 1 g | 51 | 12 × 10 × 1 | – | 1.055 mW | 8.79 | 0.0915 | terfenol-D/PZT composite |
| Kim et al. ¹⁴⁵ 2010 | PZT-5A | 0.255 g | 109.5 | 53 × 31.7 × 0.275*2 | – | ~0.53 mW | 0.57 | 0.091 | |
| Liang and Liao ¹⁴⁶ 2010 | PZT-5A | 1.44 g | 42 | 49 × 24 × 0.5 | | 2.5 mW | 4.25 | 0.02 | impedance matching circuit |
| Gu ¹⁴⁷ 2011 | PZT-5A | 0.4 g | 20.1Hz | 26 × 6.4 × 0.5*2 | 8 | 1.08 mW | 9.01 | 0.59 | low-frequency impact |
| Li et al. ¹⁴⁸ 2011 | Piezo stack | 1 g | 87 | 3141 | – | 14.6 mW | 4.65 | 0.05 | compressive mode |
| Yen et al. ¹⁴⁹ 2011 | AlN | 1.0 g | 853 | ~0.4 × 0.25 × 0.002*2 | 0.317 × 10 ⁻³ | 4.9 nW | 12.25 | 0.127 | corrugated cantilever; bimorph |
| Xu et al. ¹⁰² 2012 | PMN-PT | 3.2 g | 102 | 25 × 5 × 1*2 | 4.2 | 1.85 mW | 7.4 | 7.5 × 10 ⁻³ | flextensional transducer |
| Zhao et al. ⁹⁷ 2012 | PZT | 1.48 g | 73 | 13 × 2.5 × 1*2 | – | 8.7 μW | 0.134 | 0.64 × 10 ⁻³ | d ₁₅ mode |
| Tang and Yang ³⁸ 2012 | MFC | 0.29 g | 27.8 | 28 × 7 × 0.3 | 5.9 | 1.43 mW | 24.32 | 3.04 | piezo fiber composite |
| Dhakar et al. ¹⁵⁰ 2013 | PZT-5A | 0.2 g | 36 | 31.9 × 6.4 × 0.5 | 0.72 | 40 μW | 0.392 | 0.102 | composite cantilever |
| Wu et al. ¹⁵¹ 2013 | MFC | 0.1 g | 18 | 36 × 16 × 0.3*3 | 21.4 | ~0.75 mW | 1.45 | 1.45 | two degrees of freedom |
| Arrieta et al. ¹⁵² 2013 | PZT | 0.25 g | ~20 | 46 × 20.6 × 0.25*2 | | 7.07 mW | 14.9 | 2.49 | piezo QuickPack |
| Qiu et al. ¹⁵³ 2014 | PZT | 0.6 g | 38 | 12 × 6 × 1 | – | 0.39 mW | 5.4 | 0.1567 | magnet/PZT composite |
| Ma et al. ¹⁵⁴ 2014 | PZT-5H | 0.2 g | 93 | 30 × 3 × 3 | 5.4 | 3.18 μW | 0.012 | 2.94 × 10 ⁻³ | perpendicular electrodes |
| Zhang et al. ¹⁵⁵ 2014 | PZT | 0.29 g | 2.71 | 50 × 30 × 0.2*2 | ~282.6 | 7.7 mW | 12.83 | 1.59 | low frequency; multi-impact |
| Xiao et al. ¹⁵⁶ 2014 | PZT | 1 g | 225 | Φ25 × 0.2*4 | 198 | 10 mW | 25.48 | 0.265 | circular diaphragm array |
| Tufekcioglu and Dogan ¹⁰⁶ 2014 | PZT 5H | 2 g | 153 | Φ12.7 × 1*2 | 0.34 | 0.14 mW | 0.55 | 1.44 × 10 ⁻³ | |
| Kulkarni et al. ⁹⁹ 2014 | PZT-5A | 1 g | 620 | 5 × 5 × 0.5*4 | 106 | 0.57 mW | 11.4 | 0.119 | d ₁₅ mode; torsion excitation |
| Hung et al. ¹⁵⁷ 2015 | PZT | 3.5 g | 75 | 4 × 3.5 × 1*4 | 7.8 | 0.239 μW | 4.27 × 10 ⁻³ | 3.64 × 10 ⁻⁶ | three-axis energy harvester |
| 2015 Singh et al. ¹⁵⁸ | PZT | 4.6 g | 90 | 35 × 16.8 × 0.2 | – | 385 μW | 3.27 | 1.61 × 10 ⁻³ | bistable with the SSHI circuit |
| Sriramdas et al. ¹⁵⁹ 2015 | PVDF | 0.5 g | 30.8 | 108 | 0.63 | 8.59 μW | 0.079 | 3.3 × 10 ⁻³ | multistep and multilayer beam |
| Gong et al. ¹⁶⁰ 2015 | PZT | 0.7 g | 120.9 | 31 × 13.6 × 0.22*2 | ~23 | 6.64 mW | 35.8 | 0.760 | folded beam |
| Yang and Zu ²⁸ 2016 | PZN-PT | 0.3 g | 37.5 | 10 × 7.2 × 0.4 | 2.61 | 0.43 mW | 14.93 | 1.727 | |

(Continued on next page)

Table 3. Continued

| Ref. | Material | Excitation Amplitude; g = 9.8 ms ⁻² | Frequency (Hz) | Piezo Size (mm ³ × number) | Mass (g) | RMS Power | Power Density (mW cm ⁻³) | NPD (kg m ⁻³ × 10 ³) | Note |
|----------------------------------|-------------|--|----------------|---------------------------------------|----------|-----------|--------------------------------------|---|---|
| Wu et al. ¹⁰⁴ 2016 | Piezo stack | 0.5 g | 56 | 5918.9 | 100 | 4.76 μW | 0.804 × 10 ⁻³ | 0.033 × 10 ⁻³ | high-temperature BiScO ₃ -PbTiO ₃ |
| Yi et al. ¹⁶¹ 2017 | PZT | 3.5 g | 77.2 | 16 × 3 × 0.053 16 × 3 × 0.076 | 0.433 | 0.979 mW | 158 | 0.134 | beryllium-bronze substrate |
| Zou et al. ¹⁰³ 2017 | PZT-5H | 0.4 g | 9.9 | 40 × 10 × 1 | ~14.8 | 194 μW | 0.485 | 0.032 | compressive mode; magnet |
| He and Jiang ¹⁶² 2017 | PZT-4 | 1 g | 66.7 | 15 × 10 × 0.2 | ~6.84 | 2.35 mW | 78 | 0.812 | multi-mode chiral structure |
| Yang et al. ⁹⁰ 2017 | PZT-5H | 0.3 g | 44 | 241 | 6.34 | 1.27 mW | 5.27 | 0.610 | arc-shaped |
| Yang et al. ¹⁰⁸ 2017 | PZT-5H | 0.3 g | 22.7 | 40 × 15 × 0.5 | 100 | 15 mW | 50 | 5.78 | compressive mode |

aforementioned main applications, energy harvesters have also been explored in rain,^{163–166} pavement,¹⁶⁷ gunfire munitions,¹⁶⁸ cutting tools,¹⁶⁹ and wildlife,^{170,171} which are not covered here.

Shoes

The human body consumes a considerable amount of energy every day to perform different tasks such as speaking, eating, breathing, walking, arm lifting, and finger tapping. However, not all the kinetic energy and strain energy can be used for energy harvesters. The design of wearable energy harvesters for human motions follows the rule that the addition of the energy harvester does not interfere with normal activities or significantly alter appearance. Also, harvesters should not significantly increase the metabolic cost. Therefore, it is necessary to analyze the energy flow in body motions and figure out how much energy is available for the purpose of energy harvesting.

It is known that muscles do both positive and negative work within each motion. Positive work is done by muscles during shortening contractions whereby the torque acted by the muscles at a joint applies in the same direction as the angular velocity of the joint; Negative work is done by muscles during lengthening contractions whereby the torque applied by the muscles at a joint acts in the direction opposite to the angular velocity of the joint.^{172,173} In each motion phase, muscles work actively to generate intended motion, and they also absorb energy like brakes, i.e., negative work. The absorbed energy most of time cannot be reused but is wasted as heat.¹⁷⁴ Additionally, muscle cells usually need to do extra work to dissipate this negative work. An energy-harvesting system can be used to facilitate muscles during the negative work phase, retarding the motion, similar to a “regenerative brake” in cars. Apart from the function of dissipating the negative work, energy harvesters can also supply electricity to wearable and implantable electronic devices.

It is important to know how much energy we can harness from human body motions. Researchers have evaluated energy associated with different body motions^{175,176} under different assumptions, such as finger typing (~19 mW), breathing (~1 W), arm lifting (~60 W), and walking (~67 W). Table 4 lists available energy associated

Table 4. Available Energy in Different Human Motions for Energy Harvesters

| Joint | Work (J per Step) | % Negative Work |
|----------|-------------------|-----------------|
| ' | 1–5 | 50 |
| Ankle | 34.4 | 28.3 |
| Knee | 18.2 | 92 |
| Hip | 18.96 | 19 |
| Elbow | 1.07 | 37 |
| Shoulder | 1.1 | 61 |

Data from Riemer and Shapiro.¹⁷⁷

with different human motions for energy harvesters. Among all body motions, walking is one of the most common and energy-intensive motion. In 2011, Riemer and Shapiro¹⁷⁷ analyzed the energy consumption by muscles at each joint or segment of a body during walking. They considered an 80-kg person walking at a frequency of 1 Hz. As listed in Table 3, on average more than 1 J of energy can be harvested per step in each joint, which means over 1 W power is available for energy harvesters. Recently, Partridge et al. assumed a 10-mm deflection in shoes while walking, and estimated that the harvestable energy from shoes is 6.6 J/step on level ground, 7.47 J/step while going downstairs, and 3.12 J/step while going upstairs.¹⁷⁸

There are mainly two methods that have been explored to harvest energy from human motions: the piezoelectric effect and electromagnetic effect. The electromagnetic method is a mature technology and has been studied for decades. To obtain satisfactory power output, the input linear motions or oscillations need to be converted to high-speed rotational motions. Therefore, large-amplitude motions like knee bending and arm swing are best treated by electromagnetic energy harvesters. Compared with the electromagnetic method, harvesters using the piezoelectric effect can be designed as flexible with a smaller deformation requirement. They are thus easier to be integrated into shoes without interfering with the gait. A variety of energy harvesters have been proposed and embedded in shoes using either the electromagnetic effect^{179–181} or the piezoelectric effect. Here we mainly analyze energy harvesters in shoes using the piezoelectric effect. Only studies with experimental data are reviewed.

Harvestable energy in shoes comes mainly in three forms of excitations: the relative motion between foot and ground (deformation), the swing motion in each gait (acceleration), and the bending of the shoe sole (stretching). A variety of designs have been proposed to generate electricity by harvesting energy from one excitation or more excitations combined.

One well-known pioneering work came from the MIT Media lab¹⁸² in 2001. Although we only intend to review research in the past decade here, we cannot avoid mentioning the importance of this instructive research. Figure 15 shows the schematic of the proposed two methods. One approach is to capture energy from the process of bending the ball of the foot, using a flexible bimorph made of multi-laminar PVDF films. The other approach is to harness heel strike energy by a sandwiched curve structure, called a "dimorph." As shown in Figure 15, the dimorph consists of a beryllium-copper plate sandwiched by a pair of curved PZT-spring steel composite thin plates. For the PVDF harvester, an average power of 1.3 mW was generated at a walking pace of 0.9 Hz. Under the same excitation, the PZT harvester

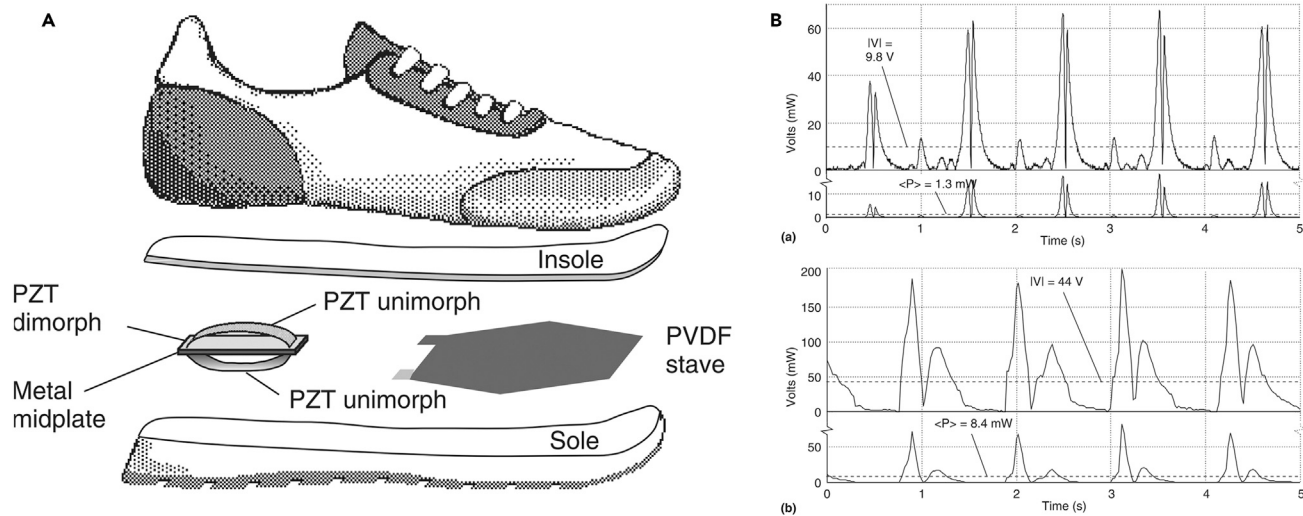


Figure 15. Shoes Energy Harvester from the MIT Media Lab

(A) Schematic.

(B) Power responses from brisk-walking tests with PVDF stave and PZT dimorph.

Reproduced from Shenck et al.¹⁸² with permission from IEEE.

generated 8.4 mW on average. The peak voltage and power can be as high as 200 V and over 50 mW, respectively. The fabricated prototype demonstrated its ability to intermittently power an active radiofrequency (RF) tag. The successful demonstration is extremely encouraging, and along with the booming wearable technologies has stimulated much research in the following years.

PEHs have been exploited to harness energy from acceleration exactions in shoes. In 2010, Moro and Benasciutti¹⁸³ carefully analyzed the characteristics of the accelerations on the heel during walking, and designed a cantilever energy harvester using piezoceramics. One main contribution of this work is that they correlated the heel acceleration data from the literature with direct experimental measurements (see Figure 16B), and quantitatively defined a standard acceleration signal. The defined excitation signal is useful in guiding other endeavors to harvest energy from heel accelerations. As shown in Figure 16B, in each gait cycle we observe an acceleration peak (6–6.5 g) instantaneously at the initial contact phase. Following that is the stance phase, which continues for about 60% of the cycle period, during which time the acceleration increases smoothly. Then in the final swing phase the acceleration along the tibial axis experiences a large oscillation. To validate the proposed energy-harvesting method and analytical model, the authors fabricated a prototype and tested it with different parameters. Figure 16A illustrates the PZT-5A bimorph ($20 \times 14 \times 0.3 \text{ mm}^3$) mounted inside the shoe heel. The tip mass was varied from 5.5 g to 16.4 g, resulting in a range of the first resonant frequency of 20–150 Hz. Excited by the acceleration in the tibial direction, the prototype achieved a maximum mean power of 0.395 mW per footstep. This work demonstrates that it is feasible to acquire on the order of 1 mW of power from heel accelerations in one direction.

Accelerations in a shoe are not always in one direction, but may vary in multiple directions. Therefore, a multi-directional harvester is expected to generate more energy. In 2017, Fan et al. proposed a composite configuration to capture vibration energy not only from the tibia direction, but also from the tangential direction of the swing motion and the sole compression. Figure 16C shows the schematic. The PEH

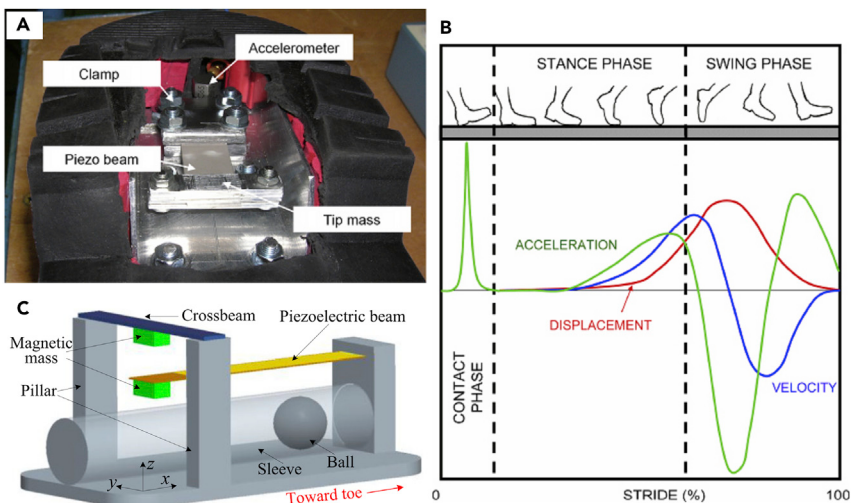


Figure 16. Devices to Harness Energy from Acceleration Exactions in Shoes

(A) Shoe-mounted piezoelectric cantilevers. Reproduced from Moro et al.¹⁸³ with permission from IOP Publishing Ltd.

(B) Displacement, velocity, and acceleration waveforms of heel over one stride. Reproduced from Moro et al.¹⁸³ with permission from IOP Publishing Ltd.

(C) Multi-directional energy harvesting. Reproduced from Fan et al.¹⁸⁴ with permission from AIP Publishing LLC.

consists of a piezoelectric cantilever beam magnetically coupled to a ferromagnetic ball and a crossbeam. The main cantilever is made of a brass substructure of $23.1 \times 7.3 \times 0.05 \text{ mm}^3$ and a PZT-5H beam of $19.1 \times 7.1 \times 0.245 \text{ mm}^3$. A steel ball of diameter (Φ) 7 mm was encapsulated in a 34-mm long polycarbonate sleeve to harvest energy from the swing motion. A cylindrical NdFeB magnet ($\Phi 3 \times 2 \text{ mm}^3$) was fixed at the free end of the cantilever, coupled with a magnet ($\Phi 5 \times 2 \text{ mm}^3$) on the fixed crossbeam. The crossbeam was connected with the insole, and was able to move up and down while walking with the help of two springs inserted in the supporting pillars. The structure was proposed to harvest energy from three directions simultaneously, but these acceleration excitations may hold a certain phase difference that causes mutual cancellation. The experiments indicated that the prototype generated 0.03–0.35 mW at the walking speed ranging from 2 km hr^{-1} to 8 km hr^{-1} .

Overall, acceleration excitations in shoes are characterized with low frequency, large amplitude, and multiple directions. Inertial PEHs generated <1 mW power from the acceleration exactions. The relatively low power output is mainly attributed to the low-input mechanical energy. Because it is not permitted to design a heavy inertial mass in a shoe-inserted inertial energy harvester, we can only capture very limited kinetic energy. Future work may explore new amplification methods to capture more inertial energy.

Compared with the acceleration excitations, deformation and stretching excitations hold more energy and are easier to be harnessed. Although the allowed deformation in a shoe is very limited, the effective load force from a body weight is at the level of several hundred newtons, which have stimulated researchers to develop a variety of strain-based harvesters.^{185,186}

For harvesting the deformation energy, PVDF films are the ideal candidates due to their outstanding flexibility. PVDF films have been widely explored in many groups

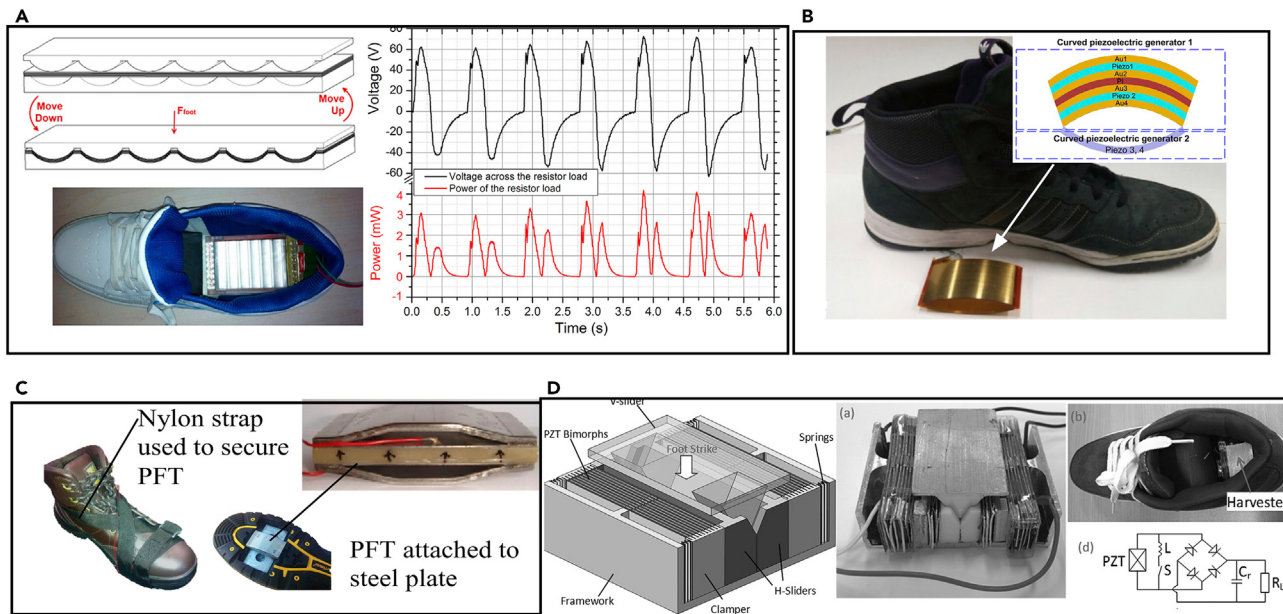


Figure 17. Devices to Harness Energy from Deformation and Stretching Excitations in Shoes

(A) PVDF wavy surfaces and the electrical responses under strike. Reproduced from Zhao et al.¹⁸⁹ with permission from MDPI AG.

(B) Curved PVDF stack. Reproduced from Jung et al.¹⁹⁰ with permission from Elsevier.

(C) PZT flex transducer. Reproduced from Daniels et al.¹⁹¹ with permission from IOP Publishing Ltd.

(D) PZT with an amplification mechanism. Reproduced from Xie et al.¹⁹² with permission from AIP Publishing LLC.

successively.^{187,188} In 2014, Zhao and You¹⁸⁹ developed a 1-mW shoe-embedded PVDF energy harvester. In the design, to attain a high power output the authors stacked eight layers of PVDF films together and sandwiched them between two wavy surfaces. As shown in Figure 17A, the stacked PVDF film ($50 \times 80 \text{ mm}^2$) was fixed on the lower plate at both ends, and the upper movable plate was activated by the foot. Once the upper plate was moved down, the PVDF film would be stretched and fit in the wavy surface. Figure 17A shows the irregular response curves of the prototype. Under brisk walking at $\sim 1 \text{ Hz}$, the prototype generated a peak-to-peak voltage of 136 V, a peak power of 4 mW, and an average power of 1 mW.

Instead of the flat pattern, PVDF has also been made in curved shapes. In 2015, Jung et al.¹⁹⁰ proposed a curved PVDF energy harvester, which was claimed to be able to light up 476 LEDs. Figure 17B illustrates the proposed energy harvester. Two 0.1-mm thick PVDF films were attached on each side of an arc-shaped polyimide (PI) (0.2 mm thick) substrate. A pair of such arc PVDF-PI composites were assembled together back to back. In the design, PVDF films experience bending stress without stretching when a load is applied on the harvester. A prototype, fabricated with four $70 \times 40 \text{ mm}^2$ PVDF films, generated an averaged open-circuit voltage of $\sim 25 \text{ V}$ and an averaged short-circuit current of $\sim 20 \mu\text{A}$, during walking at 0.5 Hz. The high performance is contributed by the large surface area (multiple layers) and high bending stress (curved structure). Theoretically, the electromechanical coupling effect of PVDF films is over 10 times weaker than that of PZT ceramics. PZT ceramics thus have a greater potential than PVDF films to generate more power from deformation and stretching in shoes. In 2013, Daniels et al.¹⁹¹ used a rectangular flexextensional transducer to harvest energy from the relative motion between foot and ground during walking (Figure 17C). The flexextensional end caps amplify the downward applied force and also protect the sandwiched piezo elements from impacts. To withstand

Table 5. Power Requirements of Different Medical Implants

| Device | Power Requirement |
|-------------------------------------|-------------------|
| Pacemaker ^{196,197} | 5–10 µW |
| Cochlear implant ^{198,199} | 100–2,000 µW |
| Drug pump ²⁰⁰ | 400 µW |
| Retinal stimulator ²⁰¹ | 250 mW |
| Neural recording ²⁰² | 1–10 mW |

the nearly 1-kN force, the piezoceramic ($52 \times 30 \times 4 \text{ mm}^3$) is covered by a pair of steel plates. The harvester prototype was placed under the sole of a boot. It generated an averaged power of 2.5 mW under 760 N at 1.4 Hz, and was able to power a wireless sensor module independently.

In 2014, Xie and Cai¹⁹² proposed a novel structure, consisting of an amplification mechanism and a stack of piezoceramic bimorphs, as shown in Figure 17D. A foot strike applies an impact force on the V-shaped slider in the vertical direction and then causes a movement of the symmetric H-shaped sliders in the horizontal direction. The horizontal movement deforms the bimorphs with one end fixed at the center and the other end inserted in comb-like clamps. The bimorphs are symmetrically deformed and an electrical potential is formed over the PZT elements. The symmetric in-phase deformation in all piezoelectric elements provides substantial convenience to the conditioning circuits that follow. The harvester has four springs that connect the static framework and two clamps to restore the V-shaped slider. A prototype, 105 g in total, was fabricated with 20 PZT-5H bimorphs ($30 \times 15 \times 0.2 \text{ mm}^3$). The prototype was embedded in the heel of a shoe and excited by a user of 68 kg. The maximum RMS power is 18.6 mW at 1 Hz (regular walking pace), and the corresponding power density over the whole volume is about 0.41 mW cm^{-3} , which is higher than that in some electromagnetic harvesters.^{180,193}

Overall current energy harvesters can generate tens of milliwatts of power from shoes. Research is being conducted to further improve the efficiency and power density of energy harvesters, and at the same time explore new applications of the shoe-inserted energy harvesters.

Pacemakers

The wide diffusion of implantable medical devices has been raising the quality of life and life expectancy. Take the artificial pacemaker, for example; it has saved over 3 million lives to date, and every year 600,000 new pacemakers are implanted in patients.¹⁹⁴ Ideally, implantable electronic devices are expected to work automatically inside bodies for years without maintenance. However, the commonly used electrochemical batteries cannot constantly supply power for long enough. It is therefore pressing to find practical methods to increase the energy density and lifespan of power sources. By harnessing energy from the nonstop body motions, energy harvesters supply a perpetual approach to achieve lifelong autonomous operations of medical implants.

Powering medical implants by harvesting a small part of energy from body motions without any side effects is a true possibility. To secure years of autonomous operations, low power consumption has become one of the most critical requirements for the design of biomedical implants.^{195,196} As microelectronics develop rapidly, implantable devices require increasingly less energy. Table 5 lists the power consumptions of five medical implants. Most of them require power less than 1 mW,

and the artificial cardiac pacemaker only consumes 5–10 mW. The required micro-watt-level power is trivial compared with the rich mechanical energy associated with body motions.

The artificial cardiac pacemaker is an intriguing application for energy harvesters and has attracted much attention from both the engineering and medical fields. The longevity of pacemakers is mainly decided by the battery lifespan. Currently pacemakers are powered by lithium-iodine cells, which theoretically can support pacemakers to operate uninterruptedly for up to 10 years. However, the lifespan of a pacemaker depends upon the frequency of use, and is usually less than 7 years, which is not satisfactory especially for the increasing number of young patients (as young as 2 years old). Also, new functions, such as biventricular pacing (three electrodes), consume more energy than current pacemakers (one electrode). Energy harvesters hold great potential to prolong the lifespan of pacemakers and supply extra power for new functions.

Design of energy harvesters for pacemakers is much more challenging than that for industrial applications because of the very limited space, which is typically less than 1 cm³. Furthermore, human motion is most of the time in a low frequency range under 10 Hz. As a rule of thumb, the smaller the size of the harvester, the higher will be the resonant frequency. This means we have to develop a compact energy-harvesting system that can work under ultra-low-frequency excitations with an ultra-high efficiency. Both the electromagnetic effect and piezoelectric effect have been explored to harvest energy for pacemakers. The mass imbalance oscillation generator in automatic wristwatches has been tested, and generated a power of 16.7 µW from the cardiac wall motion of a sheep.²⁰³ Due to the very limited space, PEHs are supposed to show better performance than electromagnetic counterparts.⁸ Here we mainly review recent research on powering pacemakers using PEHs.

There are mainly three excitation sources that have been studied for energy harvesters in pacemakers: heart beats, blood pressure gradients, and arterial wall deformation. The cyclic heart beat causes vibration and deformation of the myocardium at a frequency of 1–3 Hz.²⁰⁴ The frequency depends on a person's activity and morphology. The induced strain on the myocardium is 15%–23% in the radial direction and 9%–12% in the circumferential direction.²⁰⁵ The blood pressure gradient, in a healthy body, varies with an amplitude of about 20–100 mmHg (2.7–13.3 kPa) in right and left ventricles, and about 40 mmHg (5.3 kPa) in the arterial system.^{204,206} For arterial wall deformation, Länne et al.²⁰⁷ reported that the diameter of the distal abdominal aorta varies between 15.8 mm (blood pressure 118 mmHg) and 17.3 mm (blood pressure 64 mmHg) at a heart rate of 66 beats per minute. The diameter variation of the carotid artery is about 10% between the diastolic and systolic period.²⁰⁸ The human brachial artery experiences a diameter distension of 3.7%.²⁰⁸ Blood flow is also a possible energy source for energy harvesters. However, concerns such as the blood cell damage from rotating blades and the risk of vortex-induced thrombi impede research endeavors on flow-based energy harvesters for pacemakers.

We now review energy harvesters that use the heart motions. In early 2011, Inman's group^{209,210} started to explore the possibility of utilizing the heartbeat-induced vibration energy inside the chest to power pacemakers. A battery roughly occupies two-thirds of the volume of a pacemaker (~42 × 51 × 6 mm³ of Biotronik's device), and thus an inserted harvester should not be designed to be larger than the battery volume. Within such a small space and restricted weight, linear PEHs will have resonant frequencies much higher than that of the heartbeat excitation. To lower the

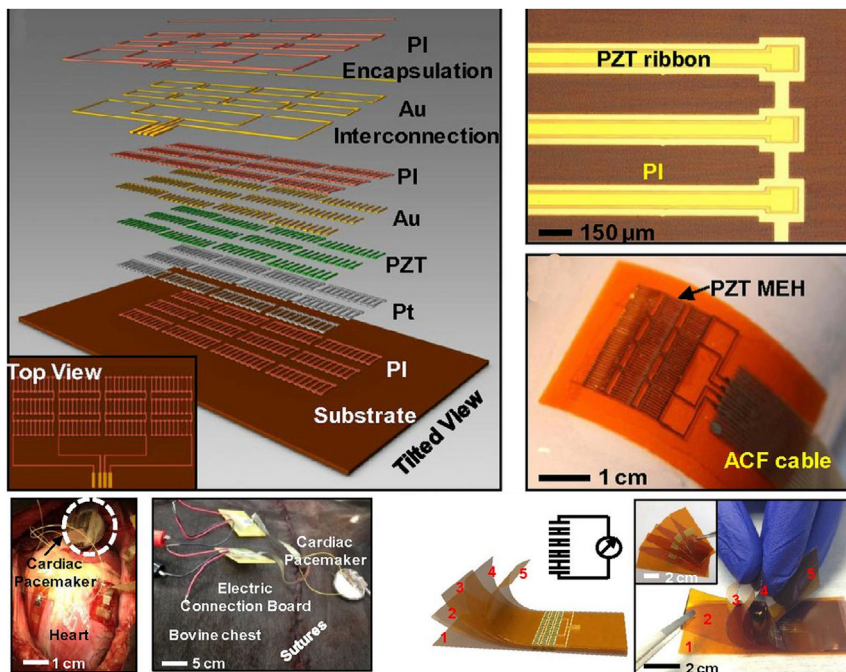


Figure 18. Conformal Piezoelectric Energy Harvesting and Storage from Motions of the Heart, Lung, and Diaphragm

Reproduced from Dagdeviren et al.²¹⁴ with permission from National Academy of Sciences.

resonant frequency, in 2017 Ansari and Karami²¹¹ proposed a fan-folded structure that consists of bimorph beams folding on top of each other. A 1-cm³ prototype was constructed with three bimorph beams (PZT-5A layer: 20 × 5 × 0.19 mm³) and a tip mass of 18.4 g. The prototype was excited by a normal heartbeat waveform from a feedback controlled shaker, and generated 16 µW power on average. As well as the fan-fold structure, other methods such as symmetric meandering configurations²¹² and multi-cantilever arrays²¹³ have also been exploited for this purpose.

In addition to rigid mechanical devices encapsulated in the solid pacemaker case, researchers have also tried to develop soft energy harvesters that can be directly attached to hearts and extract energy from the deformation of the myocardium. In 2014, Dagdeviren et al.²¹⁴ proposed a strain-based harvester for conformal energy harvesting from the contraction and relaxation motions of the heart. Figure 18 shows schematically the PZT thin-film harvester. Thin PZT ribbons (500 nm in thickness) were sandwiched between metal electrodes, fixed on a thin spin-cast PI substrate layer, and encapsulated with biocompatible materials. The harvester was further integrated with a bridge rectifier and a millimeter-scale battery for simultaneous power generation and storage. The thin PZT ribbon composite showed a superior stability and was sustained after 20 million bending cycles. The flexible piezoelectric patch was affixed on the surface of the ventricles of bovine and ovine hearts. The thin-film harvester generated a maximum open-circuit voltage of 4–5 V, and its maximum power density could reach 1.2 µW cm⁻² when using multi-layer stacks.

Similar work was reported later by Lu et al.²¹⁵ The authors argued that cows and sheep are different from human beings with regard to the cardiac anatomy, and that *in vivo* tests should be performed in conscious animals rather than in

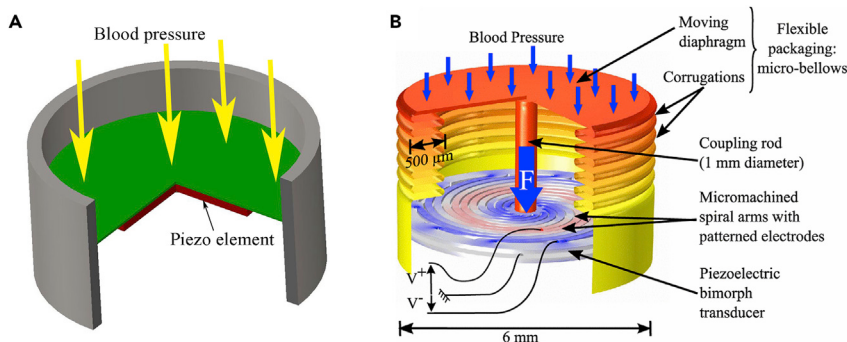


Figure 19. Harvesting Energy from Blood Pressure Gradients

(A) Schematic of piezoelectric diaphragms to harvest energy from blood pressure variations.
 (B) A micro-spiral piezoelectric transducer that captures energy from blood pressure variations.
 Reproduced from Deterre et al.²²³ with permission from IEEE.

anesthetized animals. They did experiments in swine using the similar flexible PZT ribbon composites, and obtained a peak-to-peak voltage of 2–3 V.

To improve the energy density of flexible piezoelectric transducers, Hwang et al.¹²¹ proposed a flexible energy harvester using the high-efficiency single-crystal PMN-PT. They optimized the stress-controlled exfoliating process,²¹⁶ which transferred a PMN-PT thin film from a bulk substrate onto a flexible substrate. The PMN-PT thin film had an area of $17 \times 17 \text{ mm}^2$ and was $8.4 \mu\text{m}$ thick. It was bonded on a polyurethane (PU)-coated polyethylene terephthalate (PET) substrate. Excited by a linear motor for a strain of 0.36% at a strain rate of $2.3\% \text{ s}^{-1}$, the thin film harvester generated maximum open-circuit voltage of 8.2 V and short-circuit current of 145 μA . In this study, the authors did not apply the developed harvester on a heart. Instead the PMN-PT film composite was bent by hand and the output voltage was used directly to stimulate a rat heart. Subsequently, in 2017 the same group²¹⁷ *in vivo* tested a single-crystalline PMN-PZT-Mn thin film ($20 \times 30 \times 0.02 \text{ mm}^3$) on a porcine heart, and obtained a short-circuit current of 1.75 μA and open-circuit voltage of 17.8 V. The group also presented a detailed review of thin-film flexible harvesters.²¹⁸

Next we consider methods to harvest energy from blood pressure gradients. The piezoelectric diaphragm is the most widely studied structure in this application.^{206,219–222} As shown in Figure 19A, typically the harvester consists of a substrate layer with a thin piece of piezoelectric element attached on one side. The other side is exposed to the low-frequency blood pressure variation. In the work from Mo et al.,²²¹ under a 40-mmHg pressure variation (1 Hz), 36 V and 128 μJ per cycle is generated by a $\Phi 25.4 \times 0.127\text{-mm}$ PZT-5H wafer on a $\Phi 42.4 \times 0.285\text{-mm}$ aluminum substrate. In the work from Deterre et al.,²⁰⁶ a prototype made of a $\Phi 25 \times 0.11\text{-mm}$ PZT layer on $\Phi 45 \times 0.1\text{-mm}$ brass diaphragm generated a maximum voltage of 10 V and maximum energy per cycle of 25 μJ under a 50-mmHg air pressure variation (2 Hz). This equates to average power output of about 50 μW . Here, the energy per cycle refers to the highest energy stored in the piezoelectric elements. It is calculated via the equation: half of capacitance of the piezoelectric element times squared maximum voltage over the electrodes. This calculation overestimates the harvester performance because, in an energy-harvesting system, the effective energy that can be finally consumed by a target electric load is much less than the energy stored in the piezoelectric elements. No *in vivo* tests have been performed. As these diaphragm harvesters need one side of the diaphragm structure to be

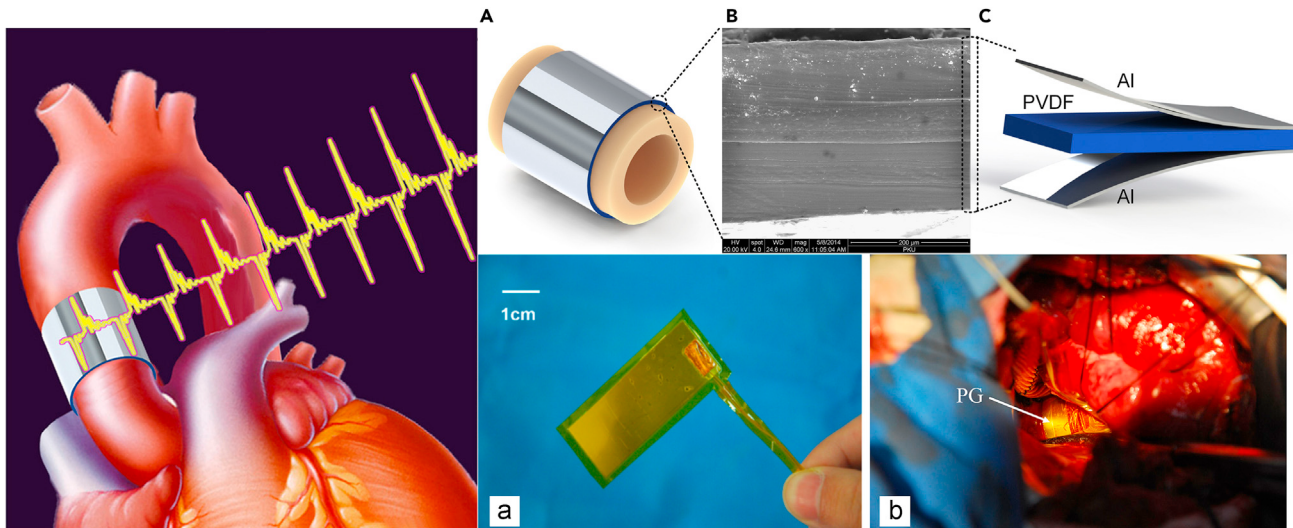


Figure 20. A PVDF Harvester that Captures Energy from the Arterial Wall Deformation

Reproduced from Zhang et al.²²⁶ with permission from Elsevier.

exposed to the blood flow, possible installation sites may be located along the endocardium and the endothelium of large arteries.

In 2014, Deterre et al.²²³ proposed a micro-spiral piezoelectric transducer associated with a novel micro-fabricated packaging that captures energy from blood pressure variations in the cardiac environment. This is intended for use as a leadless pacemaker that resides inside a heart.²²⁴ As Figure 19B shows, the proposed system consists of an ultra-flexible electrodeposited micro-bellows (21 mm^3 volume), a micro-machined spiral-shaped piezoelectric bimorph, and a 1-mm diameter coupling rod. The coupling rod is fixed on a spiral-shaped bimorph on one end, and connects the top surface of the micro-bellows on the other end. The top surface is only $12 \mu\text{m}$ in thickness so that we can regard it as a diaphragm. Both the top diaphragm and deformable bellows contribute to the total flexibility of the harvester. The article also presents an optimization of the electrode pattern and geometry of the spiral bimorph. Under an excitation of 1.5 Hz and 180 mN (corresponding to the maximal amplitude pressure variations in the left ventricle on a surface of diameter of 6 mm), the optimized prototype achieved a maximum power density of $3 \mu\text{J}/\text{cm}^3/\text{heartbeat}$. The energy conversion efficiency was calculated to be 0.57%.

Regarding methods to harvest energy from arterial wall deformations, harvesters on blood vessels are prohibited to hamper blood flow and arterial movement. Therefore, soft piezoelectric materials such as PVDF films are preferred in this application. In 2008, Potlay and Brooks²²⁵ designed a PVDF cuff surrounding arterial blood vessels. A small $28 \times 8 \times 0.028\text{-mm}^3$ PVDF film was embedded inside a 0.25-cm^3 self-curling silicone cuff. The harvester was tested on a mock artery (latex tubing). On average, 6 nW power was generated from $\sim 80 \text{ mmHg}$ blood pressure variation through the $\Phi 12.7\text{-mm}$ latex tubing. In 2015, Zhang et al.²²⁶ tested a PVDF harvester on the ascending aorta of a pig heart, as shown in Figure 20. Similar to Potlay's work, they first evaluated the performance of the flexible PVDF harvester on a latex tube. A $25 \times 56 \times 0.2\text{-mm}^3$ prototype showed a maximum output power of 681 nW and a maximum voltage of 10.3 V, respectively, under a pressure variation of 80 mmHg, 160 beats per minute. When wrapping the PVDF film around the ascending aorta of a porcine heart, a maximum voltage of 1.5 V was achieved under the heart rate

of 120 beats per minute and blood pressure of 160/105 mmHg. The implanted harvester is able to charge a 1- μ F capacitor to 1.0 V within 40 s. It is roughly estimated that the average power output is about 12.5 nW.

Overall, the last decade has witnessed an intensive study on energy harvesters for implantable devices, especially for pacemakers. A variety of rigid and flexible piezoelectric transducers have been developed with the hopes of powering artificial pacemakers by harvesting energy from heart beats, blood pressure vibrations, and blood vessel deformations. It is impossible to quantitatively compare these harvesters due to the lack of systematic reporting (excitation strength, mass, dimension, and electrical load). Generally the power output from *in vivo* tests is under 1 μ W. Energy harvesters currently are facing complex hurdles and there is a long way to go before we achieve self-powered operation of pacemakers. Most research is still in the stage of *in vitro* testing and there are few practical designs that can supply enough power for pacemakers. No energy harvesters have been integrated into pacemakers and tested *in vivo*. Furthermore, other critical issues such as biocompatibility and reliability are waiting to be properly addressed. How does one attach a solid artificial structure to soft dynamic biological tissues? How do we harvest enough energy without side effects and interference in normal organ motions? How is fatigue and degradation avoided over 10 years of operation? These open questions must be answered in a comprehensive manner analytically and experimentally before clinic trials are initiated.

Nevertheless, it is believed that energy harvesting is a logical and intriguing concept for powering medical implants and promises a game-changing technology if successful. Theoretically, energy-harvesting systems can be perpetual because, unlike batteries, they are not power reservoirs but power generators. A perpetual power source provides great flexibility in the design of future pacemakers and other medical implants. For example, to carry out maintenance and replace batteries easily, pacemakers currently are implanted under the skin of the chest (just below the collarbone) and long lead cables are used to deliver therapeutic stimulus to the heart. With a perpetual energy source, surgeons can implant newly designed compact pacemakers directly inside the heart without long lead cables. External cables are one of the leading causes of failure in implanted devices. Pacemakers are evolving with more diagnostic and telemetric functions. Demands on power consumption will be increased as the complexity of devices evolves. Energy harvesters make it possible to develop new functions without compromising the lifespan. The development of energy harvesters also supports other implantable devices such as defibrillators or carotid stimulators that require much more power than pacemakers, and the need to extend their lifespan is generally accepted. Overall the energy-harvesting technology holds great potential to prolong the lifespan of existing implantable devices with more functions, and support the emergence of new therapies. We can foresee an increasing level of research on implantable energy harvesters in material, design, and system aspects.

Tire Pressure Monitoring System

The automotive industry has a great interest in small-scale sensors for control and safety applications. Currently each vehicle is equipped with about 60 sensors, and an increasing number of sensors are being integrated into vehicles along with the rapid development of self-driving technology and electric cars. One main barrier to the trend in this context is cabling and connectors of these sensor modules. The total cable length in a modern car is more than 4 km (Auzanneau²²⁷), which adds additional weight, occupies much space, and lowers the vehicle's reliability

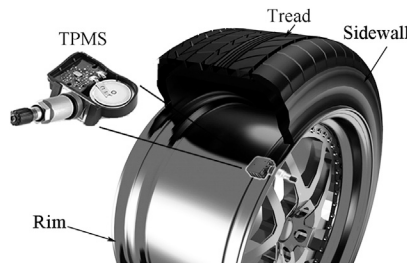


Figure 21. A TPMS Module and Its Installation on a Wheel

as a whole. These troubles can be avoided by updating sensors to be wireless. However, wireless sensor modules cannot operate automatically for a long time due to the limited capacity of embedded batteries. To address the power source issue, researchers have started to exploit on-site wasted energy in vehicles. By harvesting the tremendous vibration and deformation energy in running vehicles, energy harvesters can effectively extend the battery life, with great potential of achieving life-long autonomous operations of these small-size sensor modules. A variety of energy-harvesting methods have been proposed for different applications in the automotive industry.^{110,228–234} Here our analysis concentrates on energy harvesters for the TPMS. Tires are the only components in vehicles that directly contact the ground. They carry out multiple key tasks including supporting the vehicle load, absorbing shocks from the road, and providing grip during steering and braking; thus, tires play a determinant role in driving safety and comfort. The TPMS was initially proposed to enhance safety, but also contributes to higher fuel efficiency and longer tire life.

TPMS is a very promising application for energy harvesters, and may become one of the first commercially available energy-harvesting products. This is mainly because the TPMS market is growing extremely quickly, driven by the stringent fuel efficiency and safety regulations in the United States, Europe, and Asia. Also, there is enormous energy associated with a rolling tire that can be scavenged by energy harvesters. Furthermore, compared with medical implants, there are fewer regulations in the automotive applications. Energy harvesters can reach the market in a timely way once their performance meets requirements.

Energy harvesters for the TPMS have garnered much interest academically and commercially. One can find a variety of energy harvester-based TPMS systems in the patent literature. Bowen et al.²³⁵ and Kubba et al.²³⁶ have presented excellent reviews on tire pressure sensors and energy harvesters for TPMS application broadly via the electromagnetic, piezoelectric, electrostatic, and thermal effects. Here we give a detailed and up-to-date analysis of mechanical energy harvesters using the piezoelectric effect for TPMS, focusing on the structure design and dynamic analysis.

Figure 21 shows a TPMS module and its installation on the tire valve. A TPMS usually is composed of a sensor IC, a low-frequency interface, an RF transmitter, an antenna, and a primary battery. The sensor IC integrates a low-power MCU, an ADC module, a pressure sensor, a temperature sensor, and an accelerometer. The accelerometer is used to enable a sleep mode when the car is idle for a predefined period of time. In the run mode, tire pressure is measured and wirelessly transmitted once or several times per minute. The overall power consumption of a TPMS module highly depends on how many RF transmissions are made in every minute and how long the

Table 6. Power Consumptions of the Mainstream IC Solutions on the Market

| Company | IC Solutions | Typical Current Consumption Run mode + RF Transmission |
|-------------------|-----------------------|---|
| Infineon | SP370 | run mode: 2 mA RF: 10 mA sleep current: 0.7 µA |
| Freescale | FXTH870x | run mode: 2 mA RF: 6 mA sleep current: 0.5 µA |
| Texas Instruments | TPIC82010 | run mode: 1.53 mA RF: 10.5 mA sleep current: 0.1 µA |
| Melexis | MLX91801/2 + MLX72013 | run mode: 1 mA RF: 3.8–16.8 mA sleep current: 0.25 µA |

All data are from the datasheets of the ICs. Operation voltage of the ICs is about 1.8–3.6 V.

TPMS module stays in the sleep mode. The capacity of TPMS batteries^{235,237} is about 220–600 mAh and the typical operation lifespan is 5–10 years.

Table 6 lists the power requirements of the most commonly used TPMS chips on the market. The RF transmitter consumes the most power, requiring over 10 mA. The sleep mode, by contrast, only needs current less than 1 µA. Overall, it is estimated that on average 450 µW is required to attain a 1-Hz transmission rate for a TPMS module.²³⁸ Today's cars sit unused over 90% of the time, and thus the majority of energy stored in the battery is consumed by the sleep current.²³⁷

Energy harvesters, like the TPMS, work only when the vehicle runs. To maintain operation, harvesters should have a power output much higher than the power requirement of the TPMS in the working mode so that a part of harvested energy can be stored for the sleep mode. The power output of a harvester embedded in a TPMS is expected to be at the milliwatt level.

Available Excitations in Tires for Energy Harvesters. A rolling tire is an energy-rich environment. Energy harvesters can take advantage of either the vibration energy from the rotation, the gravitational field and the road surface, or strain energy from the deformation of the tire. Possible installation positions include the inner liner above the tread wall, the inner liner of the sidewall, and the inside and outside of the rim. Figure 22 shows the load conditions of a rolling wheel. Due to the vehicle load, the round surface of an inflated tire flattens at the tire-road interaction zone and forms an area called the "contact patch." The existence of the contact patch induces a periodic acceleration and strain change on the wheel.

The strain change associated with the cyclic deformation of a tire is considerable. Both the tire tread wall and the sidewall deform around the contact patch. The sidewall only experiences compressive strain in the radial direction, but the inner liner of the tread wall experiences compressive stress on each side of the contact patch and tensile stress within the contact patch in the circumferential direction. The maximum strain^{239,240} on the inner liner of the tread wall can be around 0.1%–0.5%. The deformation^{241–243} of the sidewall can be as high as 10–50 mm.

The vibration associated with a rolling tire contains tremendous energy. It mainly exists in three forms: gravity, the periodic and random vibrations from the tire-road interaction, and the periodic acceleration variation from the centripetal force. Gravity is always in one direction toward the earth, but structures attached on a wheel can

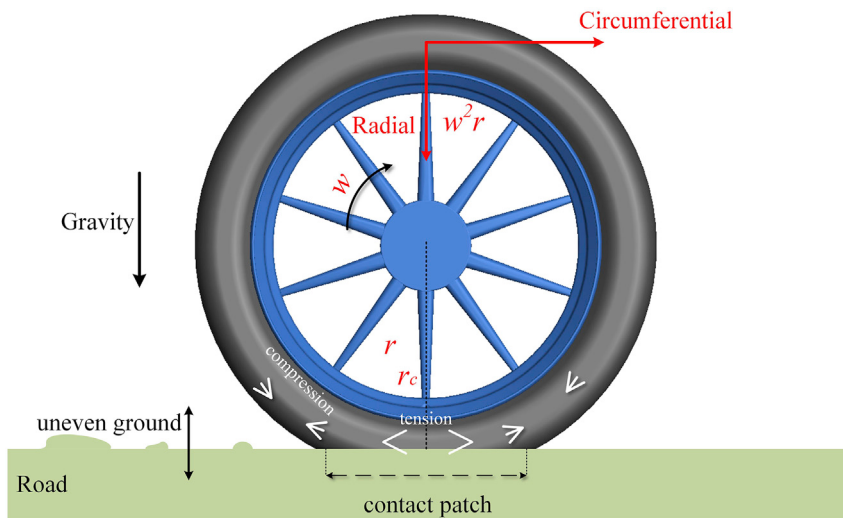


Figure 22. The Load Conditions of a Wheel Rotating on a Road

w represents the angular velocity of the wheel. r is the radius of the tire and r_c is the distance between the contact patch and the center of the wheel.

experience a periodic $\pm 1 \text{ g}$ acceleration change due to the rotation of the wheel. The frequency of the vibration follows the rotation speed of the wheel. The radial acceleration keeps at a constant value $\omega^2 r$ (ω angular velocity of the wheel; r radius of the tire) most of time per round, and drops to zero in the contact patch area. The deformation in the contact patch also causes a direction change in the circumferential (tangential) acceleration. The tangential acceleration goes up while entering the contact patch and goes down when leaving the contact patch. Figure 23 exhibits a typical acceleration value measured on a car at the speed of 80 km hr^{-1} . The tangential acceleration is $0 \pm 1,500 \text{ m s}^{-2}$. The radial acceleration is about $2,500 \text{ m s}^{-2}$ with an abrupt drop to 0 m s^{-2} in the contact area. Pooya et al.²⁴⁵ reported a peak radial acceleration of 100 m s^{-2} and tangential one of 150 m s^{-2} . The acceleration level is highly dependent the driving speed. Schaijk et al.²³¹ reported that the maximum acceleration increases from 300 m s^{-2} to $1,200 \text{ m s}^{-2}$ as the driving speed rises from 30 km hr^{-1} to 60 km hr^{-1} . The acceleration value also varies under different road conditions and with different vehicle loads. It can be in a large range of $100\text{--}4,000 \text{ g}$ ($g = 9.8 \text{ m s}^{-2}$) (Löhndorf et al.²³⁷ and JESD22-B104-B from Automotive Electronics Council), taking unexpected shocks into account. Energy harvesters designed to work in this environment must consider the extremely high acceleration to ensure the lifetime and meet automotive quality requirements.

The vibration from the tire-road interaction is unpredicted and random. There are no general characteristics shared by the vibrations from different road conditions. Löhndorf et al.²³⁷ analyzed a set of tangential acceleration data recorded at the inner liner of a tire at 50 km hr^{-1} , and found that power mainly exists in a low frequency range of $5\text{--}20 \text{ Hz}$, corresponding to the revolution period of the wheel, but also shows several peaks around 100 Hz , which should be from the tire-ground interaction. To make use of the energy from both the vibration from the tire-road interaction and the periodic acceleration, energy harvesters ought to be designed with a broad working bandwidth.

The concept of powering TPMS using energy harvesters was proposed almost at the same time as when the TPMS legislation was implemented in the United States.

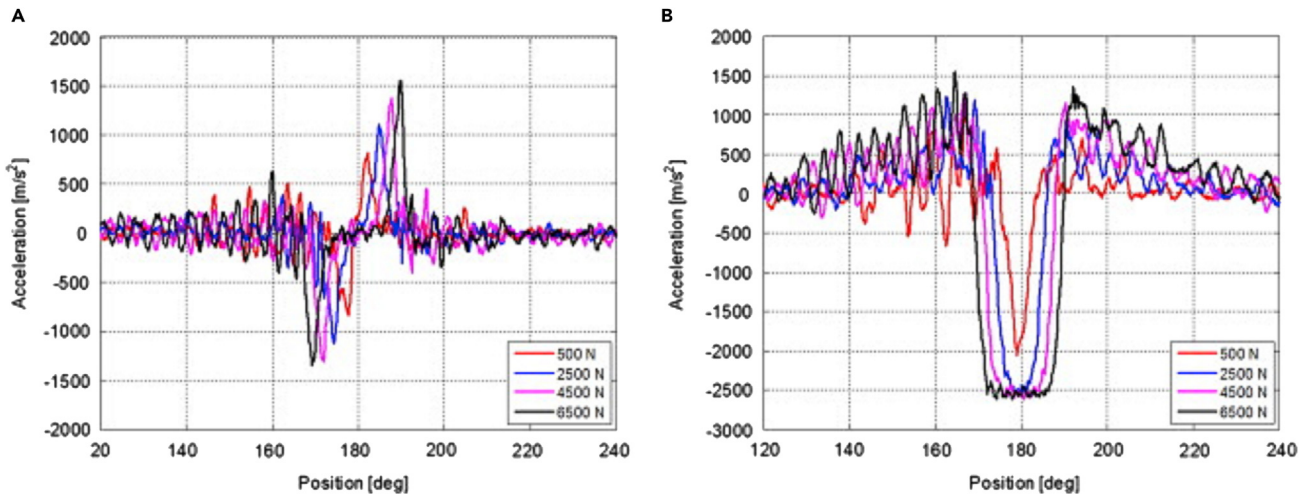


Figure 23. On-Road Acceleration Data of a Rolling Wheel with Different Vehicle Load

(A and B) Tangential direction (A) and radial direction (B). The driving speed is 80 km hr^{-1} and tire pressure is 2.6 bar. Data in (B) do not include centripetal acceleration information. Reproduced from Matilainen and Tuononen²⁴⁴ with permission from Elsevier.

TPMS suppliers first evaluated the possibility of powering TPMS using PEHs.²³⁷ Later in 2008, Roundy²⁴⁶ analyzed the problems and challenges in the design of energy harvesters for TPMS. The weight of a harvester should be much smaller than the standard maximum weight of TPMS, that is, $\sim 25 \text{ g}$. The expected lifespan approximates 150 million tire revolutions. It was estimated that a TPMS roughly requires 1.125 mJ per minute to operate. Since then, various energy-harvesting methods have been proposed, which, from the perspective of excitation sources, can be divided into two categories: vibration energy and strain energy.

Vibration Energy. Cantilever energy harvesters were first studied to power TPMS.^{247,248} A piezoelectric cantilever is mounted on the tire or rim to harness mechanical energy from the acceleration change around the contact patch and the vibration from the road surface.

In 2013, Mak et al.²⁴⁹ added a bump stop to the cantilever energy harvester to protect the structure from large deformations (Figure 24A). A theoretical model was developed to estimate the dynamic responses of cantilever energy harvesters under different conditions. The model estimated that a bimorph with PZT elements of $11 \times 5 \times 0.18 \text{ mm}^3$ is able to generate an RMS power of $178 \mu\text{W}$ with a bump stop and $298 \mu\text{W}$ without a bump stop, respectively, at a driving speed of 64.4 km hr^{-1} . The study did not consider the static deformation of the cantilever caused by the large centrifugal force that may prevent the cantilever from vibration. The configuration of a piezoelectric cantilever with end stops has also been studied by Singh et al.²⁵³ By measuring the vibration responses of a tire with different speed, load, air pressure, and road surface condition, they claimed that the ideal working frequency range is 60–80 Hz. They made a $25 \times 5 \times 0.4\text{-mm}^3$ bimorph prototype using the high-energy density material PZT-ZNN. The prototype produced $15 \mu\text{W}$ power under a harmonic excitation from a shaker at an RMS acceleration of 0.4 g and frequency of 62.5 Hz. Furthermore, they considered the fact that the vibration response of the cantilever bimorph is affected by the power management circuitry, and proposed to use a buck-boost AC-DC converter to tune the resonant frequency of the harvester. An artificial neural network (ANN)-based closed-loop system was developed to format an adaptive duty cycle for the buck-boost converter. It showed

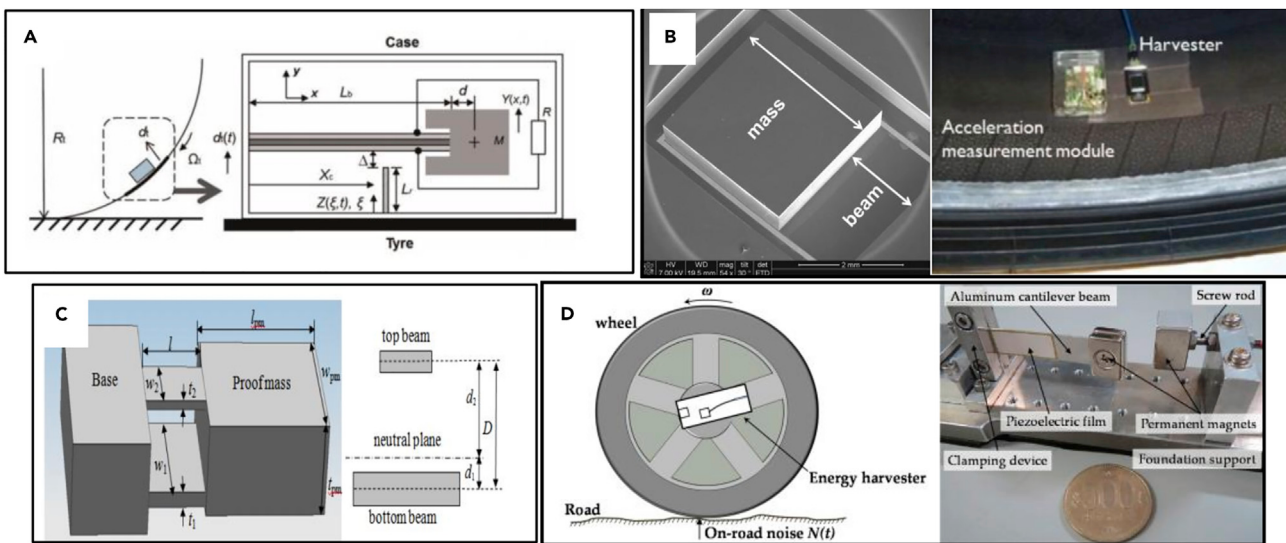


Figure 24. Cantilever Energy Harvesters Designed for TPMS

(A) Cantilever harvester with a bump stop. Reproduced from Mak et al.²⁴⁹ with permission from SAGE Publications.

(B) MEMS cantilever harvester. Reproduced from Van Schaijk et al.²³¹ with permission from SPIE and Elfrink et al.²⁵⁰ with permission from IEEE.

(C) Asymmetric air-gaped piezoelectric cantilever.²⁵¹ Reproduced from Zheng et al.²⁵¹ with permission from IOP Publishing Ltd.

(D) Stochastic resonance energy harvester for TPMS. Reproduced from Zhang et al.²⁵² with permission from MDPI AG.

that the ANN method was capable of keeping the harvester at the maximum power output condition over a broad frequency range. However, such a neural network controller may consume more energy than it adds to the energy-harvesting system.

Elfrink et al.^{231,250} fabricated an MEMS cantilever harvester as shown in Figure 24B. Under a harmonic excitation of 4.5 g and 1,011 Hz, the $3 \times 3 \times 1.7\text{-mm}^3$ AlN unimorph prototype generated a maximum power of 489 μW . When mounted on the tread wall and tested on the road at $\sim 70\text{ km hr}^{-1}$ driving speed, the prototype generated a power of $\sim 30\text{ }\mu\text{W}$ on average.

Zhang et al.²⁵¹ proposed an asymmetric air-gaped piezoelectric cantilever for harvesting energy from tires. As shown in Figure 24C, they deliberately introduced a gap into the cantilever to increase the distance between the piezoelectric element and the stress-neutral plane, and thus increased the voltage induced on the piezoelectric element. The prototype was made of an $8 \times 5 \times 0.5\text{-mm}^3$ PZT-5A plate and a 21.6-g proof mass. Due to the small size, it is impossible to match the resonant frequency of the air-gaped cantilever with the vibrations of the tire. The power response spectrum of the in-field tests showed two peaks: one at 11 Hz, corresponding to the vibrations of the tire, one at 470 Hz, corresponding to the resonant frequency of the cantilever. The prototype was not mounted on the tire-mounting side of the rim but on the opposite side so that the voltage response could be recorded via a slip ring. At a driving speed of $\sim 50\text{ mph}$, the prototype used 35 s to charge a $32\text{-}\mu\text{F}$ capacitor to 8 V and the maximum power was 47 μW .

To expand the frequency bandwidth of the cantilever energy harvester, Sadeqi et al.²⁵⁴ added a deformable support to the cantilever harvester. They considered the vibrations caused by the gravitational field in a rotating wheel and ignored the centrifugal effect in the analysis. The prototype was fixed on the rim, consisting of a piezoelectric bimorph supported by four springs at each corner. The resonant frequency of the energy harvester can be tuned by adjusting either the mass on the

bimorph or the stiffness of the springs. In-lab tests using a DC motor showed that two response peaks exist around 50 Hz and 70 Hz, and the maximum response voltage is only about 4 V. The occurrence of the low voltage response is because the soft support significantly reduced the vibration-induced stress in piezoelectric elements. Although the idea of multiple resonance in an energy-harvesting system is interesting, the inferior performance indicated that the method of introducing a soft support to cantilever harvesters is not practical.

All the aforementioned studies arranged the piezoelectric beams parallel to the tread wall surface. Zhu et al.²⁵⁵ set the cantilever harvester perpendicular to the tread wall surface on the rim to harness vibration energy from the tangential acceleration variation. In this manner, the resonant frequency of the cantilever beam can be tuned by the centrifugal force as the rolling speed varies. A prototype was made of a 70 × 7 × 0.32-mm PZT-5H unimorph and a tip mass of 11 g, and tested on the outside of a rim. It produced a peak power of 500 μW and an average power of 140 μW at a driving speed of 50 km hr⁻¹. This proposed design faces a serious installation problem. It is difficult to install a vertical piezo beam inside an inflated tire and at the same time keep it from impacts while driving.

To improve energy-harvesting efficiency, Zhang et al.²⁵² paid attention to the coupling effect of the periodic acceleration change by gravity and the random vibration from the road surface. It is known that the dynamic responses of a bistable system can be significantly enhanced with a certain probability by adding noise to a weak periodic excitation, a phenomenon known as "stochastic resonance." It has been theoretically and experimentally proved that stochastic resonance can improve the efficiency of BEHs.^{256,257} The authors studied the stochastic resonance under the rotation conditions. As shown in Figure 24D, a piezoelectric cantilever (22.9 × 10 × 0.1 mm³ PZT unimorph) was mounted outside of the tire at the center of the wheel to rule out the centrifugal effect. A pair of magnets was fixed on the stationary frame and the movable tip end of the piezoelectric cantilever to induce the required bistable nonlinearity. In-lab tests demonstrated that the excitation combined with the periodic acceleration and the on-road noise signal has advantages over the periodic acceleration excitation. On-road tests witnessed a maximum average power of 5 μW, corresponding to a power density of 0.76 μW cm⁻³ at 20 km hr⁻¹. However, it is difficult to know whether the stochastic resonance really happened in the on-road tests. The tests were performed only in a low speed range of 10–40 km hr⁻¹ on a smooth paved road. At a high speed of over 100 km hr⁻¹ or on a rugged road, the nonlinear dynamics may behave differently. The basic idea underlying the performance improvement from the stochastic resonance is that the noise signal facilitates overcoming the potential barrier and activating the intra-well dynamics.²⁵⁸ Therefore, the occurrence of the stochastic resonance requires a proper noise amplitude relative to the bistable system and the main oscillation source. In this study, the amplitude of the noise signal is comparable with that of the main periodic acceleration variation. However, such a noise and excitation condition is not guaranteed all the time in practice. Embedding nonlinear energy harvesters into TPMS faces serious issues with regard to the system robustness.

In addition to cantilevered structures, the fixed-fixed boundary condition has also been explored. Marian²⁵⁹ presented a clamped-clamped unimorph with a proof mass fixed at the center. The highest power output of 40 μW was achieved at 80 km hr⁻¹. Similarly, Jousimaa et al.²⁶⁰ fixed a piezoelectric disc on a base with a mass attached at the center, as shown in Figure 25A. It mainly utilizes the periodic radial acceleration variation of a rolling tire due to the tire radius change in each

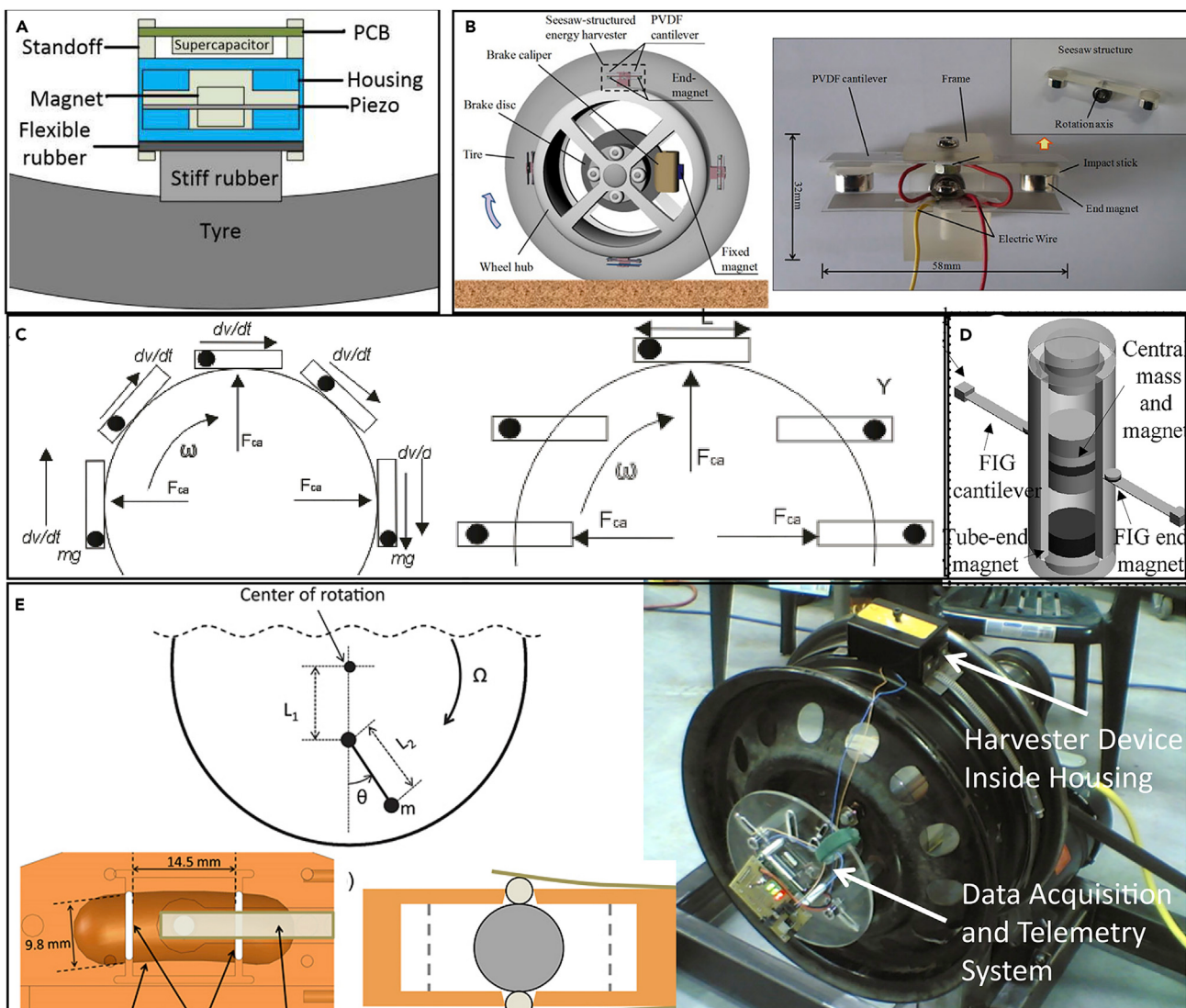


Figure 25. Different Structures for Harvesting Vibration Energy from Wheels

- (A) Fixed piezo disc for harvesting energy from the periodic radial acceleration variation. Reproduced from Jousimaa et al.²⁶⁰ with permission from IEEE.
- (B) Seesaw-structured energy harvester. Reproduced from Wu et al.²⁶¹ with permission from IEEE.
- (C) Harvesting energy from the impact of a ball on a spinning wheel. Reproduced from Manla et al.²⁶² with permission from IEEE.
- (D) The interaction of a vibrating magnet and cantilever PEHs. Reproduced from Tang et al.²⁶³ with permission from IEEE.
- (E) Offset pendulum mechanism for rotational energy harvesting.²⁶⁴ Reproduced from Roundy and Tola²⁶⁴ with permission from IOP Publishing Ltd.

rotation, as well as the periodic and random vibrations from the tire-road interaction. The prototype was made of a PZT unimorph disc of diameter 32.77 mm (Thunder TH-5C) and assembled with a circuit and a housing. The whole assembly is $35 \times 35 \times 25 \text{ mm}^3$ and weighs 65 g. The prototype produced $88 \mu\text{W}$ power on average at the excitation speed of 60 km hr^{-1} . One interesting test reported here is an endurance test. The prototype mounted inside a wheel survived for 10 min at 60 km hr^{-1} and a load of 2 kN on a tire-testing rig. The short lifetime cannot meet the requirement of the TPMS application.

In 2014, Wu et al.²⁶¹ proposed a novel seesaw-structured energy harvester for TPMS. As shown in Figure 25B, the proposed structure was constructed with a

pair of PVDF cantilevers, a seesaw beam, and two magnets at each end. The structure was fixed on a rolling wheel rim, and coupled once per round with a permanent magnet fixed on the stationary brake caliper. The swing of the seesaw structure driven by the magnetic repulsive force from the stationary magnet imposes an impulsive force on the PVDF cantilevers. It was claimed that the centrifugal force has no influence on the seesaw structure, and the harvester can work efficiently independent of the rotating speed. Excited by a motor rotating at 750 rpm ($\sim 90 \text{ km hr}^{-1}$), a prototype with a $25 \times 12 \times 0.1\text{-mm}^3$ PVDF generated a power of $5.6 \mu\text{W}$. This seesaw concept is academically appealing but may encounter cost, assembly, compatibility, and reliability issues in practice due to the complex configuration and additional magnet on the brake caliper.

In 2009, Manla et al.²⁶² proposed the concept of using the impact of a ball in a tube to harvest energy from a spinning wheel. Figure 25C shows the schematics. A small tube can be fixed on the wheel rim with both ends covered by piezoelectric plates and a free steel ball moving inside. The authors summarized two ways to install the harvester on a rotating wheel. In the first way, the tube is fixed on the edge of the rim in the tangential direction. The movement of the ball is caused by gravity and the component of the centripetal force. It was argued that this layout is not reliable because the ball will be forced to one end of the tube by the centrifugal effect when the rotating speed is high. In the second way, the tube is connected with the spinning wheel in a way that it can always stay in the horizontal direction. The acting force in this layout is the component of the centrifugal force. This study selected the second method and designed a complex mechanical system consists of one synchronous toothed belt and two pulleys to keep the harvester structure always in the horizontal direction. In experiments, a 2-cm^3 harvester was hinged on a disc of radius 5 cm, and generated on average 4 mW power at 800 rpm. There were no on-road tests reported in this paper, and it is impractical to introduce an extra belt and pulley system into a wheel to power TPMS.

Tang et al.²⁶³ also explored the tangential acceleration variation of a rotating wheel using a similar tube structure. As shown in Figure 25D, they added a pair of small piezoelectric cantilever beams outside around the centerline of the tube and magnets at the free ends of the cantilevers. A central sliding magnet is enclosed in a tube with two magnets at each end. While the central magnet slides back and forth in the tube, the outside cantilevers are bent by the magnetic force and then vibrate at their own resonant frequencies after being released. In this manner, the harvester becomes insensitive to the speed change and capable of upgrading the low-frequency vibration excitations (1–20 Hz) in wheels to high-frequency resonant vibration of the piezoelectric cantilevers. A small-size prototype with $9 \times 1.3 \times 0.14\text{-mm}^3$ PVDF-copper cantilevers generated a power of $10 \mu\text{W}$ under 1 g excitation from a shaker over a frequency range of 10–22 Hz. Its performance in a rolling wheel is unknown, but should be much lower than that excited by a shaker.^{231,250}

In 2014, Roundy and Tola²⁶⁴ also developed a tube-type energy harvester, and exploited the nonlinear dynamic characteristics of an offset pendulum to increase the working bandwidth. The authors did not really construct an offset pendulum but used a small-size curved track with a radius smaller than that of the mounted rim to produce the nonlinear behaviors of an offset pendulum. As shown in Figure 25E, the harvester is composed of a curved track, a pair of piezoelectric beams along the curved track, a steel ball that rolls in the curved track, two small balls held in conical holes, and two spring end stops. The small balls are pushed out periodically as the large steel ball rolls back and forth in the curved track, and causes deflection of the piezoelectric cantilevers. The nonlinear response of the

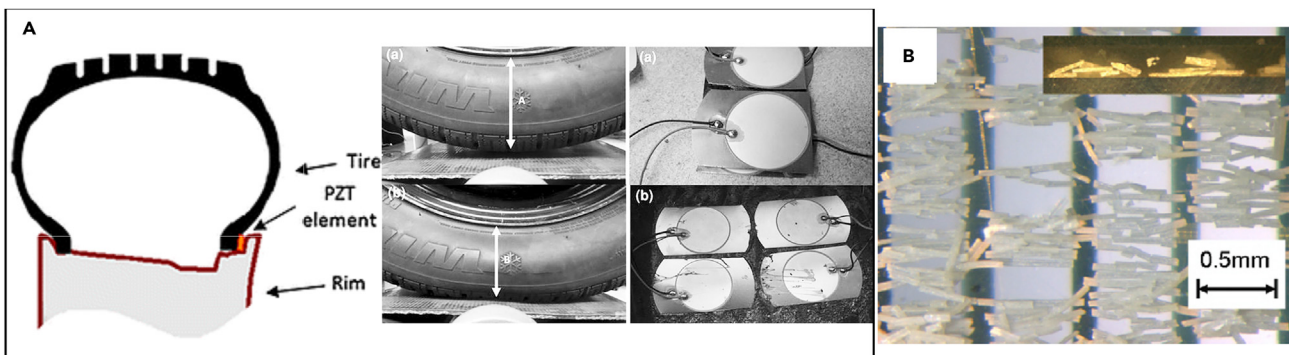


Figure 26. Harvesting Energy from the Tire Deformation

(A) PZT strain-based energy harvesting for TPMS. Reproduced from Makki et al.²⁶⁵ with permission from Springer-Verlag.

(B) PZT-polymer composite energy harvester for TPMS. PZT short fibers (light) aligned between gold electrodes (dark). Reproduced from Van den Ende et al.²⁶⁸ with permission from IOP Publishing Ltd.

steel ball is attributed to gravity, the centripetal acceleration, and the restoring force from the piezoelectric beams and the spring ends. A model was developed and predicted a power output of $\sim 10 \mu\text{W}$ at 10 mph. In the on-road tests, a prototype was assembled into a TPMS module that consumes $6.25 \mu\text{W}$ on average to make one transmission per minute. The on-road tests were performed from 10 to 155 km hr^{-1} , and the developed harvester could achieve more than one RF transmission per minute in the speed range.

Strain Energy. Makki and Pop-Iliev^{265–267} performed a series of tests on harvesting strain energy using PZT. They explored two methods, one by attaching PZT on the tread wall and the other by inserting PZT between the tire bead and the rim. The sidewall deforms periodically above the contact patch due to the vehicle weight and outward bulge. The sidewall deformation exerts an additional force to the tire bead section. To take advantage of this periodic force, the authors inserted a thin PZT element between the rim and the tire bead, as shown in Figure 26A. At 80 rpm, this method took 180 s to charge a $22\text{-}\mu\text{F}$ capacitor up to 10 V. With a matching resistance of $67 \text{ k}\Omega$, a maximum power of $70 \mu\text{W}$ was achieved.

For the tread wall method, the authors glued four PZT buzzer elements of diameter 25 mm on the inner liner of the tread wall of a tire, as shown in Figure 26A. When the tire rotated at 80 rpm (10 km hr^{-1}), the harvester produced a power of 6.5 mW with a matching resistance of $42 \text{ k}\Omega$, and took 6.76 s to charge a $22\text{-}\mu\text{F}$ capacitor to 10 V. The averaged power to the capacitor is $163 \mu\text{W}$. It is believed that the output power to the capacitor will be much higher at the impedance matching condition. A TPMS circuit was designed to test the developed harvester. The circuit on average operates at 3.0 V and 4.85 mA. In experiments, the tire-mounted PZT harvester succeeded in powering the constructed TPMS circuit for sensing and transmitting data once every 2.5 s at 60 km hr^{-1} and every 1.5 s at 100 km hr^{-1} .

The PZT attached on the tread wall can be damaged very easily due to overload or unexpected shocks. In contrast, the method of inserting PZT between the rim and the tire bead is more robust. However, this method may cause issues such as air leakage and tire imbalance. Also, the bead in a tire is strengthened by steel wires and, with high air pressure inside, the deformation in a small local area is very trivial. Nevertheless, this is a very intriguing achievement as the transmission speed is comparable with that of the TPMS powered by batteries on the market.

It has been recognized that PZT is too brittle to be used in tires directly unless elaborate stress transfer mechanisms are developed.^{268,269} Piezoelectric PVDF polymers are flexible, but exhibit a very weak piezoelectric effect. In 2012, Ende et al.²⁶⁸ fabricated a PZT-polymer composite to reach a tradeoff between the high piezoelectric effect of PZT and the excellent compliance of PVDF (Figure 26B). The PZT-polymer composite was fabricated by applying a 0.3-mm thick layer of the mixture of PU and PZT-5A powder (volume ratio 9:1) on a gold electrode PET film substrate. The dielectrophoretic (DEP) process²⁷⁰ was performed during curing of the polyurethane to form short PZT fibers. An interdigitated electrode (IDE) was used so that the cantilever could work in the more effective d_{33} mode. By attaching a PZT-polymer patch of $60 \times 10 \text{ mm}^2$ to a tire with an epoxy substrate of 0.5 mm thickness, $1.37 \mu\text{W mm}^{-3}$ was achieved. It was claimed that although the performance of the PZT-polymer composite is not as good as that of virgin MFC (micro-fiber composite) and PVDF, the composite stays relatively stable under high-temperature conditions. Lee and Choi²⁷¹ also tested a flexible piezo fiber composite patch on the inner liner of a tire. A $60 \times 10 \times 0.3\text{-mm}$ patch generated $380.2 \mu\text{J}$ energy per revolution under a 500-kg load and at 60 km hr^{-1} the power density was reported to be $1.37 \mu\text{W mm}^{-3}$.

Summary. In summary, the power output of the developed energy harvesters ranges from $10 \mu\text{W}$ to 1 mW in on-road tests. The harvester prototypes have been able to power TPMS for more than one RF transmission per minute. PZT, PVDF, and piezoelectric composites have been utilized in different forms to harvest energy from vibrations in tangential and radial directions, and strain energy on the tread wall. The strain energy on the sidewall has seldom been explored due to the extremely large deformation. The strain-based energy-harvesting method has the advantages of lighter weight and higher power output than the vibration-based counterpart, but is more susceptible to fatigue, damage, and shocks. Furthermore, attaching piezoelectric patches on a soft tire causes trouble during maintenance and also alters the elastic characteristics of the tire, which may lead to some unknown problems. In addition to reliability issues, current energy harvesters also face problems including low efficiency, poor environmental adaptability, and short lifespan.

Bridges and Buildings

One of the main applications for the wireless sensor networks (WSNs) are civil infrastructure systems such as bridges and buildings. Structure health monitoring systems on tall buildings and long-span bridges are essential for maintenance purposes (e.g., detection of early-stage degradation) and for alarm warnings (e.g., notification of earthquakes). Some systems have been successfully applied in the field, such as the wireless acceleration sensors to monitor building conditions,²⁷² and acoustic sensors for structural health prognosis in bridges.²⁷³ The WSNs are also the hardware base for the development of smart buildings²⁷⁴ and smart homes.²⁷⁵ In such systems, a myriad of wireless sensors are deployed at different locations of mega civil infrastructures. It is expected that such systems work continuously for years, but batteries in the wireless sensor nodes hold limited energy and require frequent recharge and replacement. The energy-harvesting technology supplies a remedy to the battery issue, and can significantly reduce the economic and time cost associated with the battery replacement task.

It is technically feasible to power wireless sensors using energy harvesters in civil structures.^{276,277} Tall buildings and long-span bridges are susceptible to a variety of dynamic excitations such as wind, earthquakes, traffic, and human activities, which can be used by energy harvesters to generate electricity. Vibration excitations inside

a typical English house (kitchen and utility room) were reported²⁷⁸ to be around 100 Hz, with an acceleration amplitude of 0.02–3 m s⁻². High-rise buildings ranging from 24 to 257 m in the San Francisco Bay area²⁷⁹ showed an acceleration amplitude of 0.15–0.38 g on the roof and 0.05–0.12 g on the ground floor, and vibration frequency of less than 1 Hz. For bridges, the vibration condition varies significantly, depending on weather, bridge construction, location, and traffic flow. Peigney and Siegert²⁸⁰ presented a bridge vibration of 0.03–0.3 m s⁻² and 4 Hz. Khan and Ahmad²⁸¹ presented bridge vibrations in the range of 1–40 Hz and 0.01–0.38 g. Overall, vibrations in bridges and buildings are characterized by low frequency and small amplitude.

Compared with other applications such as shoes and pacemakers, there is almost no space limitation for bridges and buildings. Therefore, relatively large-size harvesters can be designed to meet the power requirements from sensors. Here we mainly discuss small-scale energy harvesters for use in low-power electronic monitoring devices via the piezoelectric effect. Readers who are interested in the electromagnetic method are referred to other work.^{282–293}

Most research is based on the conventional cantilever energy harvester. In 2011, Erturk²⁹⁴ presented a theoretical analysis on energy harvesters in civil infrastructures using two types of excitations: vibrations and surface strain fluctuations. In the first scenario, the author considered a conventional cantilever energy harvester fixed on an arbitrary position of a slender bridge. The vibration response of a slender bridge caused by moving vehicles acts as the excitation to the cantilever harvester. In the second scenario, the dynamic surface strain variations were utilized by attaching a thin piezoelectric patch on a bridge region. Detailed theoretical analysis was presented on the two scenarios under generalized, harmonic, and white noise excitations. Furthermore, a case study using the developed distributed-parameter model was presented to evaluate the power output of a piezoceramic patch excited by real bridge strain fluctuations. A rosette strain gauge was used to measure the dynamic response of a steel multi-girder bridge (span length: 33 m). The recorded data after a fast Fourier transform analysis indicated that the major harmonic strain component lies at 22.6 Hz and the strain fluctuation amplitude is about 20 micro strain. Under such a harmonic strain fluctuation, the developed model estimated that a maximum power output of 0.13 mW can be achieved by a 30 × 30 × 0.2-mm³ PZT-5A patch.

Many models have been developed to analyze the bridge vibration response under different conditions and the power responses of the cantilever energy harvesters. Ali et al.²⁹⁵ proposed a linear SDOF model for a highway bridge with a moving point load. Zhang et al.²⁹⁶ presented a finite element model of a concrete slab-on-girder bridge for simulating the harvester performance with one passing vehicle and a continuous vehicle flow. Xie et al.²⁹⁷ presented a distributed model similar to that in the work of Erturk²⁹⁴ for a cantilever energy harvester on tall buildings. Cahill and Jaksic²⁹⁸ developed an SDOF model and via the model discussed the vibration responses of damaged and undamaged bridges affected by the road surface roughness, vehicle weight, and speed. Cahill et al.²⁹⁹ also discussed the dynamic response of a bridge traversed by trains via a finite element model. Karimi et al.³⁰⁰ proposed a distributed-parameter model whereby passing vehicles on a bridge were considered as concentrated point mass and distributed mass. Bhaskaran et al.³⁰¹ numerically analyzed an array of cantilever energy harvesters with different resonant frequencies via the finite element method in order to achieve broadband energy harvesting on bridges.

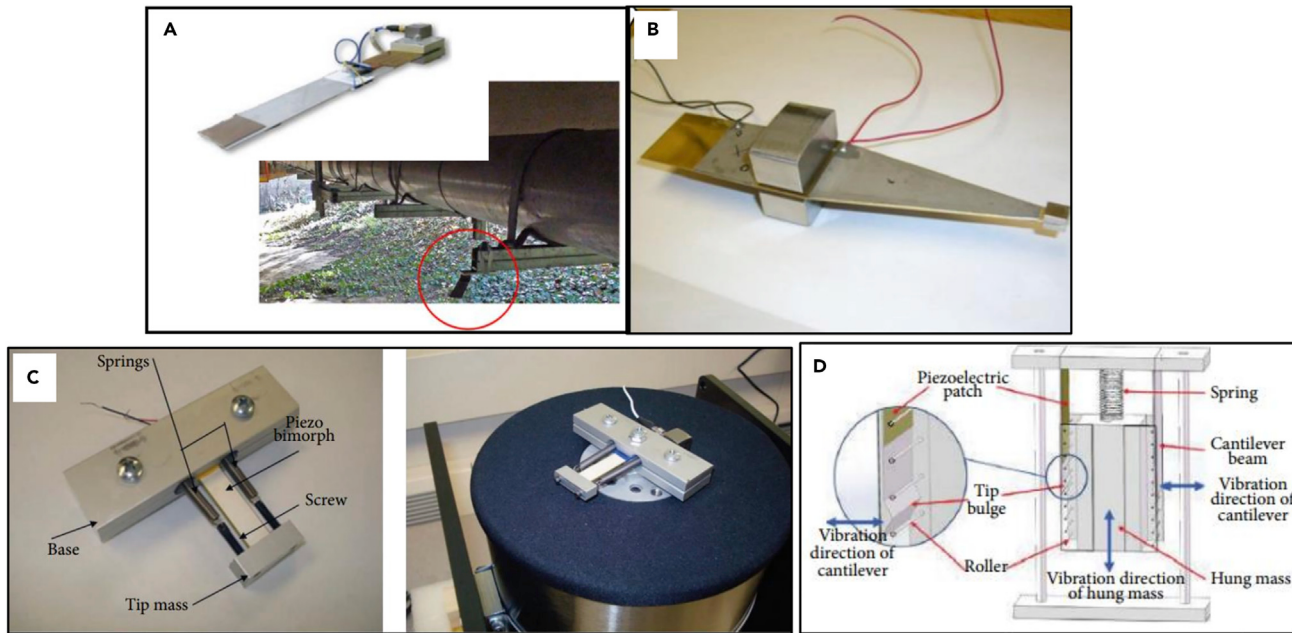


Figure 27. Energy Harvesters Developed for Bridges and Buildings

(A) Cantilever energy harvester under bridges. Reproduced from Lee et al.²⁸⁰ with permission from IOP Publishing Ltd.

(B) A segmented-type piezoelectric energy harvester. Reproduced from Lee et al.³⁰³ with permission from IOP Publishing Ltd.

(C) Cantilever harvester with an axial preload. Reproduced from Zhang et al.³⁰⁴ with permission from American Society of Civil Engineers.

(D) A multi-impact energy harvester for low-frequency vibration applications. Reproduced from Zhang et al.¹⁵⁵ with permission from IOP Publishing Ltd.

To improve the energy output, Maruccio et al.³⁰² proposed a cantilever energy harvester made of electrospinning PVDF nanofibers. They first analyzed the vibration recording of a cable-stayed bridge and identified the excitation source with an RMS acceleration of 5.87×10^{-4} – 0.0108 g and frequency of 0.92–6.39 Hz. A cantilever bimorph was then designed with 20- to 50- μm thick PVDF sheets fabricated by means of electrospinning PVDF nanofibers. The authors finally developed a finite element model and estimated that RMS voltage of 1.7–15.6 V can be generated by the harvester at different locations of the cable-stayed bridge. No prototypes and experiments were presented in this study. It is difficult to examine whether the proposed cantilever energy harvester using PVDF nanofibers has a better performance than the commonly used PZT counterpart as the piezoelectric coefficients of PVDF are much smaller than those of piezoceramics.

Cantilevered energy harvesters have also been tested on bridges. In 2013, Peigney and Siegert²⁸⁰ tested a cantilever energy harvester *in situ* on a bridge, as shown in Figure 27A. Bridge vibrations are deemed to be mainly induced by the passing traffic, and they measured the vibration conditions of a pre-stressed concrete expressway bridge located at a heavily trafficked itinerary (8,000 heavy trucks per day). The acceleration response includes successive short-time pulses, and the RMS value at different locations ranges from 0.03 m s^{-2} to 0.3 m s^{-2} . The spectral analysis of the recorded signals reveals that the main frequency components are around 4 Hz and 14.5 Hz. A cantilever harvester prototype was made of two PZT bimorphs ($46 \times 33 \times 0.76$ mm [Mide QP20W]), a steel plate of $220 \times 40 \times 0.8 \text{ mm}^3$, and a proof mass of 12 g, as shown in Figure 6. The prototype was mounted at the fixture of a water pipe under the bridge, and generated a maximum power of 30 μW .

In 2009, Lee et al.³⁰³ designed a segmented-type PEH for capture energy from the random vibration of the HVAC (heating, ventilation, air conditioning) system in a building (Figure 27B). The power spectrum of the measured data from an HVAC system indicated that the vibration is randomly distributed between 0 Hz and 150 Hz with two peaks about 0.2 g at 39 Hz and 0.1 g at 110 Hz, respectively. To make full use of the random vibration, the harvester design needs to be tailored to be able to work within multiple resonant frequencies. Traditional cantilever bimorph energy harvesters can only work at one fixed frequency around the first resonant mode where the mechanical strain on each side of the bimorph is in the same sign. The authors proposed to take advantage of the second resonant mode to capture more energy. However, in the second resonant mode, an inflection point exists in the beam where the curvature sign of deformation alters, resulting in charge cancellation. To preclude the charge cancellation effect, they separated the PZT plate into two parts near the inflection point of mechanical strain with a proof mass. As shown in Figure 27B, the proposed structure has two segments and two proof masses. The segment beam near the free end has been optimized to be a slender trapezoid via the finite element method. A prototype was fabricated with PZT-5A plates of $63.5 \times 31.8 \times 0.19$ mm³, which generated a peak open-circuit voltage of 10 V and power of 1.8 mW under the aforementioned excitation. The prototype was further tested on an HVAC system and succeeded in powering an analog temperature sensor node that requires ~ 15 µW for continuous temperature monitoring.

Considering that the vibration frequency of civil structures is usually very low, in 2012 Rhimi and Lajnef³⁰⁴ added a compressive axial preload on a cantilever PEH to reduce resonant frequency. As shown in Figure 27C, a prototype was made out of a PZT-5H bimorph with a dimension of $40 \times 10 \times 0.5$ mm³ and a pair of coil springs. The authors did not test the prototype with a bridge vibration excitation, but developed an analytical model to predict the harvester performance. The model estimated that, under an earthquake vibration recorded on a bridge, the proposed prototype could generate a maximum power of 47.23 µW. The concept of tuning the resonant frequency using axial preload has been widely studied and validated theoretically and experimentally.³⁰⁵ One should note that the resonant frequency is very sensitive to the compressive load, which may cause an unsatisfactory reliability to such pre-loaded cantilever harvesters in real applications.

In 2011, McEvoy²⁸⁸ proposed a concept of cantilever-type impact energy harvesting with the aim of harnessing the low-frequency vibrations on bridges. They designed a stopper plate directly beneath the tip end of the cantilever energy harvester so that impulsive strikes occurred in each vibration cycle. The impact causes a pair of small bimorphs attached at the tip end to vibrate at their high resonant frequencies. The concept is interesting, but no experiments were conducted on a bridge.

The impact idea has been further developed to address the low-frequency vibrations in civil structures. In 2013, Zhang et al.¹⁵⁵ proposed a multi-impact energy harvester for low-frequency vibration applications, such as bridges. Figure 27D shows the schematic of the proposed structure. It is composed of a metal frame, two vertical piezoelectric cantilever beams, and a mass-spring system. The two cantilever beams were manufactured with a triangle bulge at each tip and installed symmetrically on each side of the hung mass on the metal frame. The hung mass block is specially designed with a series of small rollers that repeatedly impact the bulges on the piezoelectric cantilevers. In this manner, the low-frequency vibration (2.71 Hz) of the spring-mass system triggers vibrations of the cantilevers around the resonant

frequency (120 Hz). It is reported that a prototype, made of $50 \times 30 \times 0.2\text{-mm}^3$ PZT plates, generated a maximum power of 7.7 mW under sinusoidal excitation of 0.29 g, 2.71 Hz (the resonant frequency of the mass-spring system). The study also presented a finite element model to calculate the vibration signal input to the energy harvester from a short span slab-on-girder bridge excited by passing vehicles. Under the simulated bridge excitation, the prototype delivered a maximum power of 2.8 mW. No in-field tests were performed in this study, and the paper does not disclose how the power is calculated. It is known that the voltage response of such impact harvesters decays exponentially in a short time. Consequently, a significant percentage of voltage responses will be too low to be used by the following circuits. Therefore, the proposed energy harvester will not be able to generate much power if applied on a bridge. Nevertheless, the concept of impact is interesting and effective for frequency up-conversion.

In 2011, Kim et al.³⁰⁶ experimentally evaluated the piezoelectric effect under various loading conditions on bridges. PZT patches were attached on a steel beam-slab type bridge specimen, and tested under various structural excitations corresponding to different traffic conditions. The experimental results indicated that energy outputs were mainly affected by the peak strain and strain increasing rate in the piezoelectric patches, which are determined by the speed and mass of moving vehicles.

Xie et al.^{307,308} successively proposed two designs for harvesting energy from high-rise buildings. The designs work like tuned mass dampers, converting the building vibration to vibration of energy harvesters first, then to electricity via the piezoelectric effect. They only presented theoretical analysis on the proposed concepts and estimated that thousands of watts of power can be generated. It is reported that the electromagnetic method is more appropriate for use in such large-scale applications.²³³

Overall, there is an increasing interest in applying PEHs in bridges and buildings. The power output of the developed PEHs ranges from several microwatts to several milliwatts. Most research focuses on the theoretical analysis of cantilever energy harvesters in bridges and buildings under different conditions. There are a few studies that report experimental data, and thus more *in situ* experiments on bridges and buildings are expected. Furthermore, although there is no strict limitation to size, new methods to scale down energy harvesters are always desirable so that harvesters can be embedded inside bridges and buildings.

Summary

This paper is devoted to reviewing state-of-the-art research aimed at high-performance piezoelectric energy harvesting. We have comprehensively analyzed different designs, nonlinear methods, optimization techniques, and materials that were explored to achieve high power output and broad frequency bandwidth. A systematic performance comparison has been conducted on recently proposed representative energy harvesters. We found that it is not appropriate to compare different designs by one figure of merit due to the complexity in dynamics, structures, and electromechanical coupling of energy-harvesting systems. Therefore, we propose to evaluate the performance of different energy harvesters using a set of metrics useful to end users, instead of one universal metric. We think performance evaluations and optimization are more appropriately conducted within specific application conditions. Here we have identified four promising applications: shoes, artificial pacemakers, TPMSs, and bridge and building monitoring systems. The excitation

characteristics of each application are analyzed and corresponding energy-harvesting methods discussed.

Although energy-harvesting technology has been intensively studied for decades, there is still a considerable gap between the achieved performance and the expected performance. Most energy harvesters are developed for a general purpose, and tested under simplified harmonic excitations. This approach provides technology that is far from ready to be used in the potential applications. Even though some application-oriented harvesters have been tested *in situ*, their reliability, stability, and compatibility have not been well examined. More research is expected to deal with these challenges. Likewise, more system-level investigations are warranted, whereby energy harvesters are integrated with power conditioning circuits, energy storage elements, sensors, and control circuits. Such research will facilitate in turning decades of research efforts on energy harvesting into tangible benefits in our daily life.

Overall, we have witnessed significant progress in energy-harvesting technology in the last decade. It continues to approach the goal of self-powered autonomous operations of wearable electronics, medical devices, automotive sensors, and wireless sensor monitoring systems.

AUTHOR CONTRIBUTIONS

Z.Y. wrote Sections 1, 2, 4, 5, and 6. S.Z. wrote Section 3. Z.Y. and S.Z. prepared figures. D.I. and J.Z. discussed and revised the manuscript. All authors contributed to the intellectual content.

REFERENCES

1. Bowen, C., Kim, H., Weaver, P., and Dunn, S. (2014). Piezoelectric and ferroelectric materials and structures for energy harvesting applications. *Energy Environ. Sci.* 7, 25–44.
2. Khan, A., Abas, Z., Kim, H.S., and Oh, I.-K. (2016). Piezoelectric thin films: an integrated review of transducers and energy harvesting. *Smart Mater. Struct.* 25, 053002.
3. Ramadan, K.S., Sameoto, D., and Evoy, S. (2014). A review of piezoelectric polymers as functional materials for electromechanical transducers. *Smart Mater. Struct.* 23, 033001.
4. Wang, Z.L. (2012). From nanogenerators to piezotronics—a decade-long study of ZnO nanostructures. *MRS Bull.* 37, 814–827.
5. Wang, Z.L., Zhu, G., Yang, Y., Wang, S., and Pan, C. (2012). Progress in nanogenerators for portable electronics. *Mater. Today* 15, 532–543.
6. Cook-Chennault, K.A., Thambi, N., and Sastry, A.M. (2008). Powering MEMS portable devices—a review of non-regenerative and regenerative power supply systems with special emphasis on piezoelectric energy harvesting systems. *Smart Mater. Struct.* 17, 043001.
7. Briscoe, J., and Dunn, S. (2015). Piezoelectric nanogenerators—a review of nanostructured piezoelectric energy harvesters. *Nano Energy* 14, 15–29.
8. Kim, S.-G., Priya, S., and Kanno, I. (2012). Piezoelectric MEMS for energy harvesting. *MRS Bull.* 37, 1039–1050.
9. Wang, Z.L., and Wu, W. (2012). Nanotechnology-enabled energy harvesting for self-powered micro-/nanosystems. *Angew. Chem. Int. Ed.* 51, 11700–11721.
10. Radousky, H.B., and Liang, H. (2012). Energy harvesting: an integrated view of materials, devices and applications. *Nanotechnology* 23, 502001.
11. Fan, F.R., Tang, W., and Wang, Z.L. (2016). Flexible nanogenerators for energy harvesting and self-powered electronics. *Adv. Mater.* 28, 4283–4305.
12. Daqaq, M.F., Masana, R., Erturk, A., and Quinn, D.D. (2014). On the role of nonlinearities in vibratory energy harvesting: a critical review and discussion. *Appl. Mech. Rev.* 66, 040801.
13. Harne, R.L., and Wang, K.W. (2013). A review of the recent research on vibration energy harvesting via bistable systems. *Smart Mater. Struct.* 22, 023001.
14. Tang, L., Yang, Y., and Soh, C.K. (2010). Toward broadband vibration-based energy harvesting. *J. Intell. Mater. Syst. Struct.* 21, 1867–1897.
15. Guyomar, D., and Lallart, M. (2011). Recent progress in piezoelectric conversion and energy harvesting using nonlinear electronic interfaces and issues in small scale implementation. *Micromachines* 2, 274–294.
16. Dicken, J., Mitcheson, P.D., Stoianov, I., and Yeatman, E.M. (2012). Power-extraction circuits for piezoelectric energy harvesters in miniature and low-power applications. *IEEE Trans. Power Electron.* 27, 4514–4529.
17. Szarka, G.D., Stark, B.H., and Burrow, S.G. (2012). Review of power conditioning for kinetic energy harvesting systems. *IEEE Trans. Power Electron.* 27, 803–815.
18. Dagdeviren, C., Li, Z., and Wang, Z.L. (2017). Energy harvesting from the animal/human body for self-powered electronics. *Annu. Rev. Biomed. Eng.* 19, 85–108.
19. Mitcheson, P.D., Yeatman, E.M., Rao, G.K., Holmes, A.S., and Green, T.C. (2008). Energy harvesting from human and machine motion for wireless electronic devices. *Proceedings of the IEEE*, 96(9): p. 1457–1486.
20. Siddique, A.R.M., Mahmud, S., and Van Heyst, B. (2015). A comprehensive review on vibration based micro power generators using electromagnetic and piezoelectric transducer mechanisms. *Energ. Convers. Manag.* 106, 728–747.
21. Hudak, N.S., and Amatucci, G.G. (2008). Small-scale energy harvesting through thermoelectric, vibration, and radiofrequency power conversion. *J. Appl. Physiol.* 103, 5.

22. Cepnik, C., Lausecker, R., and Wallrabe, U. (2013). Review on electrodynamic energy harvesters—a classification approach. *Micromachines* 4, 168–196.
23. Selvan, K.V., and Ali, M.S.M. (2016). Micro-scale energy harvesting devices: review of methodological performances in the last decade. *Renew. Sustain. Energ. Rev.* 54, 1035–1047.
24. Shaikh, F.K., and Zeadally, S. (2016). Energy harvesting in wireless sensor networks: a comprehensive review. *Renew. Sustain. Energ. Rev.* 55, 1041–1054.
25. Caliò, R., Rongala, U.B., Camponi, D., Milazzo, M., Stefanini, C., de Petris, G., and Oddo, C.M. (2014). Piezoelectric energy harvesting solutions. *Sensors (Basel)* 14, 4755–4790.
26. Uchino, K. (2010). The development of piezoelectric materials and the new perspective. In *Advanced Piezoelectric Materials*, K. Uchino, ed. (Woodhead Publishing), pp. 1–43.
27. Zhang, S., Li, F., Jiang, X., Kim, J., Luo, J., and Geng, X. (2015). Advantages and challenges of relaxor-PbTiO₃ ferroelectric crystals for electroacoustic transducers—A review. *Prog. Mater. Sci.* 68, 1–66.
28. Yang, Z., and Zu, J. (2016). Comparison of PZN-PT, PMN-PT single crystals and PZT ceramic for vibration energy harvesting. *Energ. Convers. Manag.* 122, 321–329.
29. Yuhuan, X. (1991). *Ferroelectric Materials and Their Applications* (North-Holland).
30. Pellegrini, S.P., Tolou, N., Schenk, M., and Herder, J.L. (2013). Bistable vibration energy harvesters: a review. *J. Intell. Mater. Syst. Struct.* 24, 1303–1312.
31. Wei, C., and Jing, X. (2017). A comprehensive review on vibration energy harvesting: Modelling and realization. *Renew. Sustain. Energ. Rev.* 74, 1–18.
32. Gammaitoni, L., Hänggi, P., Jung, P., and Marchesoni, F. (1998). Stochastic resonance. *Rev. Mod. Phys.* 70, 223.
33. Cottone, F., Vocca, H., and Gammaitoni, L. (2009). Nonlinear energy harvesting. *Phys. Rev. Lett.* 102, 080601.
34. Erturk, A., Hoffmann, J., and Inman, D.J. (2009). A piezomagnetoelastic structure for broadband vibration energy harvesting. *Appl. Phys. Lett.* 94, 254102.
35. Zhou, S., Cao, J., Erturk, A., and Lin, J. (2013). Enhanced broadband piezoelectric energy harvesting using rotatable magnets. *Appl. Phys. Lett.* 102, 173901.
36. Stanton, S.C., McGehee, C.C., and Mann, B.P. (2010). Nonlinear dynamics for broadband energy harvesting: investigation of a bistable piezoelectric inertial generator. *Phys. Nonlinear Phenom.* 239, 640–653.
37. Sebald, G., Kuwano, H., Guyomar, D., and Ducharme, B. (2011). Experimental Duffing oscillator for broadband piezoelectric energy harvesting. *Smart Mater. Struct.* 20, 102001.
38. Tang, L., and Yang, Y. (2012). A nonlinear piezoelectric energy harvester with magnetic oscillator. *Appl. Phys. Lett.* 101, 094102.
39. Yang, Z., and Zu, J. (2014). High-efficiency compressive-mode energy harvester enhanced by a multi-stage force amplification mechanism. *Energ. Convers. Manag.* 88, 829–833.
40. Yang, Z., Zhu, Y., and Zu, J. (2015). Theoretical and experimental investigation of a nonlinear compressive-mode energy harvester with high power output under weak excitations. *Smart Mater. Struct.* 24, 025028.
41. Stanton, S.C., McGehee, C.C., and Mann, B.P. (2009). Reversible hysteresis for broadband magnetopiezoelectric energy harvesting. *Appl. Phys. Lett.* 95, 174103.
42. Yang, Z., Zu, J., and Xu, Z. (2016). Reversible nonlinear energy harvester tuned by tilting and enhanced by nonlinear circuits. *IEEE/ASME Trans. Mechatronics* 21, 2174–2184.
43. Erturk, A., and Inman, D. (2011). Broadband piezoelectric power generation on high-energy orbits of the bistable Duffing oscillator with electromechanical coupling. *J. Sound Vib.* 330, 2339–2353.
44. Zhou, S., Cao, J., Inman, D.J., Lin, J., Liu, S., and Wang, Z. (2014). Broadband tristable energy harvester: modeling and experiment verification. *Appl. Energy* 133, 33–39.
45. Zhou, S., Cao, J., Lin, J., and Wang, Z. (2014). Exploitation of a tristable nonlinear oscillator for improving broadband vibration energy harvesting. *Eur. Phys. J. Appl. Phys.* 67, <https://doi.org/10.1051/epjap/2014140190>.
46. Kim, P., and Seok, J. (2014). A multi-stable energy harvester: dynamic modeling and bifurcation analysis. *J. Sound Vib.* 333, 5525–5547.
47. Kim, P., and Seok, J. (2015). Dynamic and energetic characteristics of a tri-stable magnetopiezoelectric energy harvester. *Mech. Mach. Theor.* 94, 41–63.
48. Zhou, S., Cao, J., and Lin, J. (2016). Theoretical analysis and experimental verification for improving energy harvesting performance of nonlinear monostable energy harvesters. *Nonlinear Dyn.* 86, 1599–1611.
49. Stanton, S.C., Owens, B.A., and Mann, B.P. (2012). Harmonic balance analysis of the bistable piezoelectric inertial generator. *J. Sound Vib.* 331, 3617–3627.
50. Harne, R., and Wang, K. (2014). On the fundamental and superharmonic effects in bistable energy harvesting. *J. Intell. Mater. Syst. Struct.* 25, 937–950.
51. Masana, R., and Daqaq, M. (2012). Energy harvesting in the super-harmonic frequency region of a twin-well oscillator. *J. Appl. Physiol.* 111, 044501.
52. Zhou, S., Cao, J., Inman, D.J., Lin, J., and Li, D. (2016). Harmonic balance analysis of nonlinear tristable energy harvesters for performance enhancement. *J. Sound Vib.* 373, 223–235.
53. Panyam, M., and Daqaq, M.F. (2017). Characterizing the effective bandwidth of tristable energy harvesters. *J. Sound Vib.* 386, 336–358.
54. Cao, J., Zhou, S., Inman, D.J., and Chen, Y. (2015). Chaos in the fractionally damped broadband piezoelectric energy generator. *Nonlinear Dyn.* 80, 1705–1719.
55. Stanton, S.C., Mann, B.P., and Owens, B.A. (2012). Melnikov theoretic methods for characterizing the dynamics of the bistable piezoelectric inertial generator in complex spectral environments. *Phys. Nonlinear Phenom.* 241, 711–720.
56. Oumbé Tékam, G., Kitio Kuimy, C., and Woaf, P. (2015). Analysis of tristable energy harvesting system having fractional order viscoelastic material. *Chaos* 25, 013112.
57. Litak, G., Friswell, M., and Adhikari, S. (2010). Magnetopiezoelectric energy harvesting driven by random excitations. *Appl. Phys. Lett.* 96, 214103.
58. Litak, G., Borowiec, M., Friswell, M.I., and Adhikari, S. (2011). Energy harvesting in a magnetopiezoelectric system driven by random excitations with uniform and Gaussian distributions. *J. Theor. Appl. Mech.* 49, 757–764.
59. Cottone, F., Gammaitoni, L., Vocca, H., Ferrari, M., and Ferrari, V. (2012). Piezoelectric buckled beams for random vibration energy harvesting. *Smart Mater. Struct.* 21, 035021.
60. Daqaq, M.F. (2011). Transduction of a bistable inductive generator driven by white and exponentially correlated Gaussian noise. *J. Sound Vib.* 330, 2554–2564.
61. He, Q., and Daqaq, M.F. (2014). Influence of potential function asymmetries on the performance of nonlinear energy harvesters under white noise. *J. Sound Vib.* 333, 3479–3489.
62. Zhao, S., and Erturk, A. (2013). On the stochastic excitation of monostable and bistable electroelastic power generators: relative advantages and tradeoffs in a physical system. *Appl. Phys. Lett.* 102, 103902.
63. Haitao, L., Weiyang, Q., Chunbo, L., Wangzheng, D., and Zhiyong, Z. (2015). Dynamics and coherence resonance of tristable energy harvesting system. *Smart Mater. Struct.* 25, 015001.
64. Su, W.-J., Zu, J., and Zhu, Y. (2013). Design and development of a broadband magnet-induced dual-cantilever piezoelectric energy harvester. *J. Intell. Mater. Syst. Struct.* 25, 430–442.
65. Su, W.-J., and Zu, J.W. (2014). Design and development of a novel bi-directional piezoelectric energy harvester. *Smart Mater. Struct.* 23, 095012.
66. Arrieta, A., Hagedorn, P., Erturk, A., and Inman, D. (2010). A piezoelectric bistable plate for nonlinear broadband energy harvesting. *Appl. Phys. Lett.* 97, 104102.
67. Leadham, S., and Erturk, A. (2014). M-shaped asymmetric nonlinear oscillator for broadband vibration energy harvesting: harmonic balance analysis and experimental validation. *J. Sound Vib.* 333, 6209–6223.
68. Arrieta, A., Neild, S., and Wagg, D. (2009). Nonlinear dynamic response and modeling of a bi-stable composite plate for applications to adaptive structures. *Nonlinear Dyn.* 58, 259–272.

69. Betts, D.N., Kim, H.A., Bowen, C.R., and Inman, D. (2012). Optimal configurations of bistable piezo-composites for energy harvesting. *Appl. Phys. Lett.* **100**, 114104.
70. Betts, D.N., Bowen, C.R., Kim, H.A., Gathercole, N., Clarke, C.T., and Inman, D.J. (2013). Nonlinear dynamics of a bistable piezoelectric-composite energy harvester for broadband application. *Eur. Phys. J. Spec. Top.* **222**, 1553–1562.
71. Zhou, S., Cao, J., Inman, D.J., Liu, S., Wang, W., and Lin, J. (2015). Impact-induced high-energy orbits of nonlinear energy harvesters. *Appl. Phys. Lett.* **106**, 093901.
72. Mallick, D., Amann, A., and Roy, S. (2016). Surfing the high energy output branch of nonlinear energy harvesters. *Phys. Rev. Lett.* **117**, 197701.
73. Lan, C., Tang, L., and Qin, W. (2017). Obtaining high-energy responses of nonlinear piezoelectric energy harvester by voltage impulse perturbations. *Eur. Phys. J. Appl. Phys.* **79**, 20902.
74. Hajj Hosseiniloo, A., Slotine, J.-J., and Turitsyn, K. (2017). Robust and adaptive control of coexisting attractors in nonlinear vibratory energy harvesters. *J. Vib. Control.* <https://doi.org/10.1177/1077546316688992>.
75. Roundy, S., Leland, E.S., Baker, J., Carleton, E., Reilly, E., Lai, E., Otis, B., Rabaey, J.M., Wright, P.K., and Sundararajan, V. (2005). Improving power output for vibration-based energy scavengers. *IEEE Pervas. Comput.* **4**, 28–36.
76. Baker, J., Roundy, S., and Wright, P. (2005). Alternative geometries for increasing power density in vibration energy scavenging for wireless sensor networks. in Proc. 3rd Int. Energy Conversion Engineering Conf. (San Francisco, CA).
77. Dietl, J.M., and Garcia, E. (2010). Beam shape optimization for power harvesting. *J. Intell. Mater. Syst. Struct.* **21**, 633–646.
78. Goldschmidtboeing, F., and Woias, P. (2008). Characterization of different beam shapes for piezoelectric energy harvesting. *J. Micromech. Microeng.* **18**, 104013.
79. Ben Ayed, S., Abdelkefi, A., Najar, F., and Hajj, M.R. (2014). Design and performance of variable-shaped piezoelectric energy harvesters. *J. Intell. Mater. Syst. Struct.* **25**, 174–186.
80. Park, J., Lee, S., and Kwak, B.M. (2012). Design optimization of piezoelectric energy harvester subject to tip excitation. *J. Mech. Sci. Technol.* **26**, 137–143.
81. Paquin, S., and St-Amant, Y. (2010). Improving the performance of a piezoelectric energy harvester using a variable thickness beam. *Smart Mater. Struct.* **19**, 105020.
82. Rupp, C.J., Evgrafov, A., Maute, K., and Dunn, M.L. (2009). Design of piezoelectric energy harvesting systems: a topology optimization approach based on multilayer plates and shells. *J. Intell. Mater. Syst. Struct.* **20**, 1923–1939.
83. Chen, S., Gonella, S., Chen, W., and Liu, W.K. (2010). A level set approach for optimal design of smart energy harvesters. *Comput. Methods Appl. Mech. Eng.* **199**, 2532–2543.
84. Nanthakumar, S., Lahmer, T., Zhuang, X., Park, H.S., and Rabczuk, T. (2016). Topology optimization of piezoelectric nanostructures. *J. Mech. Phys. Solid.* **94**, 316–335.
85. Wein, F., Kaltenbacher, M., and Stingl, M. (2013). Topology optimization of a cantilevered piezoelectric energy harvester using stress norm constraints. *Struct. Multidiscip. O.* **48**, 173–185.
86. Takezawa, A., Kitamura, M., Vatanabe, S.L., and Silva, E.C.N. (2014). Design methodology of piezoelectric energy-harvesting skin using topology optimization. *Struct. Multidiscip. O.* **49**, 281–297.
87. Nakasone, P.H., and Silva, E.C. (2009). Design of piezoelectric energy harvesting devices and laminate structures by applying topology optimization. *Proc. SPIE.* <https://doi.org/10.1117/12.816467>.
88. Zheng, B., Chang, C.-J., and Gea, H.C. (2009). Topology optimization of energy harvesting devices using piezoelectric materials. *Struct. Multidiscip. O.* **38**, 17–23.
89. Jia, Y., and Seshia, A.A. (2016). Power optimization by mass tuning for MEMS piezoelectric cantilever vibration energy harvesting. *J. Microelectromech. Syst.* **25**, 108–117.
90. Yang, Z., Wang, Y.Q., Zuo, L., and Zu, J. (2017). Introducing arc-shaped piezoelectric elements into energy harvesters. *Energ. Convers. Manag.* **148**, 260–266.
91. Stewart, M., Weaver, P.M., and Cain, M. (2012). Charge redistribution in piezoelectric energy harvesters. *Appl. Phys. Lett.* **100**, 073901–073901-3.
92. Du, S., Jia, Y., Chen, S.-T., Zhao, C., Sun, B., Arroyo, E., and Seshia, A.A. (2017). A new electrode design method in piezoelectric vibration energy harvesters to maximize output power. *Sensor. Actuator. Phys.* **263**, 693–701.
93. Erkurt, A., Tarazaga, P.A., Farmer, J.R., and Inman, D.J. (2009). Effect of strain nodes and electrode configuration on piezoelectric energy harvesting from cantilevered beams. *J. Vib. Acoust.* **131**, 011010.
94. Cho, J., Anderson, M., Richards, R., Bahr, D., and Richards, C. (2005). Optimization of electromechanical coupling for a thin-film PZT membrane: II. Experiment. *J. Micromech. Microeng.* **15**, 1804.
95. Yang, Z.B., and Zu, J. (2017). Charge Redistribution in Flexextensional Piezoelectric Energy Harvesters. *Trans Tech.*
96. Kim, M., Dugundji, J., and Wardle, B.L. (2015). Effect of electrode configurations on piezoelectric vibration energy harvesting performance. *Smart Mater. Struct.* **24**, 045026.
97. Zhao, J., Zheng, X., Zhou, L., Zhang, Y., Sun, J., Dong, W., Deng, S., and Peng, S. (2012). Investigation of a d15 mode PZT-51 piezoelectric energy harvester with a series connection structure. *Smart Mater. Struct.* **21**, 105005.
98. Malakooti, M.H., and Sodano, H.A. (2015). Piezoelectric energy harvesting through shear mode operation. *Smart Mater. Struct.* **24**, 055005.
99. Kulkarni, V., Ben-Mrad, R., Prasad, S.E., and Nemana, S. (2014). A shear-mode energy harvesting device based on torsional stresses. *IEEE/ASME Trans. Mechatronics* **19**, 801–807.
100. Ren, B., Or, S.W., Zhang, Y., Zhang, Q., Li, X., Jiao, J., Wang, W., Liu, D., Zhao, X., and Luo, H. (2010). Piezoelectric energy harvesting using shear mode 0.71 Pb(Mg_{1/3}Nb_{2/3})O₃-0.29PbTiO₃ single crystal cantilever. *Appl. Phys. Lett.* **96**, 083502.
101. Aladwani, A., Aldraihem, O., and Baz, A. (2013). Single degree of freedom shear-mode piezoelectric energy harvester. *J. Vib. Acoust.* **135**, 051011.
102. Xu, C.D., Ren, B., Di, W.N., Liang, Z., Jiao, J., Li, L.Y., Li, L., Zhao, X.Y., Luo, H.S., and Wang, D. (2012). Cantilever driving low frequency piezoelectric energy harvester using single crystal material 0.71 Pb(Mg_{1/3}Nb_{2/3})O₃-0.29PbTiO₃. *Appl. Phys. Lett.* **101**, 033502.
103. Zou, H.-X., Zhang, W.-M., Li, W.-B., Hu, K.-M., Wei, K.-X., Peng, Z.-K., and Meng, G. (2017). A broadband compressive-mode vibration energy harvester enhanced by magnetic force intervention approach. *Appl. Phys. Lett.* **110**, 163904.
104. Wu, J., Chen, X., Chu, Z., Shi, W., Yu, Y., and Dong, S. (2016). A barbell-shaped high-temperature piezoelectric vibration energy harvester based on BiScO₃-PbTiO₃ ceramic. *Appl. Phys. Lett.* **109**, 173901.
105. Kim, H.W., Batra, A., Priya, S., Uchino, K., Markley, D., Newnham, R.E., and Hofmann, H.F. (2004). Energy harvesting using a Piezoelectric "Cymbal" Transducer in dynamic environment. *Jpn. J. Appl. Phys.* **43**, 6178.
106. Tufekcioglu, E., and Dogan, A. (2014). A flexensional piezo-composite structure for energy harvesting applications. *Sensor. Actuator. Phys.* **216**, 355–363.
107. Lee, H.J., Sherrit, S., Tosi, L.P., Walkemeyer, P., and Colonius, T. (2015). Piezoelectric energy harvesting in internal fluid flow. *Sensors (Basel)* **15**, 26039–26062.
108. Yang, Z., Zu, J., Luo, J., and Peng, Y. (2017). Modeling and parametric study of a force-amplified compressive-mode piezoelectric energy harvester. *J. Intell. Mater. Syst. Struct.* **28**, 357–366.
109. Xu, T.-B., Siochi, E.J., Kang, J.H., Zuo, L., Zhou, W., Tang, X., and Jiang, X. (2013). Energy harvesting using a PZT ceramic multilayer stack. *Smart Mater. Struct.* **22**, 065015.
110. Moure, A., Rodríguez, M.I., Rueda, S.H., Gonzalo, A., Rubio-Marcos, F., Cuadros, D.U., Pérez-Lepe, A., and Fernández, J. (2016). Feasible integration in asphalt of piezoelectric cymbals for vibration energy harvesting. *Energ. Convers. Manag.* **112**, 246–253.
111. Jiang, X., Li, Y., Li, J., Wang, J., and Yao, J. (2014). Piezoelectric energy harvesting from traffic-induced pavement vibrations. *J. Renew. Sustain. Energ.* **6**, 043110.

112. Lee, A.J., Wang, Y., and Inman, D.J. (2014). Energy harvesting of piezoelectric stack actuator from a shock event. *J. Vib. Acoust.* 136, 011016.
113. Wang, X., Shi, Z., Wang, J., and Xiang, H. (2016). A stack-based flex-compressive piezoelectric energy harvesting cell for large quasi-static loads. *Smart Mater. Struct.* 25, 055005.
114. Xu, T.-B., Jiang, X., and Su, J. (2011). A piezoelectric multilayer-stacked hybrid actuation/transduction system. *Appl. Phys. Lett.* 98, 243503.
115. Morimoto, K., Kanno, I., Wasa, K., and Kotera, H. (2010). High-efficiency piezoelectric energy harvesters of c-axis-oriented epitaxial PZT films transferred onto stainless steel cantilevers. *Sensor. Actuator. Phys.* 163, 428–432.
116. Yeo, H.G., Ma, X., Rahn, C., and Trolier-McKinstry, S. (2016). Efficient piezoelectric energy harvesters utilizing (001) textured bimorph PZT films on flexible metal foils. *Adv. Funct. Mater.* 26, 5940–5946.
117. Hwang, G.T., Annapureddy, V., Han, J.H., Joe, D.J., Baek, C., Park, D.Y., Kim, D.H., Park, J.H., Jeong, C.K., Park, K.-I., et al. (2016). Self-powered wireless sensor node enabled by an aerosol-deposited PZT flexible energy harvester. *Adv. Energy Mater.* 6, <https://doi.org/10.1002/aenm.201600237>.
118. Xu, S., Hansen, B.J., and Wang, Z.L. (2010). Piezoelectric-nanowire-enabled power source for driving wireless microelectronics. *Nat. Commun.* 1, 93.
119. Tang, G., Yang, B., Liu, J.-q., Xu, B., Zhu, H.-y., and Yang, C.-s. (2014). Development of high performance piezoelectric d 33 mode MEMS vibration energy harvester based on PMN-PT single crystal thick film. *Sensor. Actuator. Phys.* 205, 150–155.
120. Erturk, A., Bilgen, O., and Inman, D.J. (2008). Performance analysis of single crystal PMN-PZT unimorphs for piezoelectric energy harvesting. in Proceedings of the ASME Conference on Smart Materials, Adaptive Structures and Intelligent Systems, SMASIS2008.
121. Hwang, G.T., Park, H., Lee, J.H., Oh, S., Park, K.I., Byun, M., Park, H., Ahn, G., Jeong, C.K., No, K., et al. (2014). Self-powered cardiac pacemaker Enabled by flexible single crystalline PMN-PT piezoelectric energy harvester. *Adv. Mater.* 26, 4880–4887.
122. Hwang, G.T., Yang, J., Yang, S.H., Lee, H.-Y., Lee, M., Park, D.Y., Han, J.H., Lee, S.J., Jeong, C.K., Kim, J., et al. (2015). A reconfigurable rectified flexible energy harvester via solid-state single crystal grown PMN-PZT. *Adv. Energy Mater.* 5, <https://doi.org/10.1002/aenm.201500051>.
123. Zeng, Z., Xia, R., Gai, L., Wang, X., Lin, D., Luo, H., Li, F., and Wang, D. (2016). High performance of macro-flexible piezoelectric energy harvester using a 0.3 PIN-0.4 Pb(Mg_{1/3}Nb_{2/3})O_{3-0.3}PbTiO₃ flake array. *Smart Mater. Struct.* 25, 125015.
124. Xu, S., Yeh, Y.W., Poirier, G., McAlpine, M.C., Register, R.A., and Yao, N. (2013). Flexible piezoelectric PMN-PT nanowire-based nanocomposite and device. *Nano Lett.* 13, 2393–2398.
125. Wu, F., and Yao, N. (2017). PMN-PT nanostructures for energy scavenging. *Semicond. Sci. Technol.* 32, 063001.
126. Chen, Y., Zhang, Y., Yuan, F., Ding, F., and Schmidt, O.G. (2017). A flexible PMN-PT ribbon-based piezoelectric-pyroelectric hybrid generator for human-activity energy harvesting and monitoring. *Adv. Electron. Mater.* 3, <https://doi.org/10.1002/aelm.201600540>.
127. Marin, A., Bressers, S., and Priya, S. (2011). Multiple cell configuration electromagnetic vibration energy harvester. *J. Phys. D* 44, 295501.
128. Beeby, S.P., Torah, R., Tudor, M., Glynne-Jones, P., O'Donnell, T., Saha, C., and Roy, S. (2007). A micro electromagnetic generator for vibration energy harvesting. *J. Micromech. Microeng.* 17, 1257.
129. Yang, Z., Erturk, A., and Zu, J. (2017). On the efficiency of piezoelectric energy harvesters. *Extreme Mech. Lett.* 15, 26–37.
130. Kim, M., Dugundji, J., and Wardle, B.L. (2015). Efficiency of piezoelectric mechanical vibration energy harvesting. *Smart Mater. Struct.* 24, 055006.
131. Akaydin, H.D., Elvin, N., and Andreopoulos, Y. (2012). The performance of a self-excited fluidic energy harvester. *Smart Mater. Struct.* 21, 025007.
132. Shafer, M.W., and Garcia, E. (2014). The power and efficiency limits of piezoelectric energy harvesting. *J. Vib. Acoust.* 136, 021007.
133. Roundy, S. (2005). On the effectiveness of vibration-based energy harvesting. *J. Intell. Mater. Syst. Struct.* 16, 809–823.
134. Liu, W.Q., Badel, A., Formosa, F., and Wu, Y.P. (2015). A new figure of merit for wideband vibration energy harvesters. *Smart Mater. Struct.* 24, 125012.
135. Cammarano, A., Gonzalez-Buelga, A., Neild, S., Burrow, S., and Inman, D. (2013). Bandwidth of a nonlinear harvester with optimized electrical load. *J. Phys. Conf. Ser.* 476, 012071.
136. Dhote, S., Yang, Z., and Zu, J. (2018). Modeling and experimental parametric study of a tri-leg compliant orthoplanar spring based multi-mode piezoelectric energy harvester. *Mech. Syst. Signal Process.* 98, 268–280.
137. Lee, B., Lin, S., Wu, W., Wang, X., Chang, P., and Lee, C. (2009). Piezoelectric MEMS generators fabricated with an aerosol deposition PZT thin film. *J. Micromech. Microeng.* 19, 065014.
138. Shen, D., Park, J.-H., Noh, J.H., Choe, S.-Y., Kim, S.-H., Wikle, H.C., and Kim, D.-J. (2009). Micromachined PZT cantilever based on SOI structure for low frequency vibration energy harvesting. *Sensor. Actuator. Phys.* 154, 103–108.
139. Park, J.C., Park, J.Y., and Lee, Y.-P. (2010). Modeling and characterization of piezoelectric d₃₃-mode MEMS energy harvester. *J. Microelectromech. Syst.* 19, 1215–1222.
140. Tang, G., Liu, J.-q., Yang, B., Luo, J.-b., Liu, H.-s., Li, Y.-g., Yang, C.-s., He, D.-n., Dao, V.D., Tanaka, K., and Sugiyama, S. (2012). Fabrication and analysis of high-performance piezoelectric MEMS generators. *J. Micromech. Microeng.* 22, 065017.
141. Minh le, V., Hara, M., Yokoyama, T., Nishihara, T., Ueda, M., and Kuwano, H. (2015). Highly piezoelectric MgZr co-doped aluminum nitride-based vibrational energy harvesters [Correspondence]. *IEEE Trans. Ultrason. Ferroelectr. Freq. Control* 62, 2005–2008.
142. Tang, G., Yang, B., Hou, C., Li, G., Liu, J., Chen, X., and Yang, C. (2016). A piezoelectric micro generator worked at low frequency and high acceleration based on PZT and phosphor bronze bonding. *Sci. Rep.* 6, 38798.
143. Song, H.-C., Kumar, P., Maurya, D., Kang, M.-G., Reynolds, W.T., Jeong, D.-Y., Kang, C.-Y., and Priya, S. (2017). Ultra-low resonant piezoelectric MEMS energy harvester with high power density. *J. Microelectromech. Syst.* 26, 1226–1234.
144. Dai, X., Wen, Y., Li, P., Yang, J., and Zhang, G. (2009). Modeling, characterization and fabrication of vibration energy harvester using Terfenol-D/PZT/Terfenol-D composite transducer. *Sensor. Actuator. Phys.* 156, 350–358.
145. Kim, M., Hoegen, M., Dugundji, J., and Wardle, B.L. (2010). Modeling and experimental verification of proof mass effects on vibration energy harvester performance. *Smart Mater. Struct.* 19, 045023.
146. Liang, J., and Liao, W.-H. (2010). Impedance matching for improving piezoelectric energy harvesting systems. in SPIE Smart Structures and Materials + Nondestructive Evaluation and Health Monitoring, International Society for Optics and Photonics.
147. Gu, L. (2011). Low-frequency piezoelectric energy harvesting prototype suitable for the MEMS implementation. *Microelectron. J.* 42, 277–282.
148. Li, X., Guo, M., and Dong, S. (2011). A flex-compressive-mode piezoelectric transducer for mechanical vibration/strain energy harvesting. *IEEE Trans. Ultrason. Ferroelectr. Freq. Control* 58, 698–703.
149. Yen, T.-T., Hirasawa, T., Wright, P.K., Pisano, A.P., and Lin, L. (2011). Corrugated aluminum nitride energy harvesters for high energy conversion effectiveness. *J. Micromech. Microeng.* 21, 085037.
150. Dhakar, L., Liu, H., Tay, F., and Lee, C. (2013). A new energy harvester design for high power output at low frequencies. *Sensor. Actuator. Phys.* 199, 344–352.
151. Wu, H., Tang, L., Yang, Y., and Soh, C.K. (2013). A novel two-degrees-of-freedom piezoelectric energy harvester. *J. Intell. Mater. Syst. Struct.* 24, 357–368.
152. Arrieta, A., Delpero, T., Bergamini, A., and Ermanni, P. (2013). Broadband vibration energy harvesting based on cantilevered piezoelectric bi-stable composites. *Appl. Phys. Lett.* 102, 173904–173904-4.

153. Qiu, J., Chen, H., Wen, Y., Li, P., Yang, J., and Li, W. (2014). A vibration energy harvester using magnet/piezoelectric composite transducer. *J. Appl. Physiol.* **115**, 17E522.
154. Ma, M., Xia, S., Li, Z., Xu, Z., and Yao, X. (2014). Enhanced energy harvesting performance of the piezoelectric unimorph with perpendicular electrodes. *Appl. Phys. Lett.* **105**, 043905.
155. Zhang, Y., Cai, C., and Zhang, W. (2014). Experimental study of a multi-impact energy harvester under low frequency excitations. *Smart Mater. Struct.* **23**, 055002.
156. Xiao, Z., Yang, T.-q., Dong, Y., and Wang, X.-c. (2014). Energy harvester array using piezoelectric circular diaphragm for broadband vibration. *Appl. Phys. Lett.* **104**, 223904.
157. Hung, C.-F., Chung, T.-K., Yeh, P.-C., Chen, C.-C., Wang, C.-M., and Lin, S.-H. (2015). A miniature mechanical-piezoelectric-configured three-axis vibrational energy harvester. *IEEE Sens. J.* **15**, 5601–5615.
158. Singh, K.A., Kumar, R., and Weber, R.J. (2015). A broadband bistable piezoelectric energy harvester with nonlinear high-power extraction. *IEEE Trans. Power Electron.* **30**, 6763–6774.
159. Sriramdas, R., Chiplunkar, S., Cuduvally, R.M., and Pratap, R. (2015). Performance enhancement of piezoelectric energy harvesters using multilayer and multistep beam configurations. *IEEE Sens. J.* **15**, 3338–3348.
160. Gong, L.-J., Pan, Q.S., Li, W., Yan, G.Y., Liu, Y.B., and Feng, Z.H. (2015). Harvesting vibration energy using two modal vibrations of a folded piezoelectric device. *Appl. Phys. Lett.* **107**, 033904.
161. Yi, Z., Yang, B., Li, G., Liu, J., Chen, X., Wang, X., and Yang, C. (2017). High performance bimorph piezoelectric MEMS harvester via bulk PZT thick films on thin beryllium-bronze substrate. *Appl. Phys. Lett.* **111**, 013902.
162. He, Q., and Jiang, T. (2017). Complementary multi-mode low-frequency vibration energy harvesting with chiral piezoelectric structure. *Appl. Phys. Lett.* **110**, 213901.
163. Wong, V.-K., Ho, J.-H., and Chai, A.-B. (2017). Performance of a piezoelectric energy harvester in actual rain. *Energy* **124**, 364–371.
164. Guigou, R., Chaillout, J.-J., Jager, T., and Despesse, G. (2008). Harvesting raindrop energy: experimental study. *Smart Mater. Struct.* **17**, 015039.
165. Wong, C.H., and Dahari, Z. (2017). Development of vibration-based piezoelectric raindrop energy harvesting system. *J. Electron. Mater.* **46**, 1869–1882.
166. Wong, V.-K., Ho, J.-H., and Sam, H.-K. (2017). On accumulation of water droplets in piezoelectric energy harvesting. *J. Intell. Mater. Syst. Struct.* **28**, 521–530.
167. Guo, L., and Lu, Q. (2017). Potentials of piezoelectric and thermoelectric technologies for harvesting energy from pavements. *Renew. Sustain. Energ. Rev.* **72**, 761–773.
168. Rastegar, J., Murray, R., Pereira, C., and Nguyen, H.-L. (2009). Event sensing and energy-harvesting power sources for gun-fired munitions. in SPIE Smart Structures Materials+ Nondestructive Evaluation and Health Monitoring. International Society for Optics and Photonics.
169. Ostasevicius, V., Markevicius, V., Jurenas, V., Ziliys, M., Cepenas, M., Kizauskiene, L., and Gyliene, V. (2015). Cutting tool vibration energy harvesting for wireless sensors applications. *Sensor. Actuator. Phys.* **233**, 310–318.
170. Shafer, M.W., MacCurdy, R., Shipley, J.R., Winkler, D., Guglielmo, C.G., and Garcia, E. (2015). The case for energy harvesting on wildlife in flight. *Smart Mater. Struct.* **24**, 025031.
171. Li, H., Tian, C., Lu, J., Myjak, M.J., Martinez, J.J., Brown, R.S., and Deng, Z.D. (2016). An energy harvesting underwater acoustic transmitter for aquatic animals. *Sci. Rep.* **6**, 33804.
172. Winter, D.A. (2009). *Biomechanics and Motor Control of Human Movement* (John Wiley & Sons).
173. DeVita, P., Helseth, J., and Hortobagyi, T. (2007). Muscles do more positive than negative work in human locomotion. *J. Exp. Biol.* **210**, 3361–3373.
174. Lindstedt, S., LaStayo, P., and Reich, T. (2001). When active muscles lengthen: properties and consequences of eccentric contractions. *Physiology* **16**, 256–261.
175. Starner, T. (1996). Human-powered wearable computing. *IBM Syst. J.* **35**, 618–629.
176. Niu, P., Chapman, P., Riener, R., and Zhang, X. (2004). Evaluation of motions and actuation methods for biomechanical energy harvesting. in Power Electronics Specialists Conference, 2004. PESC 04. 2004 IEEE 35th Annual. IEEE.
177. Riener, R., and Shapiro, A. (2011). Biomechanical energy harvesting from human motion: theory, state of the art, design guidelines, and future directions. *J. Neuroeng. Rehabil.* **8**, 22.
178. Partridge, J., and Bucknall, R. (2016). An analysis of the energy flow and energy potential from human energy harvesting with a focus on walking. *Cogent Eng.* **3**, 1215203.
179. Fu, H., Cao, K., Xu, R., Bhouri, M.A., Martínez-Botás, R., Kim, S.-G., and Yeatman, E.M. Footstep energy harvesting using heel strike-induced airflow for human activity sensing. in Wearable and Implantable Body Sensor Networks (BSN), 2016 IEEE 13th International Conference. 2016. IEEE.
180. Ylli, K., Hoffmann, D., Willmann, A., Becker, P., Folkmer, B., and Manoli, Y. (2015). Energy harvesting from human motion: exploiting swing and shock excitations. *Smart Mater. Struct.* **24**, 025029.
181. Hayashida, J.Y. (2000). Unobtrusive Integration of Magnetic Generator Systems into Common Footwear (Massachusetts Institute of Technology).
182. Shenck, N.S., and Paradiso, J.A. (2001). Energy scavenging with shoe-mounted piezoelectrics. *IEEE Micro* **21**, 30–42.
183. Moro, L., and Benasciutti, D. (2010). Harvested power and sensitivity analysis of vibrating shoe-mounted piezoelectric cantilevers. *Smart Mater. Struct.* **19**, 115011.
184. Fan, K., Liu, Z., Liu, H., Wang, L., Zhu, Y., and Yu, B. (2017). Scavenging energy from human walking through a shoe-mounted piezoelectric harvester. *Appl. Phys. Lett.* **110**, 143902.
185. Mateu, L., and Moll, F. (2005). Optimum piezoelectric bending beam structures for energy harvesting using shoe inserts. *J. Intell. Mater. Syst. Struct.* **16**, 835–845.
186. Meier, R., Kelly, N., Almog, O., and Chiang, P. (2014). A piezoelectric energy-harvesting shoe system for podiatric sensing. in Engineering in Medicine and Biology Society (EMBC), 2014 36th Annual International Conference of the IEEE. IEEE.
187. Fourie, D. (2010). Shoe mounted PVDF piezoelectric transducer for energy harvesting. *MORJ Rep.* **19**, 66–70.
188. Ishida, K., Huang, T.-C., Honda, K., Shinozuka, Y., Fuketa, H., Yokota, T., Zschieschang, U., Klauk, H., Tortissier, G., Sekitani, T., et al. (2013). Insole pedometer with piezoelectric energy harvester and 2V organic circuits. *IEEE J. Solid State Circ.* **48**, 255–264.
189. Zhao, J., and You, Z. (2014). A shoe-embedded piezoelectric energy harvester for wearable sensors. *Sensors* **14**, 12497–12510.
190. Jung, W.-S., Lee, M.-J., Kang, M.-G., Moon, H.G., Yoon, S.-J., Baek, S.-H., and Kang, C.-Y. (2015). Powerful curved piezoelectric generator for wearable applications. *Nano Energy* **13**, 174–181.
191. Daniels, A., Zhu, M., and Tiwari, A. (2013). Design, analysis and testing of a piezoelectric flex transducer for harvesting bio-kinetic energy. *J. Phys. Conf. Ser.* **476**, 012047.
192. Xie, L., and Cai, M. (2014). Increased piezoelectric energy harvesting from human footstep motion by using an amplification mechanism. *Appl. Phys. Lett.* **105**, 143901.
193. Niu, P., Chapman, P., DiBerardino, L., and Hsiao-Wecksler, E. (2008). Design and optimization of a biomechanical energy harvesting device. in Power Electronics Specialists Conference, 2008. PESC 2008. IEEE. IEEE.
194. Amar, A.B., Kouki, A.B., and Cao, H. (2015). Power approaches for implantable medical devices. *Sensors* **15**, 28889–28914.
195. Bradley, P.D. (2006). An ultra low power, high performance medical implant communication system (MICS) transceiver for implantable devices. in Biomedical Circuits and Systems Conference, 2006. BioCAS 2006. IEEE. IEEE.
196. Wong, L.S., Hossain, S., Ta, A., Edvinsson, J., Rivas, D.H., and Naas, H. (2004). A very low-power CMOS mixed-signal IC for implantable pacemaker applications. *IEEE J. Solid State Circ.* **39**, 2446–2456.

197. Padeletti, L., and Barold, S.S. (2005). Digital technology for cardiac pacing. *Am. J. Cardiol.* 95, 479–482.
198. Kim, S., Cho, N., Song, S.-J., Kim, D., Kim, K., and Yoo, H.-J. (2006). A 0.9-V 96- μ W digital hearing aid chip with heterogeneous $\Sigma-\Delta$ DAC. in Proc. IEEE Symp. VLSI Circuits.
199. Sarapeshkar, R., Salthouse, C., Sit, J.J., Baker, M.W., Zhak, S.M., Lu, T.K., Turicchia, L., and Balster, S. (2005). An ultra-low-power programmable analog bionic ear processor. *IEEE Trans. Biomed. Eng.* 52, 711–727.
200. Saati, S., Lo, R., Li, P.Y., Meng, E., Varma, R., and Humayun, M.S. (2010). Mini drug pump for ophthalmic use. *Curr. Eye Res.* 35, 192–201.
201. Weiland, J.D., Liu, W., and Humayun, M.S. (2005). Retinal prosthesis. *Annu. Rev. Biomed. Eng.* 7, 361–401.
202. Wise, K.D., Anderson, D., Hetke, J., Kipke, D., and Najafi, K. (2004). Wireless implantable microsystems: high-density electronic interfaces to the nervous system. *Proc. IEEE* 92, 76–97.
203. Zurbuchen, A., Pfenninger, A., Stahel, A., Stoek, C.T., Vandenberghe, S., Koch, V.M., and Vogel, R. (2013). Energy harvesting from the beating heart by a mass imbalance oscillation generator. *Ann. Biomed. Eng.* 41, 131–141.
204. Lentner, C. (1990). Geigy Scientific Table: Heart and Circulation, Volume 5 (CIBA).
205. Papademetris, X., and Duncan, J.S. (2000). Cardiac image analysis: motion and deformation. In *Handbook of Medical Imaging*, 2, I.M. Bankman, ed (Elsevier), pp. 675–710.
206. Deterre, M., Lefevre, E., and Dufour-Gergam, E. (2012). An active piezoelectric energy extraction method for pressure energy harvesting. *Smart Mater. Struct.* 21, 085004.
207. Länne, T., Stale, H., Bengtsson, H., Gustafsson, D., Bergqvist, D., Sonesson, B., Lecero, H., and Dahl, P. (1992). Noninvasive measurement of diameter changes in the distal abdominal aorta in man. *Ultrasound Med. Biol.* 18, 451–457.
208. Dammers, R., Stijft, F., Tordoir, J.H., Hammeleers, J.M., Hoeks, A.P., and Kitslaar, P.J. (2003). Shear stress depends on vascular territory: comparison between common carotid and brachial artery. *J. Appl. Physiol.* 94, 485–489.
209. Karami, M.A., and Inman, D.J. (2012). Powering pacemakers from heartbeat vibrations using linear and nonlinear energy harvesters. *Appl. Phys. Lett.* 100, 042901.
210. Karami, M.A., and Inman, D.J. (2011). Linear and nonlinear energy harvesters for powering pacemakers from heart beat vibrations. in *Active and Passive Smart Structures and Integrated Systems 2011*. International Society for Optics and Photonics.
211. Ansari, M., and Karami, M.A. (2017). Experimental investigation of fan-folded piezoelectric energy harvesters for powering pacemakers. *Smart Mater. Struct.* 26, 065001.
212. Sharpes, N., Abdelkefi, A., and Priya, S. (2015). Two-dimensional concentrated-stress low-frequency piezoelectric vibration energy harvesters. *Appl. Phys. Lett.* 107, 093901.
213. Alrashdan, M.H., Hamzah, A.A., and Majlis, B. (2015). Design and optimization of cantilever based piezoelectric micro power generator for cardiac pacemaker. *Microsystem Tech.* 21, 1607–1617.
214. Dagdeviren, C., Yang, B.D., Su, Y., Tran, P.L., Joe, P., Anderson, E., Xia, J., Doraiswamy, V., Dehdashti, B., Feng, X., et al. (2014). Conformal piezoelectric energy harvesting and storage from motions of the heart, lung, and diaphragm. *Proc. Natl. Acad. Sci. USA* 111, 1927–1932.
215. Lu, B., Chen, Y., Ou, D., Chen, H., Diao, L., Zhang, W., Zheng, J., Ma, W., Sun, L., and Feng, X. (2015). Ultra-flexible piezoelectric devices integrated with heart to harvest the biomechanical energy. *Sci. Rep.* 5.
216. Bedell, S.W., Fogel, K., Lauro, P., Shahrjerdi, D., Ott, J.A., and Sadana, D. (2013). Layer transfer by controlled spalling. *J. Phys. D* 46, 152002.
217. Kim, D.H., Shin, H.J., Lee, H., Jeong, C.K., Park, H., Hwang, G.-T., Lee, H.-Y., Joe, D.J., Han, J.H., Lee, S.H., et al. (2017). In vivo self-powered wireless transmission using biocompatible flexible energy harvesters. *Adv. Funct. Mater.* <https://doi.org/10.1002/adfm.201700341>.
218. Hwang, G.T., Byun, M., Jeong, C.K., and Lee, K.J. (2015). Flexible piezoelectric thin-film energy harvesters and nanosensors for biomedical applications. *Adv. Healthc. Mater.* 4, 646–658.
219. Wang, D.-A., and Liu, N.-Z. (2011). A shear mode piezoelectric energy harvester based on a pressurized water flow. *Sensor. Actuator. Phys.* 167, 449–458.
220. Kim, S., Clark, W.W., and Wang, Q.-M. (2005). Piezoelectric energy harvesting with a clamped circular plate: experimental study. *J. Intell. Mater. Syst. Struct.* 16, 855–863.
221. Mo, C., Radzinski, L.J., and Clark, W.W. (2010). Experimental validation of energy harvesting performance for pressure-loaded piezoelectric circular diaphragms. *Smart Mater. Struct.* 19, 075010.
222. Sohn, J., Choi, S.B., and Lee, D. (2005). An investigation on piezoelectric energy harvesting for MEMS power sources. *J. Mech. Eng. Sci.* 219, 429–436.
223. Deterre, M., Lefevre, E., Zhu, Y., Woytasik, M., Boutaud, B., and Dal Molin, R. (2014). Micro blood pressure energy harvester for intracardiac pacemaker. *J. Microelectromech. Syst.* 23, 651–660.
224. Reddy, V.Y., Exner, D.V., Cantillon, D.J., Doshi, R., Bunch, T.J., Tomassoni, G.F., Friedman, P.A., Estes, N.A., 3rd, Ip, J., Niazi, I., et al.; LEADLESS II Study Investigators (2015). Percutaneous implantation of an entirely intracardiac leadless pacemaker. *N. Engl. J. Med.* 373, 1125–1135.
225. Potkay, J.A., and Brooks K. An arterial cuff energy scavenger for implanted microsystems. in *Bioinformatics and Biomedical Engineering*, 2008. ICBBE 2008. The 2nd International Conference. 2008. IEEE.
226. Zhang, H., Zhang, X.-S., Cheng, X., Liu, Y., Han, M., Xue, X., Wang, S., Yang, F., Smith, A.S., Zhang, H., and Xu, Z. (2015). A flexible and implantable piezoelectric generator harvesting energy from the pulsation of ascending aorta: in vitro and in vivo studies. *Nano Energy* 12, 296–304.
227. Auzanneau, F. (2013). Wire troubleshooting and diagnosis: review and perspectives. *Prog. Electromagn. Res. B* 49, 253–279.
228. Khalatkar, A., and Gupta, V. (2017). Piezoelectric energy harvester for low engine vibrations. *J. Renew. Sustain. Energ.* 9, 024701.
229. Wang, Y.-J., Chen, C.-D., Lin, C.-C., and Yu, J.-H. (2015). A nonlinear suspended energy harvester for a tire pressure monitoring system. *Micromachines* 6, 312–327.
230. Wang, Y.-J., Shen, S.-C., and Chen, C.-D. (2012). Wideband electromagnetic energy harvesting from a rotating wheel. In *Small-Scale Energy Harvesting*, M. Lallart, ed. (InTech). <https://doi.org/10.5772/50739>.
231. van Schaijk, R., Elfrink, R., Oudenhoven, J., Pop, V., Wang, Z., and Renaud, M. (2013). A MEMS vibration energy harvester for automotive applications. *Proc. SPIE*. <https://doi.org/10.1117/12.2016916>.
232. Kim, G. (2015). Piezoelectric energy harvesting from torsional vibration in internal combustion engines. *Int. J. Auto. Technol.* 16, 645–651.
233. Zuo, L., and Tang, X. (2013). Large-scale vibration energy harvesting. *J. Intell. Mater. Syst. Struct.* 24, 1405–1430.
234. Tianchen, Y., Jian, Y., Ruigang, S., and Xiaowei, L. (2014). Vibration energy harvesting system for railroad safety based on running vehicles. *Smart Mater. Struct.* 23, 125046.
235. Bowen, C., and Arafa, M. (2015). Energy harvesting technologies for tire pressure monitoring systems. *Adv. Energy Mater.* 5, <https://doi.org/10.1002/aenm.201401787>.
236. Kubba, A.E., and Jiang, K. (2014). A comprehensive study on technologies of tyre monitoring systems and possible energy solutions. *Sensors (Basel)* 14, 10306–10345.
237. Löhdorf, M., Kvisterøy, T., Westby, E., and Halvorsen, E. (2007). Evaluation of energy harvesting concepts for tire pressure monitoring systems. *Proceedings of Power MEMS*, p. 331–334.
238. Kubba, A.E., Behroozi, M., Olatunbosun, O.A., Anthony, C., and Jiang, K. (2014). Modeling of strain energy harvesting in pneumatic tires using piezoelectric transducer. *Tire Sci. Technol.* 42, 16–34.
239. Garcia-Pozuelo, D., Yunta, J., Olatunbosun, O., Yang, X., and Diaz, V. (2017). A strain-

- based method to estimate slip angle and tire working conditions for intelligent tires using fuzzy logic. *Sensors (Basel)* 17, 874.
240. Roveri, N., Pepe, G., and Carcaterra, A. (2016). OPTYRE—A new technology for tire monitoring: Evidence of contact patch phenomena. *Mech. Syst. Signal Process.* 66, 793–810.
241. Xiong, Y., and Tuononen, A. (2015). Rolling deformation of truck tires: measurement and analysis using a tire sensing approach. *J. Terramech.* 61, 33–42.
242. Xiong, Y., and Tuononen, A. (2014). A laser-based sensor system for tire tread deformation measurement. *Meas. Sci. Tech.* 25, 115103.
243. Tuononen, A.J. (2008). Optical position detection to measure tyre carcass deflections. *Vehicle Syst. Dyn.* 46, 471–481.
244. Matilainen, M., and Tuononen, A. (2015). Tyre contact length on dry and wet road surfaces measured by three-axis accelerometer. *Mech. Syst. Signal Process.* 52, 548–558.
245. Behroozinia, P., Taheri, S., and Mirzaefar, R. (2017). An investigation of intelligent tires using multiscale modeling of cord-rubber composites. *Mech. Base. Des. Struct. Mach.* 1–16.
246. Roundy, S. (2008). Energy harvesting for tire pressure monitoring systems: design considerations. *Proceedings of Power MEMS + MicroMEMS*, Sendai, Japan: p. 9–12.
247. Moon, K.S., Liang, H., Yi, J., and Mika, B. (2007). Tire tread deformation sensor and energy harvester development for ‘Smart Tire’ applications. in *Proc. SPIE*.
248. Wu, L., Wang, Y., Jia, C., and Zhang, C. Battery-less piezoceramics mode energy harvesting for automobile TPMS. in *ASIC, 2009. ASICON’09. IEEE 8th International Conference*. 2009. IEEE.
249. Mak, K.H., McWilliam, S., and Popov, A.A. (2013). Piezoelectric energy harvesting for tyre pressure measurement applications. *J. Automobile Eng.* 227, 842–852.
250. Elfrink, R., Matova, S., de Nooijer, C., Jambunathan, M., Goedbloed, M., van de Molengraft, J., Pop, V., Vullers, R.J.M., Renaud, M., and van Schaijk, R. (2011). Shock induced energy harvesting with a MEMS harvester for automotive applications. in *Electron Devices Meeting (IEDM), 2011 IEEE International*. IEEE.
251. Zheng, Q., Tu, H., Agee, A., and Xu, Y. (2009). Vibration energy harvesting device based on asymmetric air-spaced cantilevers for tire pressure monitoring system. *Proceedings of Power MEMS*, 403–406.
252. Zhang, Y., Zheng, R., Shimono, K., Kaizuka, T., and Nakano, K. (2016). Effectiveness testing of a piezoelectric energy harvester for an automobile wheel using stochastic resonance. *Sensors* 16, 1727.
253. Singh, K.B., Bedekar, V., Taheri, S., and Priya, S. (2012). Piezoelectric vibration energy harvesting system with an adaptive frequency tuning mechanism for intelligent tires. *Mechtronics* 22, 970–988.
254. Sadeqi, S., Arzanpour, S., and Hajikolaei, K.H. (2015). Broadening the frequency bandwidth of a tire-embedded piezoelectric-based energy harvesting system using coupled linear resonating structure. *IEEE/ASME Trans. Mechatronics* 20, 2085–2094.
255. Zhu, B., Han, J., Zhao, J., and Deng, W. (2017). Practical design of an energy harvester considering wheel rotation for powering intelligent tire systems. *J. Electron. Mater.* 46, 2483–2493.
256. McInnes, C., Gorman, D., and Cartmell, M.P. (2008). Enhanced vibrational energy harvesting using nonlinear stochastic resonance. *J. Sound Vib.* 318, 655–662.
257. Zheng, R., Nakano, K., Hu, H., Su, D., and Cartmell, M.P. (2014). An application of stochastic resonance for energy harvesting in a bistable vibrating system. *J. Sound Vib.* 333, 2568–2587.
258. Wellens, T., Shatokhin, V., and Buchleitner, A. (2003). Stochastic resonance. *Rep. Progr. Phys.* 67, 45.
259. Keck, M. (2007). A new approach of a piezoelectric vibration-based power generator to supply next generation tire sensor systems. in *Sensors, 2007 IEEE*. IEEE.
260. Jousimaa, O.J., Parmar, M., and Lee, D.-W. (2016). Energy harvesting system for intelligent tyre sensors. in *Intelligent Vehicles Symposium (IV), 2016 IEEE*. IEEE.
261. Wu, X., Parmar, M., and Lee, D.-W. (2014). A seesaw-structured energy harvester with superwide bandwidth for TPMS application. *IEEE/ASME Trans. Mechatronics* 19, 1514–1522.
262. Manla, G., White, N., and Tudor, J. (2009). Harvesting energy from vehicle wheels. in *Solid-State Sensors, Actuators and Microsystems Conference, 2009. TRANSDUCERS 2009*. IEEE.
263. Tang, Q., Xia, X., and Li, X. Non-contact frequency-up-conversion energy harvester for durable & broad-band automotive TPMS application. in *Micro Electro Mechanical Systems (MEMS), 2012 IEEE 25th International Conference*. 2012. IEEE.
264. Roundy, S., and Tola, J. (2014). Energy harvester for rotating environments using offset pendulum and nonlinear dynamics. *Smart Mater. Struct.* 23, 105004.
265. Makki, N., and Pop-Iliev, R. (2012). Battery-and wire-less tire pressure measurement systems (TPMS) sensor. *Microsystem Tech.* 18, 1201–1212.
266. Makki, N., and Pop-Iliev, R. (2011). Piezoelectric power generation for sensor applications: design of a battery-less wireless tire pressure sensor. *Proc. SPIE*. <https://doi.org/10.1117/12.887112>.
267. Makki, N., and Pop-Iliev, R. Pneumatic tire-based piezoelectric power generation. in *Proc. SPIE Vol. 2011*.
268. van den Ende, D.A., Van de Wiel, H., Groen, W., and Van der Zwaag, S. (2011). Direct strain energy harvesting in automobile tires using piezoelectric PZT-polymer composites. *Smart Mater. Struct.* 21, 015011.
269. Roundy, S.J. (2003). Energy Scavenging for Wireless Sensor Nodes with a Focus on Vibration to Electricity Conversion (University of California).
270. Bowen, C., Newham, R., and Randall, C. (1998). Dielectric properties of dielectrophoretically assembled particulate-polymer composites. *J. Mater. Res.* 13, 205–210.
271. Lee, J., and Choi, B. (2014). Development of a piezoelectric energy harvesting system for implementing wireless sensors on the tires. *Energ. Convers. Manag.* 78, 32–38.
272. Torfs, T., Sterken, T., Brebels, S., Santana, J., van den Hoven, R., Spiering, V., Bertsch, N., Trapani, D., and Zonta, D. (2013). Low power wireless sensor network for building monitoring. *IEEE Sensors J.* 13, 909–915.
273. Nair, A., and Cai, C. (2010). Acoustic emission monitoring of bridges: review and case studies. *Eng. Struct.* 32, 1704–1714.
274. Arampatzis, T., Lygeros, J., and Manesis, S. (2005). A survey of applications of wireless sensors and wireless sensor networks. in *Intelligent Control, 2005. Proceedings of the 2005 IEEE International Symposium on, Mediterranean Conference on Control and Automation*. IEEE.
275. Ricquebourg, V., Menga, D., Durand, D., Marhic, B., Delahoche, L., and Logé, C. The smart home concept: our immediate future. in *E-Learning in Industrial Electronics, 2006 1ST IEEE International Conference on*. 2006. IEEE.
276. Kaur, N., and Bhalla, S. (2014). Combined energy harvesting and structural health monitoring potential of embedded piezo-concrete vibration sensors. *J. Energy Eng.* 141, D4014001.
277. Farinholt, K.M., Miller, N., Sifuentes, W., MacDonald, J., Park, G., and Farrar, C.R. (2010). Energy harvesting and wireless energy transmission for embedded SHM sensor nodes. *Struct. Health Monit.* 9, 269–280.
278. Matiko, J., Graham, N., Beeby, S., and Tudor, M. (2013). Review of the application of energy harvesting in buildings. *Meas. Sci. Techn.* 25, 012002.
279. Çelebi, M., Phan, L., and Marshall, R. (1993). Dynamic characteristics of five tall buildings during strong and low-amplitude motions. *Struct. Des. Tall Spec.* 2, 1–15.
280. Peigney, M., and Siegert, D. (2013). Piezoelectric energy harvesting from traffic-induced bridge vibrations. *Smart Mater. Struct.* 22, 095019.
281. Khan, F.U., and Ahmad, I. (2016). Review of energy harvesters utilizing bridge vibrations. *Shock Vib.* <https://doi.org/10.1155/2016/1340402>.
282. Cao, M., and Zuo, L. (2014). Energy harvesting from building seismic isolation with multi-mode resonant shunt circuits. in

- ASME 2014 Dynamic Systems and Control Conference, (American Society of Mechanical Engineers).
283. Shen, W., Zhu, S., Zhu, H., and Xu, Y. (2016). Electromagnetic energy harvesting from structural vibrations during earthquakes. *Smart Struct. Syst.* 18, 449–470.
284. Zhu, D., Beeby, S.P., Tudor, M.J., White, N.M., and Harris, N.R. (2013). Novel miniature airflow energy harvester for wireless sensing applications in buildings. *IEEE Sensors J.* 13, 691–700.
285. Khan, F.U. and I. Ahmad. Vibration-based electromagnetic type energy harvester for bridge monitoring sensor application. in Emerging Technologies (ICET), 2014 International Conference. 2014. IEEE. \
286. Orfei, F., Mezzetti, C.B., and Cottone, F.. (2016). Vibrations powered LoRa sensor: An electromechanical energy harvester working on a real bridge. in *SENSORS, 2016 IEEE*. \
287. Takeya, K., Sasaki, E., and Kobayashi, Y. (2016). Design and parametric study on energy harvesting from bridge vibration using tuned dual-mass damper systems. *J. Sound Vib.* 361, 50–65.
288. McEvoy, T., Dierks, E., Weaver, J., Inamdar, S., Zimowski, K., Wood, K.L., Crawford, R.H., and Jensen, D. (2011). Developing innovative energy harvesting approaches for infrastructure health monitoring systems. in Proceedings of the 37th Design Automation Conference, Parts A and B.
289. Galchev, T., Kim, H., and Najafi, K. (2011). Micro power generator for harvesting low-frequency and nonperiodic vibrations. *J. Microelectromech. Syst.* 20, 852–866.
290. Tang, X. and L. Zuo. (2011). Simulation and experiment validation of simultaneous vibration control and energy harvesting from buildings using tuned mass dampers. in American Control Conference (ACC), 2011. IEEE.
291. Galchev, T., McCullagh, J., Peterson, R., and Najafi, K. (2011). Harvesting traffic-induced vibrations for structural health monitoring of bridges. *J. Micromech. Microeng.* 21, 104005.
292. McCullagh, J., Galchev, T., Peterson, R., Gordenker, R., Zhang, Y., Lynch, J., and Najafi, K. (2014). Long-term testing of a vibration harvesting system for the structural health monitoring of bridges. *Sensor. Actuator. Phys.* 217, 139–150.
293. Jung, H.-J., Kim, I.-H., and Jang, S.-J. (2011). An energy harvesting system using the wind-induced vibration of a stay cable for powering a wireless sensor node. *Smart Mater. Struct.* 20, 075001.
294. Erturk, A. (2011). Piezoelectric energy harvesting for civil infrastructure system applications: moving loads and surface strain fluctuations. *J. Intell. Mater. Syst. Struct.* 22, 1959–1973.
295. Ali, S.F., Friswell, M., and Adhikari, S. (2011). Analysis of energy harvesters for highway bridges. *J. Intell. Mater. Syst. Struct.* 22, 1929–1938.
296. Zhang, Y., Cai, S.C., and Deng, L. (2014). Piezoelectric-based energy harvesting in bridge systems. *J. Intell. Mater. Syst. Struct.* 25, 1414–1428.
297. Xie, X., Wu, N., Yuen, K.V., and Wang, Q. (2013). Energy harvesting from high-rise buildings by a piezoelectric coupled cantilever with a proof mass. *Int. J. Eng. Sci.* 72, 98–106.
298. Cahill, P., Jaksic, V., Keane, J., O'Sullivan, A., Mathewson, A., Ali, S.F., and Pakrashi, V. (2016). Effect of road surface, vehicle, and device characteristics on energy harvesting from bridge–vehicle interactions. *Comput. Aided Civ. Infrastruct. Eng.* 31, 921–935.
299. Cahill, P., Nuallain, N.A.N., Jackson, N., Mathewson, A., Karoumi, R., and Pakrashi, V. (2014). Energy harvesting from train-induced response in bridges. *J. Bridge Eng.* 19, 04014034.
300. Karimi, M., Karimi, A., Tikani, R., and Ziae Rad, S. (2016). Experimental and theoretical investigations on piezoelectric-based energy harvesting from bridge vibrations under travelling vehicles. *Int. J. Mech. Sci.* 119, 1–11.
301. Bhaskaran, P.R., Rathnam, J.D., Koilmani, S., and Subramanian, K. (2017). Multiresonant frequency piezoelectric energy harvesters integrated with high sensitivity piezoelectric accelerometer for bridge health monitoring applications. *Smart Mater. Res.* 2017, <https://doi.org/10.1155/2017/6084309>.
302. Maruccio, C., Quaranta, G., DeLorenzis, L., and Monti, G. (2016). Energy harvesting from electrospun piezoelectric nanofibers for structural health monitoring of a cable-stayed bridge. *Smart Mater. Struct.* 25, 085040.
303. Lee, S., Youn, B.D., and Jung, B.C. (2009). Robust segment-type energy harvester and its application to a wireless sensor. *Smart Mater. Struct.* 18, 095021.
304. Rhimi, M., and Lajnef, N. (2012). Tunable energy harvesting from ambient vibrations in civil structures. *J. Energy Eng.* 138, 185–193.
305. Leland, E.S., and Wright, P.K. (2006). Resonance tuning of piezoelectric vibration energy scavenging generators using compressive axial preload. *Smart Mater. Struct.* 15, 1413.
306. Kim, S.-H., Ahn, J.-H., Chung, H.-M., and Kang, H.-W. (2011). Analysis of piezoelectric effects on various loading conditions for energy harvesting in a bridge system. *Sensor. Actuator. Phys.* 167, 468–483.
307. Xie, X., Wang, Q., and Wang, S. (2015). Energy harvesting from high-rise buildings by a piezoelectric harvester device. *Energy* 93, 1345–1352.
308. Xie, X., and Wang, Q. (2016). Design of a piezoelectric harvester fixed under the roof of a high-rise building. *Eng. Struct.* 117, 1–9.